G-Safety
SCIENCE FOR GLOBAL SAFETY

The 6th International Symposium on Water Environment Systems

---with Perspective of Global Safety

(November 29th – December 1st, 2018)

Department of Civil and Environmental Engineering

Graduate School of Engineering

Tohoku University

TOHOKU
UNIVERSITY

Sponsors

http://www.g-safety.tohoku.ac.jp/

Tohoku University, Main Administration Office Organization for Leading Graduate School Program of Tohoku University, Sendai, Miyagi 980-8578, Japan

http://www.eng.tohoku.ac.jp/

Tohoku University, Graduate School of Engineering, Sendai, Miyagi 980-8579, Japan

ORGANIZERS

Dr. So Kazama (Professor, Tohoku University)

Dr. Yu-You Li (Professor, Tohoku University)

Dr. Daisuke Komori (Associate Professor, Tohoku University)

Dr. Daisuke Sano (Associate Professor, Tohoku University)

SECRETARIES

Assistant Professor, Toshimasa Hojo
toshimasa.hojo.b5@tohoku.ac.jp

Assistant Professor, Yoshiya Touge
yoshiya.touge.a6@tohoku.ac.jp

DC Student, Jialing Ni
jialing@dc.tohoku.ac.jp

DC Student, Yemei Li
li.yemei.s5@dc.tohoku.ac.jp

DC Student, Noriko Uchida
noriko.uchida.s8@dc.tohoku.ac.jp

DC Student, Grace Puyang Emang
grace.puyang.emang.r2@dc.tohoku.ac.jp

Research Student, Ying Song
song.ying.q2@dc.tohoku.ac.jp

PARTICIPANTS

Tohoku university	**Japan**
Name	**Identity**
Yemei Li	Student
Siti Nur Fatihah Binti Moideen	Student
Ying Song & Weikang Qi (Tohoku Univ. & BUCT)	Student
Yuanfan Zhang	Student
Chenglei Xie	Student
Yujie Chen	Student
Chaimaa Mribet	Student
Jialing Ni	Student
Aijun Zhu	Student
Hiroshi Iwano	Student
Runda Du & Jinmei Sun(Tohoku Univ. & TJU)	Student
Bo Feng	Student
Ming Cong	Student
Eli Hendrik Sanjaya(Tohoku Univ. & SUM)	Student
Noriko Uchida	Student
Grace Puyang Emang	Student
Chatuphorn Somphong	Student
Qing Chang	Student
Mbugua Jacqueline Muthoni	Student
Vempi Satriya Adi Hendrawan	Student
Sopha Soliya	Student
Akihiro Ichiba	Student
Koji Sakamoto	Student
Ryosuke Inomata	Student
Keitaro Yamada	Student
Andri Taruna Rachmadi	Postdoctoral researcher
Sital Uprety	Student

Fukushima University	**Japan**
Name	**Identity**
Thuy Thi Thanh LE	Student
Chris Leong	Student

Tianjin University	**China**
Name	**Identity**
Ping Gu	Professor
Guanghui Zhang	Associate Professor

Korea Institute of Civil Engineering and Building Technology	**Korea**
Name	**Identity**
Seongsim Yoon	Senior Researcher

Universiti Teknologi Malaysia	**Malaysia**
Name	**Identity**
Khairunnisa ABDUL HALIM	Visitor scholar

Venue

Graduate School of Engineering, Aobayama campus, Tohoku University

Lectures and oral presentations

Room 101, Engineering Laboratory Complex building(総合研究棟) (C10)

Posters exhibition

Room 201, Engineering Laboratory Complex building (総合研究棟) (C10)

Dinner party

Center hall Aoba restaurant (工学部中央棟)

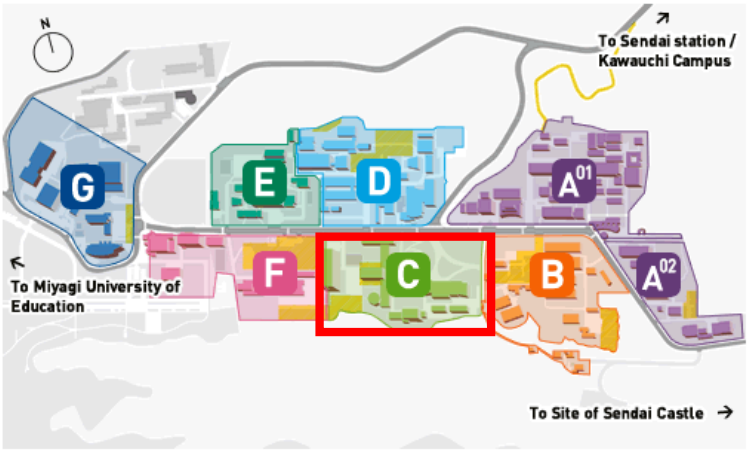

A01 Mechanical and Aerospace Engineering
A02 Quantum Science and Energy Engineering
B Materials Science and Engineering
C Center Square
D Electrical Engineering and Applied Physics
E Applied Chemistry, Chemical Engineering and Biomolecular Engineering
F Civil Engineering and Architecture
G Various Area

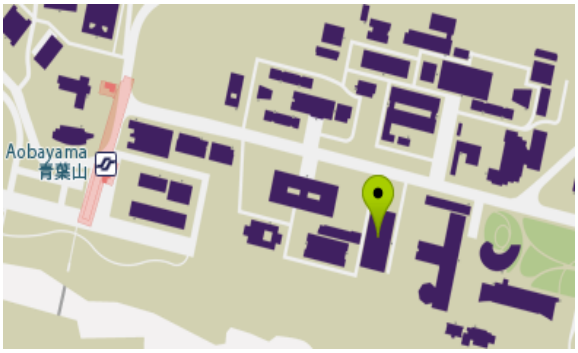

Engineering Laboratory Complex building(総合研究棟)

Access to Aobayama Campus

(Subway)

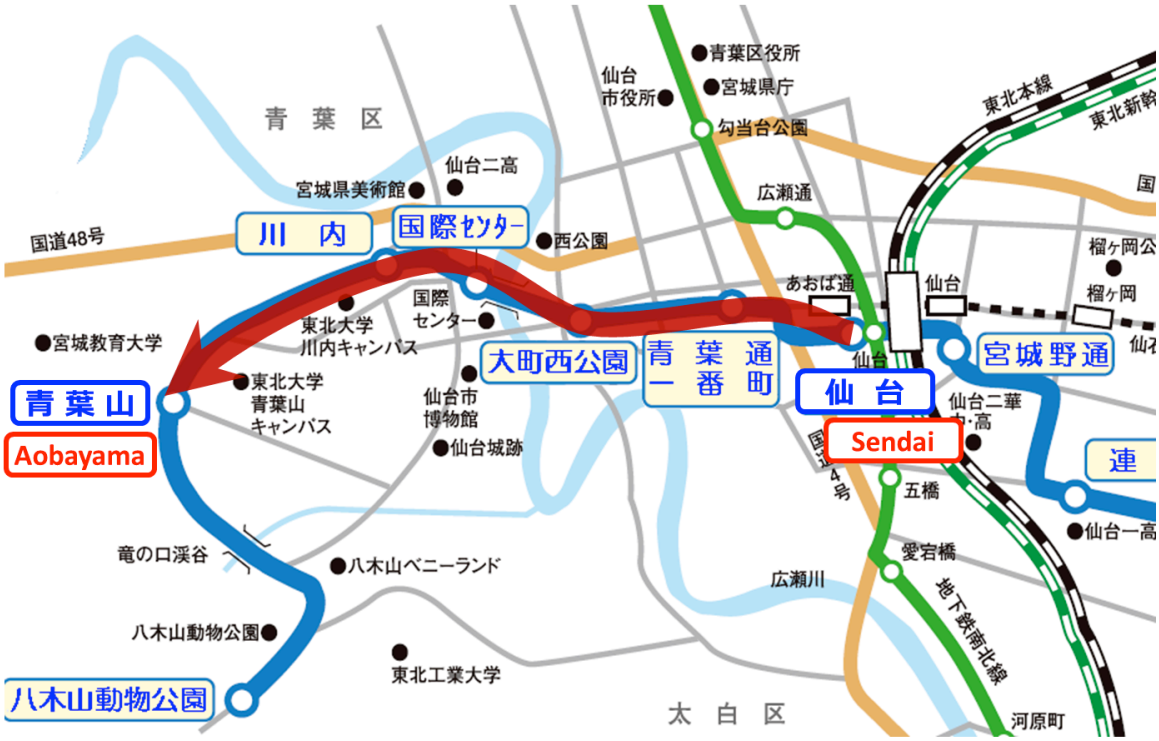

Map of **East-west line subway(地下鉄　東西線)** in Sendai

Please take this subway line and get off on the stop **Aobayama（青葉山）**.

Tips

If you start from Sendai Station, please make sure you are entering **East-west line subway（地下鉄　東西線）** rather than South-north line subway（**地下鉄　南北線**） nor JR station.

Program

Thursday, 29 Nov 2018

Fieldwork

The reconstruction of Minami-gamo sewage treatment plant

・2011/3/11 Tsunami hitting the Sewage Facilities

・Remains of 311-tsunami shocking on the wall of pump station

・Plan view of the sewage facilities

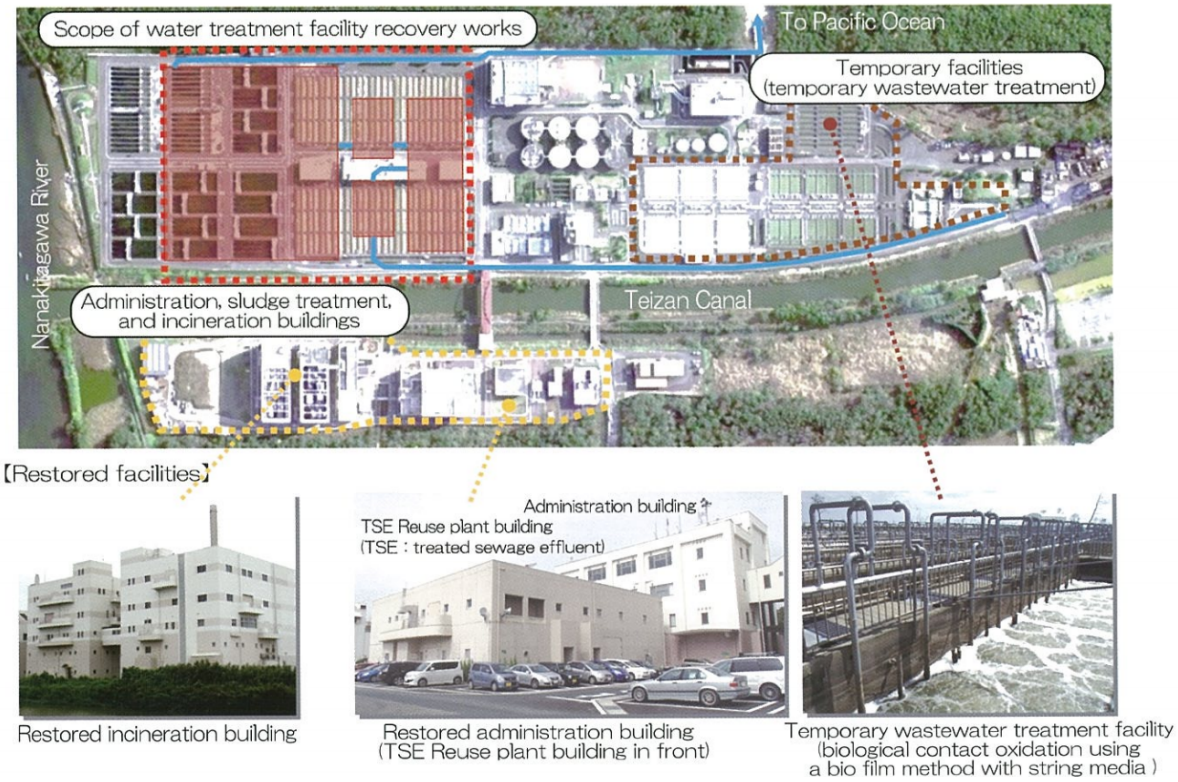

・Location of Minami-gamo sewage treatment plant

Friday, 30 Nov 2018

The 6th International Symposium on Water Environment Systems

Place: Room 101, Engineering Laboratory Complex building, Tohoku University

09:00 ~ 09:10 **Opening address**

09:10 ~ 09:20 **Memorial photo**

Session I

09:20 ~ 09:50 Development of urban flood disaster prediction techniques using weather forecasting information: a case study of Seoul, Korea
Seongsim Yoon
Korea Institute of Civil Engineering and Building Technology

09:50 ~ 10:20 Evaluation of landslide hazards in North Vietnam using TRIGRS model under impact of climate change
Thuy Thi Thanh LE
Fukushima University

10:20 ~ 10:50 Estimating runoff in perennial and ephemeral catchments: a disaggregated flow duration curve approach
Chris Leong
Fukushima University

10:50 ~ 11:00 **Coffee break**

Session II

11:00 ~ 11:30 Characteristics and seasonal flactuations of invertebrate species eDNA concentration in forest, agriculture, and urban river
Noriko Uchida
Tohoku University

11:30 ~ 12:00 Forest fire severity estimation for the 2017 Kamaishi forest fire
Grace Puyang Emang
Tohoku University

12:00 ~ 13:00 **Lunch break**

13:00 ~ 14:00 **Poster exhibition**

Place: Room 201, Engineering Laboratory Complex building, Tohoku University

- Beach Nourishment as an Adaptation to Future Beach Loss due to Sea Level Rise in Thailand
  Chatuphorn Somphong
  Tohoku University
- The impact of spatial discretization scale on urban hydrological modeling performance and prediction
  Qing Chang
  Tohoku University
- Using MODIS to detect crop type changes in the Aral Sea Basin in the 21st Century
  Mbugua Jacqueline Muthoni
  Tohoku University
- Remote estimation of rice crop yield using MODIS Vegetation Indices data:
  A case study of Solo river basin rice field, Indonesia
  Vempi Satriya Adi Hendrawan
  Tohoku University
- Preliminary study of grape farmers' perception to changing climate in Takahata city, Yamagata prefecture, Japan
  Sopha Soliya
  Tohoku University
- Estimation of woody debris recruitment by landslides:
  A Case study of Typhoon Lionrock in Iwaizumi, Japan
  Akihiro Ichiba
  Tohoku University
- Evaluation and sensitivity analysis for surface and bottom snowmelt process by runoff analysis
  Koji Sakamoto
  Tohoku University
- Estimation of nutrient distribution in Mekong river floodplain using satellite images
  Keitaro Yamada
  Tohoku University

- Long-term change and spatial anomaly of precipitation in Osaka, Japan

  Ryosuke Inomata

  Tohoku University

- Performance of sewage treatment and bioenergy production using duckweed

  Hiroshi Iwano

  Tohoku University

- Mesophilic and Thermophilic Temperature Phased Anaerobic Digestion of Paper Waste Containing Food Waste: the Effects of Hydraulic Retention Time

  Aijun Zhu

  Tohoku University

- Use of PMA-PCR for revelation of viable microbial members in anaerobic digesters

  Jialing Ni

  Tohoku University

- Optimization of cultivation of humic-reducing bacteria based on ORP/pH feedback

  Runda Du & Jinmei Sun

  Tohoku University & Tianjin University

- The effects of pre-acidification on the granule sludge perperties in the anaerobic treatment of starch wastewater

  Bo Feng

  Tohoku University

- Development of urban resource recovery system by methane fermentation and disposal waste water treatment

  Ming Cong

  Tohoku University

- Co-digestion of food waste and sewage sludge in Anaerobic Membrane Reactor

  Yemei Li

  Tohoku University

	▪ The potential appearance of free-chlorine resistant norovirus after disinfection process in wastewater Andri Taruna Rachmadi *Tohoku University*

Session III

14:00 ~ 14:30	The effectRemoval of Cesium from Simulated Wastewater by a Countcurrent Two-stage Adsorption-Microfiltration Process of organic matter on one-stage anammox process Ping Gu & Guanghui Zhang *Tianjin University*
14:30 ~ 14:50	Biohydrogen Production (BHP) and Biomethane Production (BMP) Potential from Palm Oil Mill Effluent (POME) Khairunnisa ABDUL HALIM *Universiti Teknologi Malaysia*
14:50 ~ 15:00	**Coffee break**

Session IV

15:00 ~ 15:20	Methane Fermentation Treatment of Fish Processing Wastewater by A Self-agitated Anaerobic Baffled Reactor (SA-ABR) Eli Hendrik Sanjaya *Tohoku University & State University of Malang*
15:20 ~ 15:40	The Potential Anaerobic Digestion Treatment for Palm Oil Mill Effluent (POME) Siti Nur Fatihah Binti Moideen *Tohoku University*
15:40 ~ 16:00	Assessment of slaughterhouse wastewater treatment plant using a combination of UASB and Activated Sludge Chaimaa Mribet *Tohoku University*
16:00 ~ 16:20	Using microbial quantification for Water, Sanitation and Hygiene (WASH) intervention study in rural Nepal Sital Uprety

	Tohoku University
16:20 ~ 16:35	**Coffee break**

Session V

16:35 ~ 16:55	Nitrogen removal performance of an anammox membrane reactor operated at 25℃ with increasing sludge loading rate Ying Song & Weikang Qi *Tohoku University &Beijing University Of Chemical Technology*
16:55 ~ 17:15	Successful Operation Performance of Partial Nitritation and Anammox Reactor Treating Low- Yujie Chen *Tohoku University*
17:15 ~ 17:35	The combination application study of anaerobic fermentation and anammox technology in waste organic matter control Chenglei Xie *Tohoku University*
17:35 ~ 17:55	Simultaneous Nitrogen and Phosphorus Recovery using an anammox Expanded Bed Reactor at Low Temperature Yuanfan Zhang *Tohoku University*
17:55 ~ 18:15	**Closing speech**
18:15 ~ 20:00	**Dinner party**

Development of urban flood disaster prediction techniques using weather forecasting information: a case study of Seoul, Korea

○Seongsim Yoon[1*]

[1]Department of Land, Water and Environment Research, Korea Insitute of Civil Engineering and Building Technology, Gyeonggi-do 10223, Korea

*E-mail: ssyoon@kict.re.kr

Abstract

This research developed the urban flash flood forecasting techniques and real-time system in order to prevent urban flash flood damages in Seoul and Metropolitan areas, Korea. The real-time flood forecasting system provides predicted inundation map, river risk information, and flash flood index in mountainous area using the forecast rainfall. The forecast rainfall is estimated from the numerical weather prediction model and radar to secure the lead time for evacuation. This system can offer flood disaster information and support the decision of evacuation to reduce the damage for the citizens and the government.

Keywords: Urban flood forecasting system, Seoul, Numerical weather prediction model

1. Introduction

The recent changes in climate and abnormal weather phenomena have resulted in increased occurrences of localized torrential rainfall. Urban areas in Korea have suffered from localized heavy rainfall, including the notable Seoul flood disaster in 2010 and 2011. The urban hydrological environment has changed in relation to precipitation, such as reduced concentration time, a decreased storage rate, and increased peak discharge. These changes have altered and accelerated the severity of damage to urban areas. In order to prevent such urban flash flood damages, we have to secure the lead time for evacuation through the flood forecasting system with the forecast rainfall. For Seoul and Metropolitan area, the urban flood forecasting system is developed using numerical weather prediction model (NWP).

2. Urban flash flood forecasting techniques

In order to provide effective flood forecast information for Seoul and the metropolitan area, this research developed three techniques considering the type of flood, 1) urban inundation prediction technique for roads and low-lying ground, 2) Flash flood risk prediction technique for mountainous area 3) Risk prediction technique of the river due to rising river water level. In particular, in order to support the decision-making in flood prevention effectively, we developed a real-time system and display six-hour advanced prediction information in cooperation with high resolution weather forecast information (Yoon and Lee, 2016).

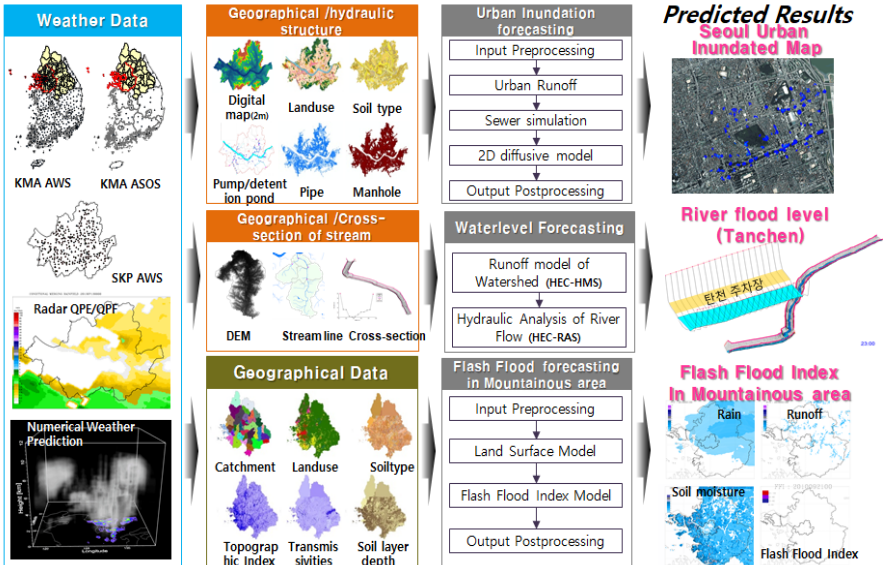

Figure 1. Concepts of urban flash flood information production

2.1 Seoul Inundation forecasting technique

The process of producing urban inundation forecasting information is divided into high resolution rainfall data production, urban runoff analysis model construction, two-dimensional flood analysis model construction, and real-time connection.

For urban flood discharge estimation, SWMM (Storm Water Management Model) is set up over the whole area of Seoul, Korea. SWMM estimates the surface and pipe flow in the sewer system of the urban area through the RUNOFF and EXTRAN modules. For urban inundation simulation, the model is based on the two-dimensional shallow water equation of continuity and momentum. When surcharging occurs at manholes, a two-dimensional diffusion model was adopted to simulate inundation on the surface by routing overland flow with the sources coming from surcharging flow. This spatial resolution of inundation model is 6m. The real-time urban flood forecasting system is consisted of these models and also uses rainfall as input. Figure 2 shows the results of inundation simulation for the 50-year probability rainfall through Seoul inundation forecasting technique (Choi et al., 2015; Lee and Yoon, 2017).

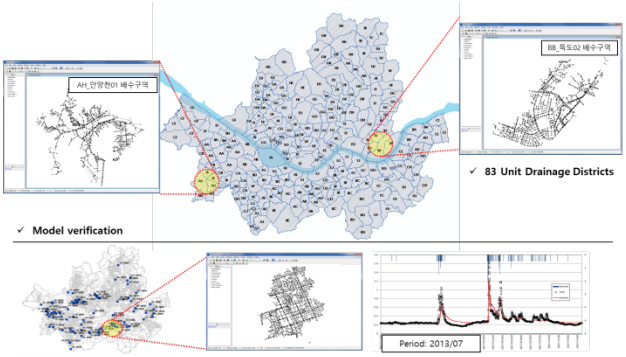

Figure 2. Pipe network data set-up in Seoul

2.2. Risk prediction technique for Tan River

There are about 40 urban rivers, with Han River as the main stream in Seoul. These rivers are used as space for leisure and parking lots. In the recent years (2009 to 2014), the parking places and people had experienced damages caused by floods.

A technique to predict the rise of the waterlevel was used to reduce flood damage at river in this study. Especially, in order to secure the lead time for evacuation in the case of heavy rainfall, it is necessary not only to utilize the high-resolution rainfall prediction of KMA, but also to reduce the time-consuming runoff estimation. This forecasting technique is based on the determined waterlelvel scenarios.

HEC-HMS, a rainfall-runoff model, was constructed on the Tan River watershed in order to simulate the upstream inflows, and the tributary inflows to the main stream were required. A total of 143 rainfall scenarios were used as inputs to the HEC-HMS to simulate the lateral flow of the Yangjae Stream and the upstream flow of the Yangjae Bridge, and the HEC-RAS model was constructed to simulate the river water level. The water level information of 25 meter cross section interval from Han river junction to Daegok bridge was obtained and a total of 143 water level scenarios were calculated. The flood criteria are set such as alert, warning and severe flood warning depends on the maximum water level from all scenarios.

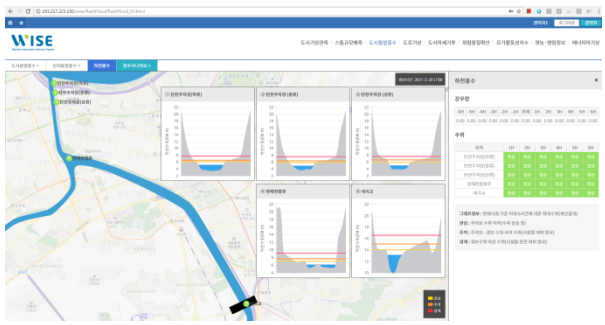

Figure 3. Risk warning using waterlevel of Tan river

2.3 Flash flood forecasting technique in mountainous area

Flash floods can be defined as a phenomenon in which signs of flooding like rapids appear in a short time within six hours after rainfall occurs in small mountainous catchment areas (~10 km^2).

In order to predict the sudden flood in the mountainous area, it is necessary to predict the localized heavy rain and surface runoff analysis technique. Therefore, this study generated the gridded flash flood index using the gridded hydrologic components of TOPLATS land surface model and statistic flash flood index model. The study area is the national capital region of Korea, and 38 flash flood damages had occurred from 2009 to 2012. The spatio-temporal resolutions of land surface model are 1 h and 1 km, respectively. The gridded meteorological data is generated using the inverse distance weight method with automatic weather stations (AWSs) of Korea Meteorological Administration (KMA). The hydrological components (e.g., surface runoff, soil water contents, and water table depth) of cells corresponding to the positions of 38 flood damages reasonably respond to the cell based hourly rainfalls. Under the total rainfall condition, the gridded flash flood index shows 71% to 87% from 4 h to 6 h in the lead time based on the rescue request time and 42% to 52% of accuracy at 0 h, which means that the time period of the lead time is in a limited rescue request time. From these results, it is known that the gridded flash flood index using the cell based hydrological components from land surface model and the statistic flash flood index model have a capability to predict flash flood in the mountainous area (Lee et al., 2016).

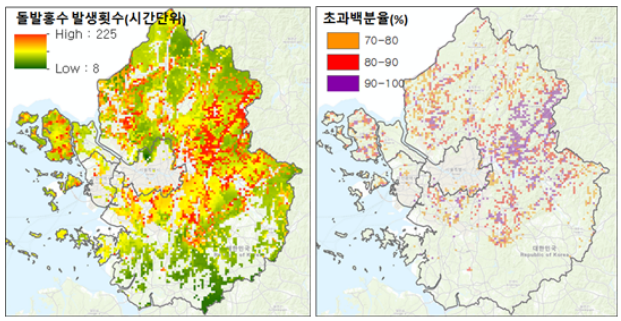

Figure 4. Flash flood occurrences and risk ratio

3. Seoul Inundation Analysis Prediction System

We developed a real-time Seoul inundation analysis prediction system using each flash flood technique with observed rainfall and forecasted rainfall of NWP model. The system provides the predicted inundation map for the next one to three hours, and Tan river flood risk information, such as alert / warning / severe flooding water level that is calculated every hour, includes cross-sectional information at five points and rainfall information of Tan river from the last six hours to the future six hours. Flash flood index is provided in the metropolitan area using forecasted rainfall of NWP through the system.

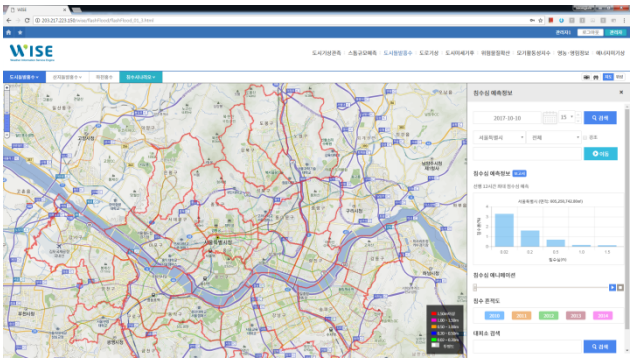

Figure 5. Seoul inundation analysis system

4. Conclusions

This study developed urban flood prediction technique for Seoul and metropolitan areas. In particular, we used forecasted rainfall from KMA to secure lead time. We estimated high resolution inundation map, mountain flash flood index, and river flood risk information reflecting the various flood occurrence mechanisms. Through this research, the citizens and the government can easily obtain the flood disaster information and can act on the evacuation to reduce the damage.

References

1) Byongju Lee, Sumin Choi, Seongsim Yoon, Youngjean Choi : The Evaluation of TOPLATS Land Surface Model Application for Forecasting Flash Flood in mountainous areas, J. Korea Water Resour. Assoc. 49(1), pp. 19-28, 2016.
2) Byongju Lee, Seongsim Yoon : Development of Grid based Inundation Analysis Model(GIAM), J. Korea Water Resour. Assoc. Vol. 50, No. 3, pp. 181-190, 2017.
3) Seongsim Yoon, Byongju Lee: Development of urban flash flood forecasting technique, water for future, 49(9), 2016.
4) Sumin Choi, Seongsim Yoon, Byongju Lee, Youngean Choi : Evaluation of High-Resolution QPE data for Urban Runoff Analysis, J. Korea Water Resour. Assoc. 48(9), pp.719-728, 2015.

Evaluation of landslide hazards in North Vietnam using TRIGRS model under impact of climate change

○Thuy Thi Thanh LE[1*], Seiki Kawagoe[1]
[1]Faculty of Symbiotic Systems Science, Fukushima University, Fukushima 960-1296, Japan
*E-mail: lethanhthuy.wru@gmail.com

Abstract
This paper evaluates the probability of landslide occurrence through the regional application of a physical model TRIGRS considering the roles of a triggering parameter (rainfall) in relation to conditioning factors under the influence of the warming climate. The scenario-base approach is adopted basing on various options such as rainstorm events and land-cover condition. Comparing to the decline of Fs in case of changing rain-event from actual storm in 2013 to 24-hour-PMP (126.9 mm – 332.4 mm rise in rainfall amount), the average value of factor of safety in the whole region decreased significantly when the downpour total of 24-hour-PMP increased by 21.7 mm – 169.1 mm in additional 24 hours to reach the magnitude of 48-hour-PMP. In addition, under the same amount of the storm-rain and storm duration, for example 24-hour-PMP, the landslide prone areas would expanse in case of changing the storm distribution from type 1 (peak rainfall locates at the beginning of the storm) to type 3 (peak precipitation appears at the end of the storm). The slope stability also reduced when the land cover changed such as from forest cover (Land-use 2010) to crop land and construction site (Land-use 2015). Interestingly when the whole region was assumed to be replaced by soil (Ha02), a significant reduction of Fs was shown when compared to the option of changes in land-use database (Ha12) and changes in soil-depth option (Ha33). The findings therefore provide an important information for local authorities in developing adequate land-management in the Cau river basin considering the relationship between landslide-prone area and changes in land-cover situation.

Keywords: Landslide, TRIGRS, PMP, North Vietnam

1. Introduction
Landslide has been evaluating as a major hazard to the society because of their catastrophic consequences. Governing by the hilly terrain in addition to higher frequencies of extreme precipitation , rainfall-induced landslides are considered as one of the major risks in Northeast region, in parallel with severe hazards from floods and debris flows. In Vietnam, a developing nation, land-falls were triggered not only by heavy intensity rainfalls, but human activities such as slope-cut and tree-cutting as well. It is a clear evidence that economic development has brought about the expansion of urbanization to the whole country, including hilly region in Northeast Vietnam; a large number of transportation routes and other infrastructures have been constructed and rehabilitated in mountainous area. Vegetation cover on hill-slopes has been rapidly replaced by bared land due to exploiting activities such as slope cutting for houses, mining and deforestation. Extreme climatic event in a relationship with changes in land cover condition could burden the slope stability and result in destructive impacts to the communities' safety. In 2012, the Vietnamese Government deployed a national project 2012-2020 to produce the landslide inventory maps in mountainous provinces. However, it is quite difficult to obtain records of slope failure in mountainous regions that locate far from populated areas; the project therefore set up investigations along main traffic routes to map historical landslides related to the man-made slope failures along transportation arteries and residential construction. In addition, recent studies analyzed the landslide risks in North Vietnam often based on statistical method for a regional scale; the determination

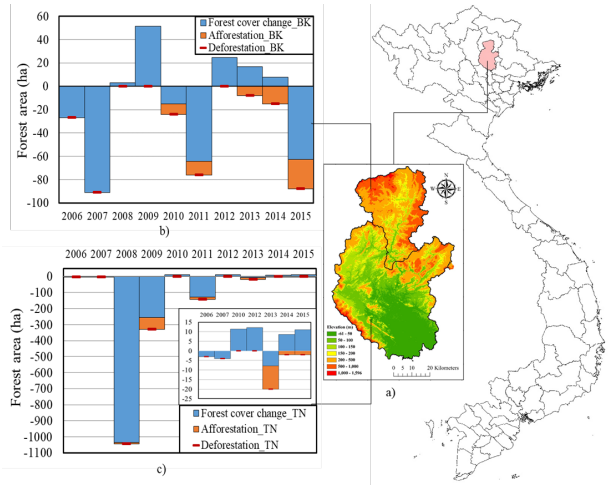

Fig. 1: a) Elevation distribution of study area; b) Deforestation and afforestation data from 2006 to 2015 in Bac Kan; c) Deforestation and afforestation data from 2006 to 2015 in Thai Nguyen

method however was mainly applied in a local scale. This paper hence would like to evaluate the probability of landslide occurrence through the regional application of a physical model considering the roles of a triggering parameter (rainfall) in relation to conditioning factors under the influence of the warming climate.

2. Study area
The study site in this paper covered the area of Cau river basin belonging to Bac Kan and Thai Nguyen provinces. This

catchment is covered by a mixture of mountainous and hilly terrain condition (Fig. 1a) with average annual precipitation of 1360 (Cho Ra) - 2572 mm (Diem Mac). The highest 24-hour precipitation in each rainy month varies from 294 mm (May) to 374.9 mm (August), the largest 24-hour rainfall was 496.1 mm at Ky Phu station on 1978/10/04. According to the national statistic data, during period 2011-2016, the population in Bac Kan rose by 18.6 thousand to reach the population of 319 thousand people in 2016 with the population density of 65.64 people/km^2. A rapid growth rate of Thai Nguyen's population from 1139.4 thousand (2011) to 1227.4 thousand people (2016) led to the higher population density in this province (348.03 people per km^2 in 2016). The population growth required higher pressure in settlement issues in the whole region. New residential areas in relation to inadequate land-use management brought about a significant reduction of forest cover in this region (Fig. 1b & 1c).

3. Methodology and database

In this paper, the landslide susceptibility is analysed based the deterministic method using a physical model: TRIGRS (Transient Rainfall Infiltration and Grid-Based Region Slope-Stability Analysis model) model. This FORTRAN program utilizes analytical solutions of partially differential equations that represent 1-D vertical subsurface flow in either saturated or unsaturated conditions. An infinite slope stability model is then used to assess the spatial and temporal occurrences of landslides. The pore-water pressure and the value of factor of safety (Fs) are calculated on a cell-by-cell basis and can be operated in the geographic information system [1]. This model could be applied to analyze the impacts of rainfall flow on the stability of soil, thus is often used for rainfall induced shallow landslides. It evaluates the changes in the transient pore-pressure and the safety factors due to rainfall infiltration. This program requires input parameters including soil physics, hydro-geology, slope condition, as well as rainfall intensities and durations. Regarding to the characteristics of the Cau River basin in Bac Kan and Thai Nguyen provinces, the infiltration model for initially unsaturated conditions of finite depth of the bedrock was selected; the soil profile was divided into two main layers (Fig. 2) including a saturated zone beneath the water table,

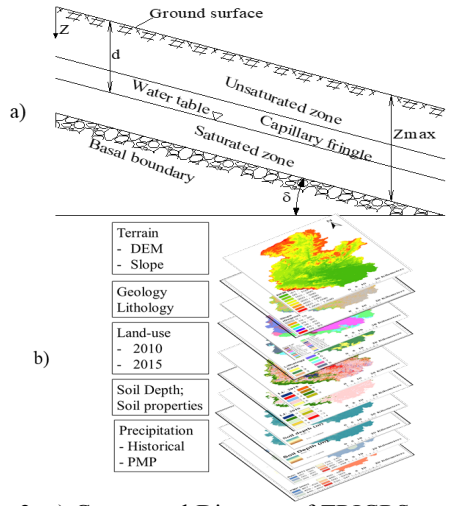

Fig. 2: a) Conceptual Diagram of TRIGRS model; b) Basic input layers for TRIGRS model.

and an unsaturated zone expanding to the ground surface [2]. The dimensionless Fs at depth Z was derived from the balance between the downslope component of the gravitational driving stress and the resisting stress for saturated soils (Iverson 2000). By separating the time-variant term and the steady terms, Iverson (1991) defined Fs as in equation (1):

$$F_s(Z,t) = \frac{\tan\varphi}{\tan\delta} + \frac{c - \Psi(Z,t)\gamma_W \tan\varphi}{\gamma_s Z \sin\delta\cos\delta} \quad (1)$$

Where φ is the soil friction angle (^{o}); δ is the slope angle (^{o}); c is the cohesion (kN/m^2),; γ_s is the unit weight of soil (kN/m^3); γ_w is the unit weight of water (kN/m^3); Z is the depth below the ground surface (m); t is the time (sec); ψ refers to the ground water pressure head as a function of depth Z and time t (m);

In addition to the Digital elevation model providing information of terrain condition, information of soil and precipitation are discretized and assigned in each cell to simulate rainfall infiltration and vertical flow through the unsaturated zone. In this study, a scenario-based approach is adopted for landslide risk assessment under extreme weather condition; main input layers for TRIGRS model was shown in (Fig. 2). Thickness of topsoil is often coincides with the failure depth, and is considered as one major parameter for slope-stability evaluation. However, this information is not often mapped, and is not feasible for field investigation in a large scale region. It therefore its spatial distribution is often predicted based on empirical relationship between terrain attributes and thickness of soil. In this study, we applied the method of Saulnier (1997) [3] to evaluate soil depth in each pixel with the assumption of decreasing linear function between effective soil depth and topographic slope (eq. 2):

$$Z_i = Z_{max}\left[1 - \frac{tan\delta_i - tan\delta_{min}}{tan\delta_{max} - tan\delta_{min}}\left(1 - \frac{Z_{min}}{Z_{max}}\right)\right] \quad (2)$$

In which Z_{min} and Z_{max} refer to minimum and maximum values of effective soil depths; δ_{min} and δ_{max} are the minimal and maximal values of slope angle; Z_i and δ_i represent the soil depth and slope angle at the calculated cell i.

To evaluate the role of vegetation cover on the hilly slope, in this paper, we considered the contribution of root systems to the shear strength (s) by additional cohesion component (Δc) following the Mohr-Coulomb formulation [4] (eq. 3):

$$s = c + \sigma_N\, tan\varphi = (c_s + \Delta c) + \sigma_N\, tan\varphi \quad (3)$$

Where the cohesion c in equation (1) in vegetation cover area is the sum of soil cohesion c_s (kN/m^2) and apparent cohesion provided by roots (root cohesion) Δc (kN/m^2); σ_N refers to the normal stress on the shear plane (kN/m^2). For simplicity, in this paper the influence of tree –surcharge is ignored, and the mechanical impact of tree cover on the shear strength of soil with vegetation cover is represented only by the root cohesion (Δc).

4. Results

In order to simulate shallow landslide under different extreme precipitation, it is necessary to evaluate spatial and temporal distribution of storm events. We firstly analyzed 68 heavy storms events from 1960-2016 in three provinces in Northeast (Bac Kan, Tuyen Quang, and Thai Nguyen) and found out that typical forms of rainstorm in this region differ not only in rain durations (from 5 hours in Tuyen Quang on

Table 1: Total rainfall amount regarding to historical rainfall (H) in 2013 and 24-hour PMP, and 48-hour-PMP (mm)

Station	Rainstorm in 2013	24hr-PMP	48hr-PMP
Bac Kan	186.3	482.1	651.3
Cho Don	178.2	493.8	572.8
Phu Thong	294.0	420.9	524.7
Dinh Hoa	189.0	468.9	552.9
Dai Tu	164.7	497.1	542.9
Thai Nguyen	222.2	499.0	520.7
Pho Yen	200.7	496.2	529.3
Vo Nhai	250.0	492.4	530.7

Table 2: Calculation options for factor of safety using TRIGRS (Fs_abcd)

[Fs_abcd] Option	a Rainfall event	b Rainfall distribution	c Land use	d Soil depth
H	Historical event			
a		Actual distribution		
0			Bare soil	
1	24-hour PMP	Type 1	USGS 2010	Case 1
2	48-hour PMP	Type 2	JAXA 2015- 100m resolution	Case 2
3		Type 3	JAXA 2015- 50m resolution	Case 3

For example: Fs_Ha32 refers to the factor of safety (Fs) for an option applying the historical rainfall event (a=H) having an actual distribution (b=a) using JAXA land-use in 2015 with 50 m resolution (c=3), and soil depth case 2 (d=2).

1984/6/22 to 53 hours in Bac Kan on 1990/9/21) but the hourly-distributions as well. Duration of almost all heavy storm events were often below 48 hours with three main distribution types: i) Type 1: peak rainfall locates at the beginning of the storm; ii) Type 2: peak rain locates at the middle of the storm time; and iii) Type 3: peak precipitation appears at the end of the storm (Fig. 3). In addition, within the period 2010-2016 , the average annual rainfall in Bac Kan and Thai Nguyen provinces varied from 1391 mm (2011) to 2029 mm (2013); the highest values of the maximum-1-day precipitation at most rain-stations occurred in the year 2013. Heavy rainstorm events in 2013 also led to a large number of landslides problems across the region; for example, according to the report of Bac Kan province, the road 258 from Bac Kan to Ba Be (40 km) were closed for 1 month and repaired for about 3 months as the results of landslide occurrences after the downpour in May 2013. Additionally, under the influence of a changing climate, increases of temperature are believed to drive higher intensity of precipitation in many regions throughout the world. The magnitudes of extreme rainstorm have been estimated using the Probable maximum precipitation (PMP) [5] . The evaluation of PMP was implemented using the moisture maximization method. The value of a heavy rainstorm in 2013, 24-hour-PMP, and 48-hr-PMP are shown in Table 1. Regarding to other input data in TRIGRS, we gathered information of soil and hydro-geology from literature reviews and field investigation; average values were then

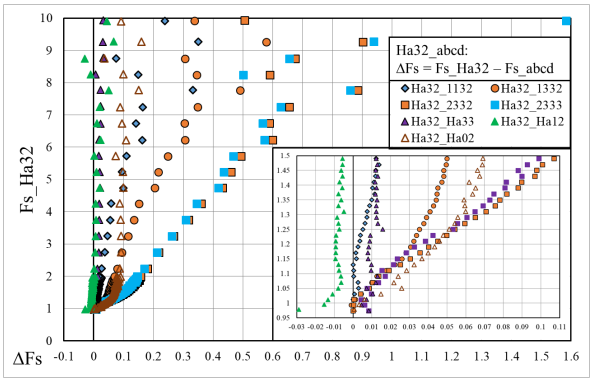

Fig. 4: Relationship between factor of safety for option Ha32 (Fs_Ha32) and delta Fs (ΔFs) [difference between Fs_Ha32 and factor of safety for other options]

selected regarding to main geology regions. In addition to the worst case of bared land across the region (the cohesion c in equation (1) refers to the soil cohesion c_s), the land-use data obtaining from two main sources -USGS 2010 and JAXA 2015- was put in the model to set up scenarios (Table 2); the cohesion c in equation (1) is the sum of the soil cohesion c_s and the root cohesion Δc . Applying the Saulnier method [3] (Eq. 2), information of average depth of top soil was gathered from recent studies and reports, and was set up in three options including i) case 1: upper value of soil depth (1.1 m – 4 m) based on lithology map across the whole region; ii) case 2: average value of soil depth (0.5 m – 3 m) based on lithology map and geology distribution across the whole region; iii) case 3: average value (0.5 m – 3 m) of soil depth based on geology distribution and rainfall regions. Since the information of groundwater table was unavailable, it was assumed that the initial groundwater table was at the bottom of the weather soil layer in summer time without antecedent rain.

Based on options of rainstorm amount, rainfall distribution, land-use condition, and soil depth assumption, we computed the factor of safety for the whole region of Cau river basin. In case of actual rainstorm distribution, we calculated the factor of safety Fs regarding to two options of soil-depth (case 2 and case 3) as well as the changes in land-use option, i.e. from land use database in 2010 (USGS) (Ha12) to land-use database in 2015 (JAXA) (Ha32 & Ha33) in addition to the worst option of land cover with bare soil (Ha02). To estimate the changes in Fs, we consider the option Ha32 as a base case and compute the difference between Fs_Ha32 and factor of safety for other scenarios (Fig 4). Within the range of below 1.5 in the value of Fs_Ha32, the option Ha12 (land cover in 2010) obtained higher threshold of ΔFs; in other words, the slope stability reduced when the land cover changed such as from forest cover (2010) to crop land and construction site (2015). Interestingly when the whole region is assumed to be replaced by soil (Ha02), a significant reduction of Fs was shown when compared to the option of changes in land-use database (Ha12) and changes in soil-depth option (Ha33). When the rainstorm amount changed from actual event (Ha32) to 24-hour-PMP (1132 and 1332) and 48-hour-PMP (2332 and 2333), the factor of safety Fs also declined in the whole basin. Overall the top file values of average ΔFs in the whole basin are 0.196 (Ha32_2333),

0.189 (Ha32_2332), 0.097 (Ha32_1332), 0.069 (Ha32_Ha02), and 0.040 (Ha32_1132).

5. Conclusions

In conclusion, under the changes in climatic condition, extreme precipitation would result in higher probability of unstable regions. It is noted that under the same amount of the storm-rain and storm duration, for example 24-hour-PMP, the landslide prone areas would expanse in case of changing the storm distribution from type 1 (scenario 1132) to type 3 (scenario 1332). Comparing the rise of ΔFs in case of changing rain-event from actual storm in 2013 to 24-hour-PMP (126.9 mm – 332.4 mm rise in rainfall amount), the factor of safety still decreased significantly when the downpour total of 24-hour-PMP increased by 21.7 mm – 169.1 mm in additional 24 hours to reach the magnitude of 48-hour-PMP (Fig 4). This reveals the importance of three major components of a storm events including rain-amount, rain-duration, and rain-distribution to the stability condition of hilly site. The findings also provide an important information for local authorities in developing adequate land-management in this river basin considering the relationship between landslide-prone area and changes in land-cover situation.

Acknowledgements

This research was supported by the Vietnamese Government scholarship (project 911); and the Social Implementation Program on Climate Change Adaptation Technology (SI-CAT) of MEXT, Japan.

References

1. Baum, R. L., Savage, W. Z., Godt, J. W.: TRIGRS — A Fortran Program for Transient Rainfall Infiltration and Grid-Based Regional Slope-Stability Analysis, Version 2.0. *US Geol Surv Open-File Rep*. 2008;(2008-1159):75. doi:Open-File Report 2008–1159.
2. Baum, R. L., Godt, J. W., Savage, W. Z.: Erratum: Estimating the timing and location of shallow rainfall-induced landslides using a model for transient, unsaturated infiltration. *J Geophys Res*. 2010;115(F03013):1-26. doi:doi:10.1029/2009JF001321.
3. Saulnier, G.-M., Beven, K., Obled, C.: Including spatially variable soil depth in TOPMODEL. *J Hydrol*. 1997;202:158-172.
4. Pollen-Bankhead, N., Simon, A.: Enhanced application of root-reinforcement algorithms for bank-stability modeling. *Earth Surf Process Landforms*. 2009;34:471-480. doi:10.1002/esp.1690.
5. WMO.: Manual on Estimation of Probable Maximum Precipitation (PMP)., 2009.

Estimating runoff in perennial and ephemeral catchments: a disaggregated flow duration curve approach.

○Chris Leong[1*], Yoshiyuki Yokoo[1]

[1]Graduate School of Symbiotic Systems Science and Technology, Fukushima University, Fukushima 960-1296, Japan

*E-mail: leongchris3@gmail.com

Abstract

The flow duration curve (FDC) is a simple tool that has been used over decades in hydrologic studies. The use of simplistic hydrologic models is important to further development of models relating to ungauged catchment runoff estimations. Therefore, this study uses the FDC and disaggregates it into three parts, high, middle, low and attempts to make reasonable runoff estimations in each part. Based on previous literature, it was determined that FDC high flow part was controlled by precipitation, herein the Curve Number method was used for runoff estimations in the high flow parts and the middle flow parts could use mean monthly flow (MMF). For the low flow part of the FDC, evapotranspiration was suggested be an important controlling factor. Therefore, perennial and ephemeral catchments were used because of the different nature of the FDC shapes especially at the low flow ends. The results show reasonable runoff estimations in the perennial catchments low flow sections and can be comparable to the MMF, therefore, using either approach is suitable. For the ephemeral catchment, the runoff did not have proper estimations. Further analysis on ephemeral catchments identify precipitation index as a suitable tool for making runoff estimations in the low flow part of the FDC.

Keywords: Flow duration curve, Disaggregation, Runoff estimation, Mean monthly flow, Precipitation and aridity index

1. Introduction

The flow duration curve (FDC) is a simple and easy to use hydrologic tool that has provided valuable insight into hydrological nature of catchments. This study the second part of a preceding one, aims to make potential runoff estimations in the low flow section of the FDC. The first study by Leong and Yokoo (2017) disaggregated the FDC into three sections namely, high, middle and low flow sections based on the Yokoo and Sivapalan (2011) proposal. The difference between the two studies is the latter disaggregated the FDC into two part, high and low. A principal finding of the Yokoo and Sivapalan (2017) was that the FDC high flow part was controlled by precipitation and the middle flow parts could use mean monthly flow (MMF) for runoff estimation. The authors suggested that for the low part of the FDC, evapotranspiration could be an important controlling factor. Using the information from this research, the Leong and Yokoo study used a calibrated curve number method to estimate high flows and for the middle flow part the results confirmed that the MMF can be used for runoff estimations. This study aims to bring light to the low flow section. This study uses perennial and ephemeral catchments because of the different nature of the FDC shapes.

2. Methodology

There are three distinctive methods used, first is the hydrograph separation, storage estimation and lastly a Tank model. The hydrograph separation method by Hino and Hasebe (1984) was first used to separate the runoff into two runoff components (fast and slow runoff). Secondly, the method by Chiba and Yokoo (2015) was used to estimate storage. This method improves a storage estimation method by Kobayashi and Yokoo (2013). The Kobayashi and Yokoo (2013) storage estimation method had combined the nonlinear storage estimation method by Kirchner (2009) and the Hino and Hasebe (1984) hydrograph separation method. Lastly a process based Tank model by Yokoo *et al*., (2017) similar to the Suguwara (1995) Tank model but with few applied differences was used to make runoff estimations.

3. Results and Concluding Discussion

By using these methods, the results show the perennial catchment making proper runoff estimations in the low flow sections and is comparable to the MMF, meaning that because perennial catchments have continuous runoff either approach is suitable. However, for the ephemeral catchment, the runoff estimation did not have a desired outcome. Therefore, for this study the authors isolated the ephemeral catchments runoff estimations. Focusing on the short falls of the Yokoo *et al*., (2017) Tank model, where it does not include evapotranspiration which can be an important factor especially in dry ephemeral catchment regions. Two factors that stand out in ephemeral catchments annual data is the lack of precipitation and the high evapotranspiration. Based on this, two indices are calculated, the aridity and precipitation indices. By performing regression analysis of the two indices for each catchment at selected runoff percentiles, a generalized regression equation was obtained for each selected percentile. Inputting the indices into the generalized

regression equation will give the runoff estimates based on the aridity and precipitation. The results show the precipitation index making sound runoff estimations more than the aridity index, resulting in the conclusion that for the studied ephemeral catchments usual climate is the import controlling factor

References

1) Chiba takahiko, Yokoo yoshiyuki : Revision estimation method of watershed-scale rainwater storage and its effect, Journal of JSCE B1 (Hydraulic Engineering), 71(4), 289-294, 2015.
2) Hino mikio, Hasebe masahiko : Identification and prediction of nonlinear hydrologic systems by the filter-separation autoregressive (AR) method: Extension to hourly hydrologic data, Journal of Hydrology, 68(1), 181-210, 1984.
3) Kirchner James : Catchments as simple dynamical systems: Catchment characterization, rainfall-runoff modeling, and doing hydrology backward, Water Resources Research, 45(2), 2009.
4) Leong Chris, Yokoo yoshiyuki : Estimating flow duration curve in the humid tropics: a disaggregation approach in Hawaiian watersheds, Hydrological Research Letters, 11(4), 175-180, 2017.
5) Suguwara M : Tank Model. In Computer Models of Watershed Hydrology, Singh VJ (ed), Water Resources Publications, pp.165-214, 1995.
6) Syuhei kobayashi, Yokoo yoshiyuki : Estimating watershed-scale storage changes from hourly discharge data in mountainous humid watersheds: toward a new way of dominant process modeling, Hydrological Research Letters, 7(4), 97-103, 2013.
7) Yokoo yoshiyuki, Chiba takahiko, Shikano yudai, Leong Chris : Identifying dominant runoff mechanisms and their lumped modeling: a data-based modeling approach, Hydrological Research Letters, 11(2), 128-133, 2017.
8) Yokoo yoshiyuki, Murugesu Sivapalan : Identifying dominant runoff mechanisms and their lumped modeling:a data-based modeling approach, Hydrology and Earth System Sciences, 15(9), 2805-2819, 2011.

Characteristics and seasonal flactuations of invertebrate species eDNA concentration in forest, agriculture, and urban river

○Noriko Uchida[1*], So Kazama[1] , Kubota Kengo[1] , Shunsuke Aita[1]

[1]Graduate School of Engineering, Tohoku University, Sendai 980-8579, Japan

*E-mail: noriko.uchida.s8@tohoku.ac.jp

Abstract

The concentration of total DNA and invertebrate species DNA were quantified from the samples that were collected from rivers that had different land use property (i. e. forest, agriculture, urban). The sampling had been conducted from March of 2017 to May 2018, in Natori river basin, Miyagi Prefecture, Japan. From the observation results, total DNA concentration in forested rivers showed significantly low value comparing with agricultural and urban rivers. Concentration of invertebrate species DNA showed maximum value on December for all rivers. That may be resulted from decreasing of dilution effect because of small river discharge and increasing of riparian animal's population. Specific discharge of invertebrate species DNA of urban river was the largest in 3 land used rivers. This study clarified that different terrestrial land use influenced the amount of eDNA load to basin. Furthermore, the dynamics of eDNA concentration were varied by season and land use. Thus, we should consider land use of inflowing river to basin and sampling season when we try to evaluate basin ecosystem by eDNA methods.

Keywords: Invertebrate species, Environmental DNA, Land use, qPCR, Watershed ecosystem

1. Introduction

Exploitations and climate changes have resulted in habitat deterioration of wild animals. To conserve wild life, it is required to understand distribution of keystone or rare species[1)]. Additionally, in streams, understanding assemblage component (population size or faunal composition) of stream invertebrate is fruitful to assess biological diversity [2)]. Monitoring of aquatic wild life has been practically carried out by visual observation, and fishing in several manners. However, in terms of monitoring in broader scale or longer term, these conventional methods are time- and effort- consuming, require special skills to identify species and involve observer errors or bias.

Environmental DNA (eDNA) is remarked as to be a breakthrough method for biological monitoring. eDNA is originated by organism's bodies and metabolites, and exists in environmental samples such as water, soil, and air [3)]. By detecting species specific genome sequences in a given environmental samples using molecular biological methods (e.g. PCR, Next Generation Sequencing) presence / absence of a target species can be determined with high accuracy. Remarkably, it is already verified that using eDNA method is more efficient to know species composition or existence than conventional monitoring methods by Minamoto *et al.* [4)]

Taking environmental sample less sampling effort and time than animal trap or capturing or visual detection, and this advantage will enhance broader and longer biological monitoring. In fact, some reports surveyed animal habitat distribution [5)] and found biological construction with high accuracy [6)]. To make eDNA method more practically usable, fundamental knowledge such as eDNA maintain time or flow-down distance [7, 8)] has been accumulated. Specifically, water quality such as water temperature[9)], turbidity and pH[10)] have correlation with eDNA preservation and degradation time. Consequently, eDNA concentration should be characterized by terrestrial land use type because water quality indices are influenced by land uses.

In this study, we aim to find relationship between terrestrial land use and eDNA concentration, especially in aquatic invertebrate species. To meet this target, we focused on small rivers with 3 different type of land use and measured total DNA concentration and invertebrate species DNA concentration for 1 year.

2. Methodologies

We sampled eDNA at 2 forest rivers, 2 agricultural rivers, and 2 urban rivers which are included Natori River basin in northeast Japan (Fig. 1 and Table. 1). The samplings were monthly conducted at no-rain day, through March 2017 to May 2018 except 22th July 2017 to 26th August 2017 because of one month-continuous rain. Invertebrate species are targeted as eDNA detection because invertebrate species exist even though river environment is totally different (i.e. forest, agriculture, and urban river).

We collected 4.5L of water from surface to sterilized plastic container by gloved hands. The sampled stream water was transported to the laboratory and kept in the cold condition following previous reports [11)]. Subsequently, filtering process was conducted immediately in the same day. The water samples were then filtered by the vacuum filtration with 47mm diameter glass-fiber filters (normal pore size, 0.7μm; Whatman) and GF/D filter (Whatman, diameter 90mm, normal pore size 0.27μm) as a pre-filter. These samples were wrapped in commercial aluminum foil and zipped plastic bag and stored in -20ºC until DNA extraction. DNA was extracted from filters by combination of Phenol-Chloroform-Isoamyl alcohol method and ethanol precipitation to

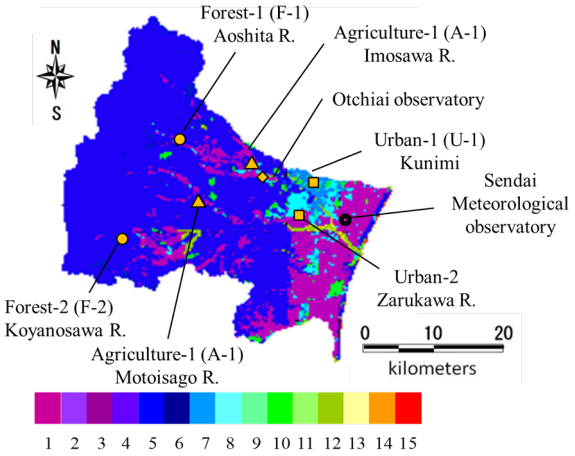

Fig. 1. Field observation points on land use map in Natori River basin, Miyagi Prefecture. Circles represent forest sites, triangles represent agricultural sites, and squares represent urban sites. Each sampling sites is written with land use type, display name, and river or place name. The black rhomboid represents Ochiai river observatory and the double circle represent Sendai meteorological observatory. Land use types are classified by 15 color: Agriculture (1~4), Forest (5, 6), Urban (7 ~10), and others.

enrichment DNA concentration. To remove PCR inhibitor, DNA samples were purified using PCR Inhibitor Removal Kit (Zymo Research). Finally, concentration of the total extracted DNA was measured using Qubit ®3.0 (Thermo Fisher Scientific Inc). In this report, we called this measured DNA concentration as "total DNA" because it contained not only invertebrate species but also other organisms such as microbe vertebrate species, and algae DNA.

Mitochondrial DNA (mtDNA) was employed as the target genetic marker because copy number of mtDNA in stream water could be larger than that of nuclear DNA per cell so that detection rate is expected to be higher. We used a universal primer targeting mtDNA cytochrome *c* oxidase subunit 1 (CO1), which is divergent among all animal phyla [12]. We amplified the target DNA fragments of the samples using the PCR primers designed to amplify invertebrate-specific loci from the CO1 region. A 658 bp fragment from CO1 region was amplified with the following primer pair; LCO1490 (5'-GGT CAA CAA ATC ATA AAG ATA TTG G-3') and HCO2198 (5'-TAA ACT TCA GGG TGA CCA AAA AAT CA-3')[8]. We initially validated the primers on tissue samples for a larva of the caddis fly species (*Stenopsyche marmorata*) which was also sampled in the study catchment.

The qPCR was performed using SYBR®Premix Ex Taq (TaKaRa) and LightCycler®2.0 (Roche). The condition of qPCR consists of an initial incubation at 95ºC for 20 seconds followed by 40 cycles of 95ºC for 5 seconds, 53ºC for 30 seconds, 72ºC for 1 minute. Fragment size of amplicons was verified with agarose gels electrophoresis and qPCR products were purified using a MicroSpin S-400 Columns (GE Life Science). Further, we set a template DNA which was extracted from tissue of *S. marmotara* and amplified it using the above primer pair. Then we created a dilution series from the PCR products of as standard DNA thorough $1.0x10^1$ to $1.0x10^7$ (copies/µl) and conducted qPCR for environmental samples.

At the same time of water sampling, we measured average flow velocity (AEM1-D, electromagnetic flow velocimeter) and average water depth in one cross section of each sampling site and calculated river discharges.

3. Result

3.1. Comparing eDNA concentration in each land use

Over annual monitoring results of total DNA concentration an invertebrate species DNA concentration in forest, agriculture, and urban rivers were showed in **Fig. 2**. Forest rivers (F-1, F-2) total DNA median value were about 0.15~ 0.49 times of one of agriculture river (A-1) and both urban river (U-1, U-2). By Mann-Whitney *U* test, median of total DNA in F-1 and F-2 were significantly different from A-1, U-1, and U-2. On the other hand, agriculture river A-2 total DNA was higher than both of forest rivers but was not significantly different statistically. This may be related that land use of A-2 watershed is 40% of agriculture area and 60 of forest area besides A-1 had 80% of agriculture area. A-2 might have agriculture and forest characteristics and did not show clear agricultural pattern. Invertebrate DNA (inv. DNA) concentration in F-1 and U-1, F-1 and U-1 showed significant differences. The inv. DNA median of F-1 was 0.43 times; F-2 was 0.58 times of U-1.

Table 1. Field information

River type	River/place name	Display name	Location (N. Latitude, E. Longitude)	Elevation (m)	Catchment Area (km^2)
Forest River	Aoshita R.	F-1	38.34107, 140.65442	360.0	4.813
	Koyanosawa R.	F-2	38.21021, 140.54447	361.4	27.750
Agriculture River	Imosawa R.	A-1	38.30602, 140.76431	121.6	17.625
	Motoisago R.	A-2	38.24180, 140.63376	209.0	12.563
Urban River	Kunimi	U-1	38.26907, 140.84255	37.9	0.125
	Zarukawa R.	U-2	38.22217, 140.84882	30.9	1.063

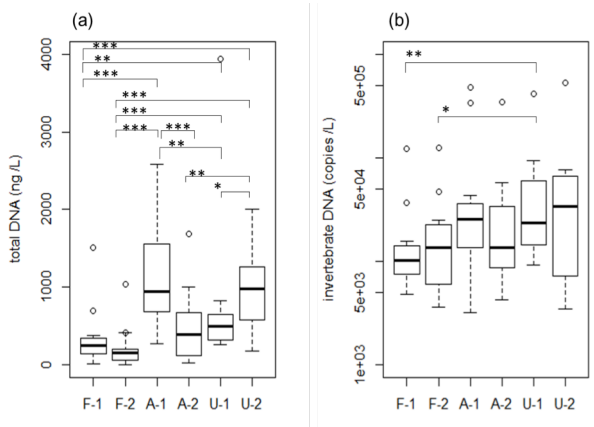

Fig. 2. Concentration of total DNA (a) and invertebrate DNA (b) in each river. Forest rivers showed significant lower concentration compared with other land use rivers (***: p<0.01, **: p<0.05, *: p<0.1). Horizontal bars in box plots represent median (50 percentile), and upper ends of boxes represent 75 percentiles, and lower ends of boxes represent 25 percentiles. Open circles represent outlier values that are 1.5 times larger than maximum datum and 1.5 times smaller than minimum datum.

3.2. Seasonal fluctuation of invertebrate DNA

Inv. DNA concentration in every river demonstrated maximum value at December (1.0 x10^5 copies/L order) even though the land use types were different. Generally, inv. DNA had increased through October to December, and had gradually decreased after January to May. This fluctuation trend was observed commonly in all survey rivers. According to fluctuation of March to July in 2017, inv. DNA will recover after May and decrease towards summer season.

4. Conclusion

This study monitored that eDNA concentration of invertebrate species in different land use types for over a year. It is usual that survey area is located or includes various kind of terrestrial land use types but land use impact to eDNA detection had not been remarked. The monitoring result in this report demonstrated that terrestrial condition characterized eDNA concentration, especially from river water from urban area contained high eDNA concentration. Secondary, seasonal fluctuations pattern of eDNA were common among forest, agriculture, and urban rivers. From this result, winter season may be suitable to get high eDNA concentration in case of invertebrate species. To clearly interpret biological information from eDNA survey, further understanding of eDNA dynamics in the field should be required.

Acknowledgements

This research was partly supported by the Ministry of Education, Science, Sports and Culture through a Grant-in-Aid for Scientific Research (grant nos. 25241024, Yasuhiro Takemon, 26630247, Kozo Watanabe, 26820196, Kei Nukazawa) and Japan society for the Promotion of Science (JSPS) Research Fellowship (grant no. 256493). We express deep appreciating for all of supports.

References

1) Hurlbert, A. H., Jetz W.: Species richness, hotspots, and the scale dependence of range maps in ecology and conservation. PNAS. 104 (33): 13384-13389. 2007
2) Heino, J.: Biodiversity of aquatic insects: spatial gradients and environmental correlates of assemblage-

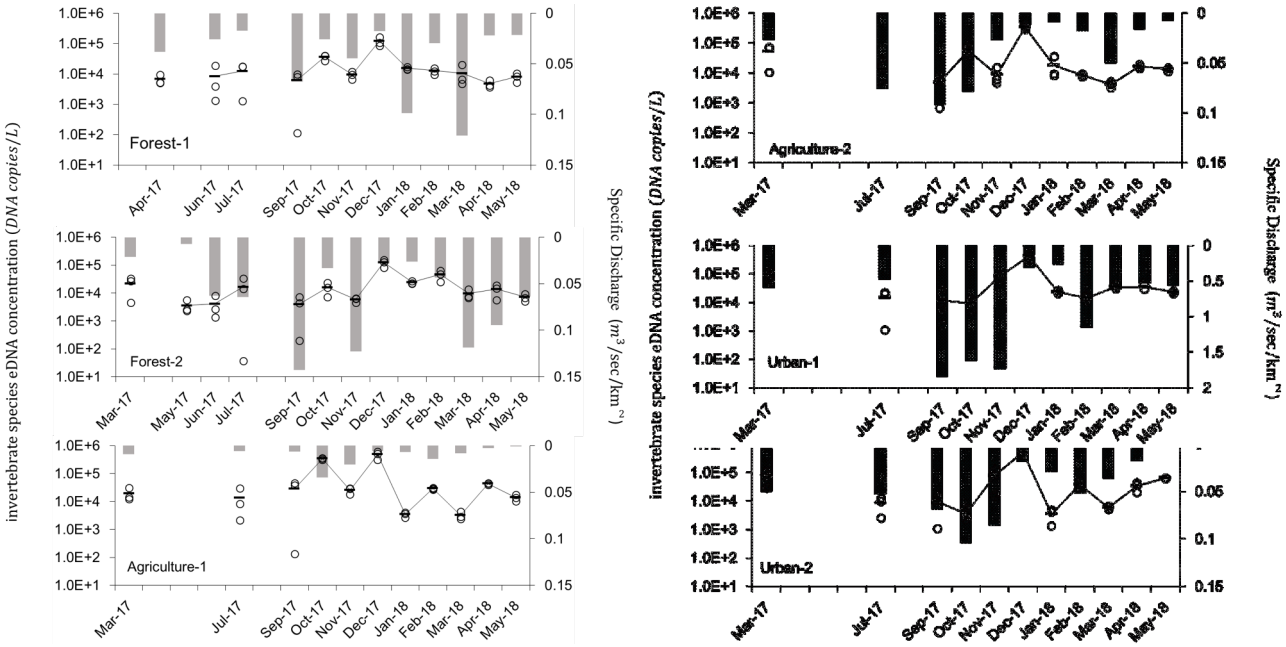

Fig. 3. Seasonal change of invertebrate species eDNA concentration (copies/L) at each sites (March 2017 to May 2018). Open circles represent measured data (n=3), and small black rectangles represent average value of them in left axis. Gray bar represents observed specific discharge (m/sec/km^2) that discharges are divided by catchment areas in right axis.

level measures at large scales. Freshwater Reviews. 2: 1-29, 2008

3) Rees, H. C., Maddison, B. C., Middleditch, D. J., Patmore, J. R. M., Gough K. C.: The detection of aquatic animal species using environmental DNA-a review of eDNA as a survey tool in ecology, Journal of Applied Ecology. 51: 1450-1459, 2014
4) Minamoto, T., Yamanaka, H., Takahara, T., Honjo, M. N., Kawabata, Z.: Surveillance of fish species composition using environmental DNA, Limnology, 13 (2): 193-197. 2012
5) Port J.A., O'Donnell J.L., Romero‐MaraccciniO. C., Leary P. R., Litvin S. Y., Nickols K. J., Yamahara K. M., Kelly R.P.: Assessing vertebrate biodiversity in a kelp forest ecosystem using environmental DNA. Molecular Ecology. 25 (2): 527-541. 2015
6) Miya M., Sato Y., Fukunaga T., Sado T., Poulsen J. Y., Sato K., Minamoto T., Yamamoto S., Yamanaka H., Araki H., Kondoh M., Iwasaki W.: MiFish, a set of universal PCR primers for metabarcoding environmental DNA from fishes: detection of more than 230 subtropical marine species. Royal Society Open Science. 2 (7): 150088. 2015
7) Nukazawa K., Hamasuna Y., Suzuki Y.: Simulating the Advection and Degradation of the Environmental DNA of Common Carp along a River. Environmental Science & Technology. DOI: 10.1021. 2018
8) Tsuji S., Uchio M., Sakurai S., Minamoto T., Yamanaka H.: Water Temperature-Dependent Degradation of Environmental DNA and Its Relation to Bacterial Abundance. PLOS ONE. 12 (4): e0176608, 2017
9) Strickler, K. M., FremierA. K., Goldberg C. S.: Quantifying Effects of UV-B, Temperature, and PH on EDNA Degradation in Aquatic Microcosms. Biological Conservation. 183 : 85‐92, 2015
10) Fukumoto S., Ushimaru A., Minamoto T.: A basin‐scale application of environmental DNA assessment for rare endemic species and closely related exotic species in rivers: a case study of giant salamanders in Japan. British Ecological Society. 52 (2): 358-365. 2015.
11) Folmer, O., Black, M., Hoeh, W., Lutz, R., Vrijenhoek, R.: DNA primers for amplification of mitochondrial cytochrome c oxidase subunit 1 from diverse metazoan invertebrates, Molecular Marine Biology and Biotechnology. 3: 294-299. 1994

Forest fire severity estimation for the 2017 Kamaishi forest fire

○Grace Puyang Emang[1*], Yoshiya Touge [1], So Kazama[1]
[1]Graduate School of Engineering, Tohoku University, Sendai 980-8579, Japan

*E-mail: grace.puyang.emang.r2@dc.tohoku.ac.jp

Abstract
The 2017 Kamaishi forest fire occurred for 14 days from 8th till 22nd May 2017 and the total burnt area was 413 ha which is greater than the total burnt area for the whole Japan in 2016. This burnt area was estimated based on burnt and unburned area. However, in the burnt area itself, there were differences of fire severity observed. The objective of this research was to estimate the fire severity in this burnt area using Normalized Difference Vegetation Index (NDVI) and post fire observations of stem-bark char height, h_c and crown scorch height, h_s. The results shows that NDVI and h_s has stronger relationship than h_c suggesting both are sensitive towards fire severity on leaves while h_c is related to fire severity on stem-bark.

Keywords: Fire severity, NDVI, Post-fire observations, Kamaishi

1. Introduction
Forest fire occurs annually in developed and developing countries. Between 2010 till 2014, forest and field fire are reported annually with an average of 1635 cases and an average annual loss at approximately 576 million yen (Statistic Bureau Japan, 2018). Forest fire causes not only economic loss but also losses of animals' habitat and food resources.

Ecosystem of the forest is also affected based on fire severity as increased in sedimentation yield and concentration was observed in burned watershed in Oldman River Basin, Alberta (Silins *et al.*, 2009) and in Colorado Front Range, higher sedimentation production rate was found in high severity forest fire than moderate and low severity forest fire (Benavides-Solorio and MacDonald, 2005). Most research focused on estimation of burnt area and hotspots using remote sensing data such as NDVI (Kasischke and French, 1995) but in burnt area, various degree of fire severity exist and can be seen from loss of vegetation.

Fire severity is used to measure the loss or change of the above and below ground organic matter (Keeley, 2009) such as char height and scorch crown height. This research will use NDVI and char height on stem- bark, h_c and height of scorch on crown, h_s to estimate the fire severity in the 2017 Kamaishi Forest Fire.

2. Study area
In the last 42 years, Kamaishi had three major fire incidents with burnt area of 200 ha, 392 ha and 130 ha in Kamaishi Hamacho, Kamaishi Higashimae-cho and Kamaishi Toni-cho respectively and recently, in Kamaishi Heita with an estimated burnt area of 413 ha (Touge *et al.*, 2018), the study area for this research as shown in Fig. 1. This indicates that Kamaishi is prone to forest fire and burnt areas were wide.

Fig.1 Historical large scale forest fire occurring in Kamaishi

3. Methodology
3.1 Remote sensing data
NDVI which were cloud free from Landsat 8 were used in this research for the period of 2017. These images were then processed to create a two weeks average in an image and subsequently, $NDVI_{diff}$ were computed by subtracting the post-fire image from the pre-fire image.

3.2 Post-fire observation: stem-bark char height, h_c and scorch crown height, h_s
Two types of post-fire observations were made, namely stem-back char height, h_c and scorch crown height, h_s. For every 30 m, a tree was observed of its fire severity by measuring the char height on its stem bark, h_c and the scorch height on its crown, h_s. The observation were made in the estimated burnt area and in total 650 points of h_c and h_s respectively were collected.

4. Results and discussion

To estimate the fire severity of the 2017 Kamaishi forest fire, corresponding $NDVI_{diff}$ with 650 points of h_c and h_s were extracted and plotted in dots distribution maps as shown in Fig. 2.

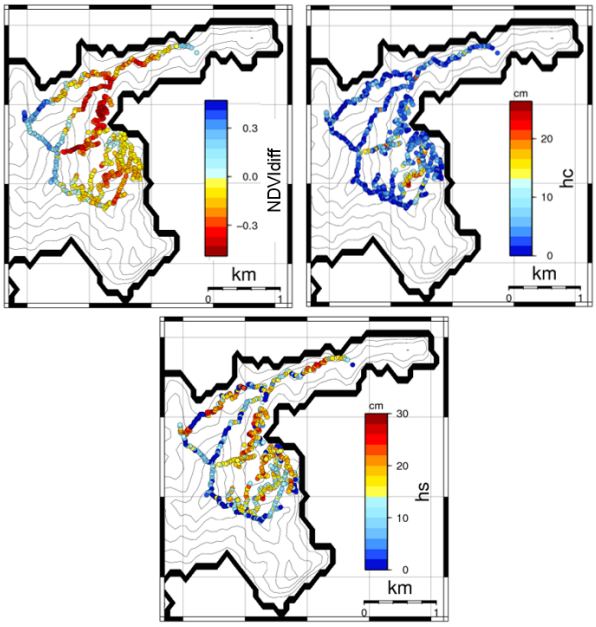

Fig. 2 Distribution of $NDVI_{diff}$, h_c and h_s

The results indicate $NDVI_{diff}$ and h_s can show more variation of fire severity than h_c. However, $NDVI_{diff}$ has a slight stronger relationship with h_c (R = 0.29) than h_s (R = 0.27) as shown in Fig. 3a and 3b.

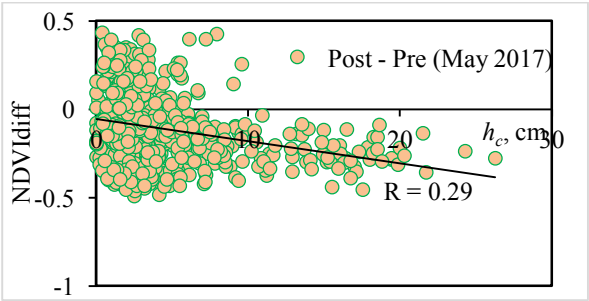

Fig. 3a

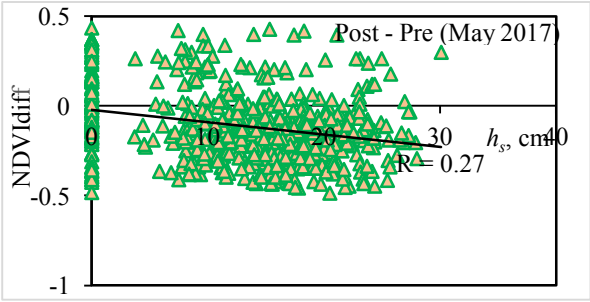

Fig. 3(b)

Fig. 3a and 3b Correlation between $NDVI_{diff}$, h_c and h_s respectively

This suggests using direct value of h_c and h_s would not be a good indicator for fire severity as it may represent only the height of fire but by taking into account the h_c and h_s in relation to its total stem-bark height and crown height respectively, it could be a better representative of fire severity.

5. Conclusions

All three observation indicates variation of fire severity with $NDVI_{diff}$ and h_s exhibiting the most variations. Moreover, results indicate using rate of h_c and h_s based on its overall stem-bark height and crown height could offer a better estimation of fire severity. These results open new prospects for estimating the fire severity in the 2017 Kamaishi forest fire more definite.

6. Acknowledgements

We wish to thank Nohmura Foundation for Membrane Structure's Technology for their generous financial assistance.

References

1) Benavides-Solorio JDD, MacDonald LH: Measurement and prediction of post-fire erosion at the hillslope scale, Colorado Front Range. International Journal of Wildland Fire 14(4), 457–474, 2005.
2) Kasischke ES, French NHF: Locating and estimating the areal extent of wildfires in alaskan boreal forests using multiple-season AVHRR NDVI composite data. Remote Sensing of Environment 51(2), 263–275, 1995.
3) Keeley JE: Fire intensity, fire severity and burn severity: A brief review and suggested usage. International Journal of Wildland Fire 18(1), 116–126, 2009.
4) Silins U, Stone M, Emelko MB, Bladon KD: Sediment production following severe wildfire and post-fire salvage logging in the Rocky Mountain headwaters of the Oldman River Basin, Alberta. Catena 79(3), 189–197, 2009.
5) Statistic Bureau Japan: Japan Statistical Yearbook 2018
6) Touge Y, Emang GP, Kazama S, Takahashi Y, Sasaki K: Introduction of the Tohoku Forest Fires on May 2017; case in Kamaishi city of Iwate Prefecture and Kurihara city of Miyagi Prefecture, 自然災害科学 J. JSNDS 36(4), 361–370, 2018

Removal of Cesium from Simulated radioactive water by a Countcurrent Two-stage Adsorption-Microfiltration Process

○Zhang Guanghui, Xu Xiaotian, Gu Ping*, Xu Yao
Department of Environmental Engineering, School of Environmental Science and Engineering, Tianjin University, Tianjin 300072, China.
*E-mail: guping@tju.edu.cn

Abstract

A hybrid process of adsorption, coagulation and ultrafiltration was developed to remove cesium from the simulated radioactive water, which could effectively alleviate membrane fouling without seriously deteriorating decontamination performance. In the meanwhile, a simple calculation method was established based on the Freundlich adsorption isotherm, and it could accurately predict the cesium concentration in the effluent. When the dosages of cupric ferrocyanide were 0.025 g/L and 0.04 g/L, respectively, ignoring the influence of sludge discharge, the relative errors between the experimental and calculation values were no more than 10%. As a result, the calculation method could be used to determine the consumption of cupric ferrocyanide at a given requirement for the effluent.

Keywords: Copper ferrocyanide, Cesium, Carrying-adsorption, ultrafiltration, radioactive water

1. Introduction

Fukushima nuclear leakage accident in 2011 caused the worldwide extensive research on the radioactive pollutions, among which the released nuclides including ^{137}Cs, ^{134}Cs, ^{90}Sr and so on, has drawn considerable attention due to their long half-life, high biological toxicity and strong mobility in the receiving water body.

Copper ferrocyanide (CuFC) is a highly efficient and environmentally friendly adsorbent, and it could remove the radioactive cesium ions from water or wastewater. When the radioactive ^{137}Cs and non-radioactive ^{133}Cs simultaneously existed in the water or wastewater, after adsorption and solid-liquid separation, the decontamination factor for cesium based on the radioactivity concentration was equal to that based on the mass concentration. This result explicitly answered that ^{137}Cs and ^{133}Cs own the same decontamination characteristics.

The effects of the initial concentration of cesium, CuFC dosage and coexisting ions on the adsorption by CuFC was evaluated by the means of Freundlich adsorption isotherm and response surface methodology (RSM). A novel index called volumetric distribution coefficient (Kvd) was proposed to comprehensively evaluate the adsorption process. Based on the calculation results, it could be found that there existing an optimum initial cesium concentration, at which the highest decontamination factor could be obtained at a certain dosage of CuFC. In the application for the engineering, artificially dosing ^{133}Cs to increase cesium concentration to a suitable level could significantly improve ^{137}Cs removal. This method was named as carrying-adsorption. When the dosage of CuFC was 0.08 g/L and the initial cesium concentration was 2500 μg/L, respectively, the decontamination factor could achieve 1.65×10^5.

A hybrid process of adsorption, coagulation and ultrafiltration was developed to remove the cesium ions from the simulated radioactive water and it could effectively alleviate the fouling rates of the membrane without seriously deteriorating decontamination performance. In the meanwhile, a simple calculation method was established based on the Freundlich adsorption isotherm, which could accurately predict the concentrations of the cesium in the effluent. When the dosages of CuFC were 0.025 g/L and 0.04 g/L, respectively, ignoring the influence of sludge discharge, the relative errors between the experimental and calculation values were no more than 10 percent. That is to say, if the cesium level in the effluent is determined, the dosage of CuFC could be predicted very quickly. As a result, the calculation method could be used to determine the consumption of cupric ferrocyanide at a given level in the treated water.

Considering the upgrade of WTP and emergency water supply in the radioactive nuclear accidents. We tried the test that the ultrafiltration was substituted by the sand filtration, and the hybrid process of adsorption, coagulation and filtration was also explored for the removal of the cesium from drinking water. The process could also highly and safely remove the cesium ions in the simulated radioactive water, and it could be compatible with the existing facilities in the water treatment plants. The development of the processes would provide the technical supports for large-scale applications to cope with the radioactive cesium pollution caused by the nuclear leakage or accident.

2. Acknowledgements

The authors would like to thank the Ministry of Science and Technology, China, for the funding support under the Major Science and Technology Program for Water Pollution Control and Treatment (2015ZX07406006) and National Natural Science Foundation of China for the funding support (51238006).

Biohydrogen Production (BHP) and Biomethane Production (BMP) Potential from Palm Oil Mill Effluent (POME)

○Khairunnisa ABDUL HALIM[1]*, Muhammad Faiezul PAUZI[1] & Ee Ling YONG[1]
[1]Department of Environmental Engineering, School of Civil Engineering, Faculty of Engineering, University Teknologi Malaysia, 81310 UTM Johor Bharu, Johor Darul Takzim, Malaysia.
*E-mail: khairunnisaabdulhalim17@gmail.com

Abstract
Biogas production from the POME treatment system has been extensively studied. High organic content in raw POME is a good source for biogas production via anaerobic digestion. Nonetheless, 80% of the palm oil millers still persist with ponding treatment system due to lower operational and maintenance cost. Owing to the large treatment areas and long retention time, high-rate anaerobic digestion treatment system was developed. However, unstable and low yield of biogas production the treatment paradigm has shifted to multi-stage anaerobic digester. Presently, most studies focused on the biogas production performance but evaluation on the biogas production potential under controlled temperature is still lacking. Therefore, this study performs a batch scale thermophilic-mesophilic anaerobic digestion evaluating biohydrogen and biomethane production of POME at different organic loading rate (7.5 – 44 g COD/L). The potentials are termed as BHP and BMP, respectively. Highest hydrogen production in BMP test was attained at 44 g COD/L, i.e. 112.1 mL-H_2, after 5 days. Meanwhile, methane production (540.7 mL-CH_4) was spotted also peaked at 44 g COD/L within 45 operational days. Both BHP and BMP revealed that biogas production using a multi-stage anaerobic treatment system provide a better yield.

Keywords: biohydrogen, biomethane, production potential, palm oil mill effluent.

1. Introduction
Palm oil industry is one of the larger agricultural industries in Malaysia where about 20 million tonne of crude palm oil (CPO) was produced in 2017. However, along the clarification and extraction of the CPO massive production of byproduct known as palm oil mill effluent (POME) was generated. Roughly 3.35 million tonnes of oily-thick-sluggish POME was produced at every million tonne of palm oil processed. Proper waste management needs to be implemented to avoid the pollution of water bodies that can severely affect the aquatic biodiversity.

POME has preference of high organic contaminants concentrations and biodegradable, best to be treated biologically through anaerobic process. Conventional ponding treatment system has been employed for decades due to low cost and manpower needed. Although anaerobic treatment has been implemented to treat fresh POME, this process alone is unable to achieve the standard discharged limit outlined by the Department of Environment (DOE), Malaysia. Furthermore, the inefficient anaerobic activities will impede the production of biogas leading to unstable yield. Consequently, millers chose to flare the biogas (*e.g: methane*) to the atmosphere contributing to global warming.

Currently, methane gas generated from a single-staged anaerobic digestion system ranged between 0.012 to 0.9 L-CH_4/g-COD. The unstable performance and low yield in biogas production made the millers to persevere with ponding treatment system. The limitations of the single-stage anaerobic process altered the pattern of ideas of the researchers by introducing principle of multi-stage anaerobic digestion in order to enhance the biogas. Nevertheless, the studies on the hydrogen and methane production potential from POME through two-stage anaerobic digestion under controlled temperature are still limited.

Thus, this study monitors and evaluates the production of hydrogen and methane from a batch sequence of thermophilic-mesophilic anaerobic digestion.

2. Materials and Methods

2.1 Seed sludge preparation
Sludge was collected from closed anaerobic digester from Palm Oil Mill, Felda Penggeli, Wilayah Tenggara, Johor Malaysia. The sludge has the following characteristics: pH=7.46; total suspended solids (TSS)=59.5 g/L; and volatile suspended solids (VSS)=11 g/L. Seed sludge was heated at 95°C for 1 hour to inhibit the methanogens and enrich the hydrogen producing bacteria, prior to the BHP test. Meanwhile, for BMP test, the anaerobic sludge without heat treatment was first degassed by incubating at 37°C for 5 days before used as an inoculum to the test.

2.2 Feedstock
The fresh POME was collected from same palm oil mill, characterized and stored at 4°C prior to any test to avoid biodegradation to the sample. The fresh POME has following characteristics: pH=4.89; TSS=19.6-22.0 g/L; VSS=2.0-2.4 g/L; and COD=22-44 g/L.

2.3 Biohydrogen Production (BHP) and Biomethane Production (BMP) Potential
The experiments were carried out in batch conditions, using a 550-mL Schott bottles. The glass bottle was initially added with 50-mL of inoculum and 150-mL of POME, without any nutrient supplement. These experiments were carried out at four different concentrations of 7.5, 15 and 44 g/L. The reaction flasks were purged with nitrogen; tighten and incubate at 55°C for 5 days HRT. The reaction flask was manually swirled every day and maintained at the static

condition at desired conditions. The hydrogen production was monitored daily.

After 5 days, the bottles were opened, and another 150-mL of anaerobic sludge without heat treated were added into the reaction flasks. Reaction flasks were purged with nitrogen again before the closed flasks were held at 37°C and incubated for 45 days, for methane evaluation. The flasks were manually swirled every day at first 5-7 days; and 2-3 days once for the entire experimental period; and then later maintained static at desired condition.

The hydrogen and methane gases production were evaluated by applying wet displacement method in which 5% NaOH displaced was considered as volume of hydrogen and methane generated, respectively.

3. Results and Discussion

3.1 Biohydrogen Production (BHP) Potential

Figure 1 illustrates the cumulative hydrogen production from POME at different loading rate. Throughout the experimental period, 112.1 mL-H_2 was obtained at 44 g-COD/L loading rate; 89.5 mL-H_2 at 15 g-COD/L and 78.9 g-COD/L at 7.5 g-COD/L.

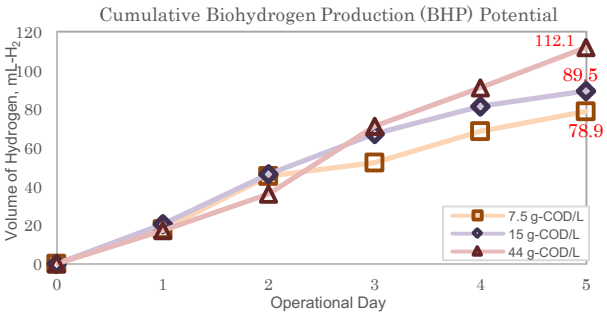

Figure 1 Cumulative biohydrogen production of POME at different loading rate in a batch experiment.

It shows that the biogas production is increase with loading rate. However, at low loading rate as 7.5 and 15 g-COD/L stiffen increment trend was spotted from day 0 to 2 while at 44 g-COD/L this trend was seen from day 0 to 3. From this, it can be concluded that fast degradation occurs at low loading rates.

3.2 Biomethane Production (BMP) Potential

Figure 2 demonstrates the cumulative methane production from POME at different loading rate. Methane gas production was cumulated about 540.7 mL-CH_4 within 5 to 50 of operational days at 44 g-COD/L; 212.2 mL-CH_4 at 7.5 g-COD/L and 185.4 mL-CH_4 at 15 g-COD/L. These trends were predictable and support the logic that high volume of methane gas will be produced at high loading rate. Nevertheless, at the end of operating period of day 46 to 50, slight increment trend was spotted at 7.5 g-COD/L indicates that substrate degradation still occurs although the production is unstable.

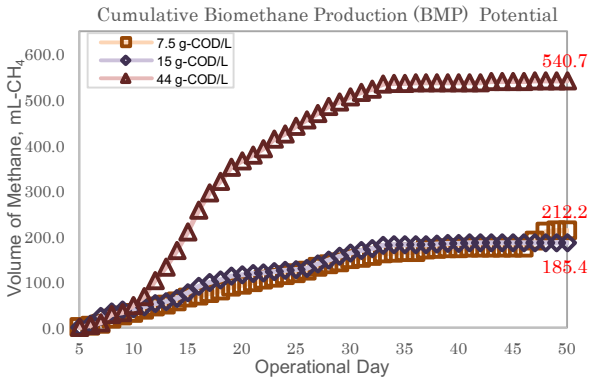

Figure 2 Cumulative biomethane production of POME at different loading rate in a batch experiment.

Each concentration displays sudden increment before slowly reach to the steady state at the end of the experimental time. At 7.5 g-COD/L and 15 g-COD/L, maximum daily methane production is at day 8 and 7, respectively before the production started to decrease while at 44 g-COD/L was at day 16. This supports the theory that substrate fermentation to generate methane requires about 15 days.

4. Conclusions

- Throughout the 5 days of BHP test, 112.1 mL-H_2 was observed at 44 g-COD/L loading rate; 89.5 mL-H_2 at 15 g-COD/L and 78.9 g-COD/L at 7.5 g-COD/L.
- Approximately 540.7 mL-CH_4 of methane gas production was attained within 45 operational days of BMP test at 44 g-COD/L; 212.2 mL-CH_4 at 7.5 g-COD/L and 185.4 mL-CH_4 at 15 g-COD/L.
- Replication of BHP and BMP test is needed to validate the findings - that will be carried out in the future work.

5. Acknowledgements

The authors would like to thank Japan International Cooperation Agency for the financial support through AUN/SEED-Net Collaborative Research (CR) grant. The cooperation from Palm Oil Mill, Felda Penggeli, Wilayah Tenggara, Johor also was acknowledged.

Methane Fermentation Treatment ofFish Processing Wastewater by A Self-agitated Anaerobic Baffled Reactor (SA-ABR)

○Eli Hendrik SANJAYA[1,2]* and Yu-You LI[1]
[1] Department of Civil and Environmental Engineering, Tohoku University, 6-6-06 Aoba, Aramaki, Aoba-ku, Sendai, Miyagi, 980-8579, Japan.
[2] Department of Chemistry, State University of Malang (Universitas Negeri Malang), Jl. Semarang No. 5, Malang, East Java, 65145, Indonesia.
*E-mail: eli.hendrik.fmipa@um.ac.id

Abstract
New design of self-agitated anaerobic baffled reactor (SA-ABR) was developed for methane fermentation treatment of fish processing wastewater (FPW). The performance, in term of gas production, organic removal, and inhibition of ammonia and salinity were investigated during 263 days by changing the hydraulic retention time (HRT) and organic loading rate (HRT) from 100 to 10 days and from 0.461 to 4.905 g/L/day. FPW which had TCOD, proteins, carbohydrates and lipids of 46.90, 6.83, 1,37 and 4.04 g/L, respectively, was used as substrate. Overall, the SA-ABR had very good performance. Gas production was increased by increasing the OLR and little bit fluctuating when the OLR 2.934 and 4.905 gCOD/L/day. Methane composition and pH were quite stable about 70-80% and 7.9 to 8.1, respectively. COD, proteins, and carbohydrates removal were stable about 82.48, 76.05, and 60.72%, respectively. However, these were gradually decreased when the OLR was about 2.706 gCOD/L/day. This pattern was also similar to TS, VS, SS, and VSS conversion removal. There were not significantly ammonia, VFA, and salinity inhibitions. However, it was needed advance studies of SA-ABR for optimization with the higher OLR or shorter HRT.

Keywords: methane fermentation, self-agitated anaerobic baffled reactor (SA-ABR), fish processing wastewater

1. Introduction
Generally, world capture fisheries and aqua culture production always grow up as reported by FAO (2016). On the other hand, the most utilization of fish it selves is for food. Hence, fish processing industry will be increased along with the human population growth.

Most of the fish processing industries are located along the coasts, and they have historically discharged their liquid waste directly into the sea or into the estuaries, with little or no treatment at all (Veiga et al., 1994). FPW is containing high levels of organic substances such as fat, soluble proteins, acetic acid, and carbohydrates, phosphorus, and nitrogen (Renata et al., 2015). Therefore, it will cause eutrophication.

Moreover, the biodegradable level of organic matter is usually high along with the potential for bioenergy production using an anaerobic process (Rollon et al., 2002). Panpong et al. (2014) and Rollon et al. (2002) have investigated the anaerobic digestion of fish processing wastewater by using UASB, it show COD removal 92% and 96.8%, respectively. The other study showed that the results of anaerobic digestion of fish wastewater processing of MBR were better than those of CSTR in the removal of total organic carbon with efficiencies from 97.9% to 98.6%. Nevertheless, salinity with increasing OLR aggravates fouling in MBR while leads to deterioration of sludge settle ability and effluent quality in CSTR (Jemli et al., 2015).

On the other hand, FPW has some limitations in anaerobic digestion such as high salinity, protein and oil content. These compounds can inhibit fermentation process by each own way.

Various of anaerobic bioreactor were developed for anaerobic digestion, such as upflow anaerobic sludge blanket (UASB), continuously stirred tank reactor (CSTR), anaerobic membrane bioreactor (AnMBR) and baffled reactor. The first anaerobic baffled reactor (ABR) was developed by Bachmann (1983). Then, many researchers have been working on baffled reactor and resulting several advantages. ABR has faster granulation process (HutnÏan, M. et al., 1999), higher microbial diversity in every chamber, good resilience to hydraulic and organic shock loads, prevent the sludge wash-out (Tanikawa, D., 2017 and Motteran et al., 2013), high resistance in environmental parameters such as pH and alkalinity (Rongrong et al., 2011; Zhong and Yang, 2012), simple design low cost for construction and operating (Tanikawa, D., 2017; Ji et al., 2009).

Since many superiorities of the ABR, our research group has developed new ABR called self-agitation anaerobic baffled reactor (SA-ABR). The SA-ABR has been investigated and the result show that SA-ABR is comparable in digestion performance to the completely stirred tank reactor (CSTR) (Kobayashi and Li, 2011). On the other hand, The SA-ABR also has been simulated in computational program to investigate the fluid dynamics of the reactor. The result show that the necessary periodical mixing is performed by the biogas generated during the process. It is applicable for the waste substrate fermentation treatment, especially for medium and small scale reactor (Qi et al., 2013). Therefore, the SA-ABR is compatible to be applied in fish processing industry since majority the fish industries in the world are small up to medium scale (Nations, 2007).

The aim of this research are to investigate the performance of SA-ABR in methane fermentation of FPW in term of COD conversion; biogas production; ammonia, VFA, and salinity inhibition.

2. Materials and Methods
2.1 Reactor design and operation

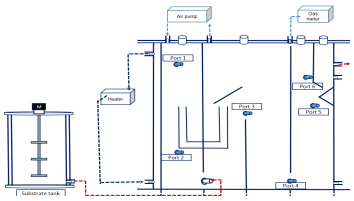

Fig. 1. SA-ABR Design

The reactor design is shown on Fig.1 with working volume 10.4 L (total volume 15.4 L), temperature 35±1°C, substrate tank with stirrer. The seed sludge was taken from anaerobic wastewater treatment SEN-EN Sendai City and granular sludge from slaughter house wastewater treatment.

2.2 Analysis

Analyses of pH, alkalinity, COD, protein, carbohydrate, lipid, NH_4^+, TS and TVS were performed according to the Japan standard methods (JSWA, 1997). VFA was determined by gas chromatography (Agilent-6890). Biogas composition was measured by a gas chromatograph (SHIMADZU GC-8A). In addition, Free ammonia (FA) was calculated according to Hansen et al (1998) formula.

3. Results and Discussion

3.1 Substrate profile

As substrate, fish processing wastewater had been characterized. pH, TAN and VFA were gradually increased during in substrate tank with the average 7.14, 4.719 g/L and 16.886 g/L, respectively. On the other hand, TS, VS, SS, VSS, COD, protein, carbohydrate, and lipid were vice versa. They would be decreased during in substrate tank, the averages were 8.21, 2.69, 1.59, 1.22, 46.90, 6.83, 1.37, and 4.04 g/L. These phenomena because some bacteria which were originally from FPW were working at substrate tank.

3.2 Performance and stability of fermentation process

Overall, the performance of SA-ABR in treatment of fish processing wastewater was very good. Gas production were increased by increasing the OLR and little bit fluctuating when the OLR 2.934 and 4.905 gCOD/L/day. Methane composition and pH were quite stable about 70-80% and 7.9 to 8.1, respectively. Based on the VFA concentration, it was indicated that ammonia inhibition at the beginning and at the middle of OLR 1.253 gCOD/L/day, the total VFA were more than 12.000 mg/L. However, it was very good when the HRT 15 to 10 days, the free ammonia (FA) less than 110mg/L. The SA-ABR had very good performance in resilience of ammonia inhibition. In the previous studies of chicken manure fermentation by Anaerobic Membrane Bioreactor (AMBR), the fermentation process had a good performance when TAN concentration lower than 5000mg/L (Niu et al., 2013).

Salinity were also investigated in term of the sodium concentration. Sodium content in substrates were not more than 3341 mg/L. On the other hand, there were sodium concentration accumulation in the reactor 317 to 2121 mg/L. However, these were far from the salinity inhibition since the previous research show that inhibition would be happened when the concentration more than 4000 mg/L (Aslan and Şekerdağ, 2016; Feijoo et al., 1995; Wang et al., 2017; Zhang et al., 2017).

In addition, the substrate conversions were evaluated in several form, these were COD, protein, carbohydrate, TS, VS, SS and VSS. The COD, protein, and carbohydrate removal were stable about 82.48, 76.05, and 60.72%, respectively. However, these were gradually decreased when the OLR reached 2.706 gCOD/L/day. Similar pattern upon TS, VS, SS, and VSS removal. The performance data can be more clearly when the OLR were increase as shown on Fig. 2.

4. Conclusions

The SA-ABR has shown satisfying performance in treated FPW. The COD conversion was 82.48% with methane content in gas production 70-80%. There was not significantly ammonia, VFA, and salinity inhibition. However, it was needed advance studies of SA-ABR for optimization with the higher OLR or shorter HRT.

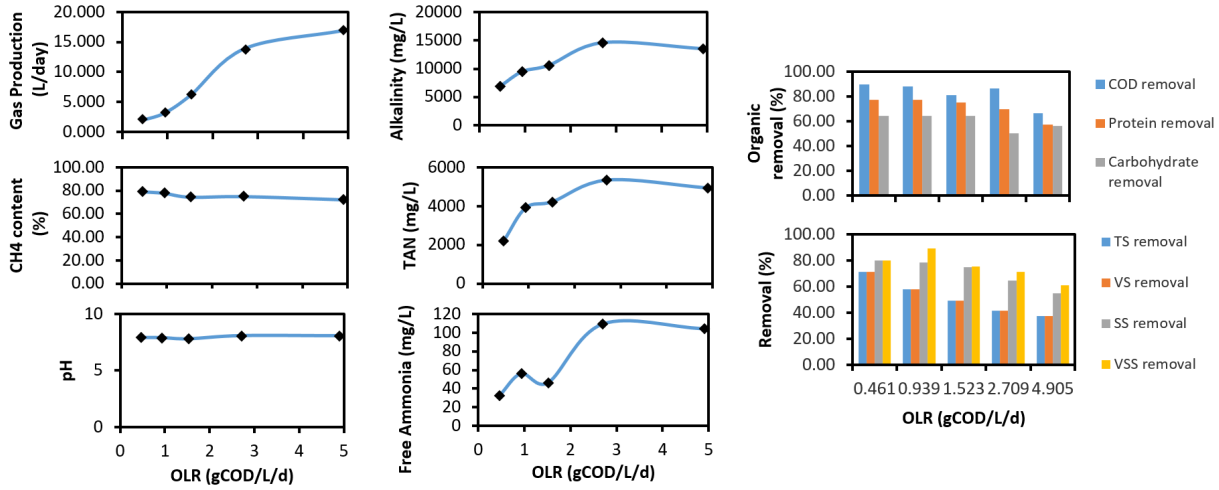

Fig. 2. SA-ABR Performance in Fish Processing Wastewater Fermentation When the OLR Was Increase

The Potential Anaerobic Digestion Treatment for Palm Oil Mill Effluent (POME)

○Siti Nur Fatihah MOIDEEN[1]* & Yu-You LI[1,2]

[1]Graduate School of Environmental Studies, Tohoku University, 6-6-06 Aza-Aoba, Aramaki, Aoba-ku, Sendai, Miyagi 980-8579, Japan.

[2]Department of Civil and Environmental Engineering, Graduate School of Engineering, Tohoku University, 6-6-06 Aza-Aoba, Aramaki, Aoba-ku, Sendai, Miyagi 980-8579, Japan.

*E-mail: siti.nur.fatihah.binti.moideen.t3@dc.tohoku.ac.jp

Abstract

Palm oil is primarily used in the developing countries. Palm oil is coming from oil palm trees which can only grow in the tropical country. Malaysia, is one of the palm oil main producer in the world after Indonesia. However, this industry has contributed to the massive generation of palm oil mill effluent (POME). POME having high content of organic content and it became abundancies as the industry kept growing. Thus, a promising treatment system is required in order to treat POME accordingly and became harmless to the environment. Anaerobic digestion is favorable treatment since this treatment able to degrade organic matters in POME and emit biogas as the end product. Generally, 85% of Malaysian palm oil mill adopting conventional anaerobic pond to treat POME, hence, it is required to explore advance treatment method since conventional method leads to excessive emissions of greenhouse gaseous to the atmosphere. This paper reviews the potential treatment for POME. A part of that, the prospective treatment also reviewed.

Keywords: Palm oil mill effluent (POME), organic content, anaerobic digestion, treatment system

1. Introduction

In 2016, the production of 3.8 tons of oil per hectare has been produced in 2016. Globally, the palm oil production increased from 15.2 million tons in 1995 to 62.6 million tons in 2015. Malaysia is the second largest producer of palm oil and it is the main leading industry. The production of crude palm oil is more than 13 million tons per year and covers about 11% of total plantations land area.

However, the drawback from persistent demand of palm oil is the generation of vast amount of palm oil mill effluent (POME). As stated by Vijaya *et al*. (2008), in every tons of crude palm oil (CPO), 3.05 tons of POME was generated. Moreover, in 2015 itself, almost 60.88 million tons of POME produced by the palm oil industry in Malaysia (Choong *et al*., 2018).

Basically, Malaysian palm oil industries adapting conventional treatment plant to treat POME. The disadvantages of this conventional method are large land area required and excessive emission of greenhouse gaseous emitted to the environment. As cited by Poh and Chong (2010) from Ma *et al*. (1993), 85% of Malaysian palm oil mill adapting low cost ponding system to treat POME.

There are plenty of published papers discussing about the effective POME treatment and also it potential in producing biogas from the degradation process of organic matters in POME.

Hence, this article is representing general review on POME production from fresh fruit bunch (FFB), the characteristics of POME and the potential treatment system for POME treatment and biogas generation.

2. From FFB to POME: The Process

2.1 Oil Processing

The process of palm oil from oil palm started when fresh fruit bunch (FFB) were brought to the mill and been sterilized. During sterilization phase, huge amount of fresh water was utilized. Then, sterilized fruits were stripped and the fruits were detached from empty fruit bunch (EFB). The fruits flow to the digester and converted into homogeneous oily mash. In pressing phase, the press cake was separated from the mixture oil, water, debris and other material and discarded as dirty crude oil.

The solid press cake and palm nuts and fed into depericarper. The crude oil was clarified and the oil was sifted based on its density. The oil from top were skimmed off and flows to the next step. The final CPO is then cooled and stored.

The lower layer of sludge is separated using separator and the final liquid waste; POME flows to the cooling pond for biogas production.

2.2 POME Characteristics

The characteristics of POME were varies depending upon the time of sample withdrawn from the mill. Commonly, POME having colloidal suspension of 95-96% of water, 0.6 -0.7% of oil and 4-5% total solids including 2-4% of suspended solid (Ahmad *et al*., 2003).

POME is rich in organic carbon and having BOD more than 20 gL^{-1}. Moreover, POME contains nitrogen compound around 0.2 gL^{-1} and 0.5 gL^{-1} of total nitrogen.

Table 1: Characteristic of raw POME (*source*: Malaysian Palm Oil Board, MPOB, 2017)

Parameter	POME (average)
pH	4.2
Oil and grease	4000
Biochemical oxygen demand (BOD)	25,000
Chemical oxygen demand (COD)	51,000
Total solid	40,000
Suspended solid	18,000
Total volatile solid	34,000
Ammoniacal nitrogen (NH_3-N)	35
Total nitrogen	750

All values are in mgL^{-1} except pH

2.3 Anaerobic Treatment of POME

POME is in high organic properties, thus, anaerobic process is the most appropriate method of treating POME. Biological treatment has many benefits compared to other method (i.e. aerobic and facultative process). The advantages of biological treatment are less energy demand, minimum sludge accumulation and most valuable point is methane production from efficient breakdown of organic matter by anaerobic bacteria (Rincón *et al*., 2006; Iskandar *et al*., 2018).

Even though by conventional method could generate methane gas, the liberation of methane gas to the atmosphere will affecting the ozone layer thus eventually causing greenhouse effect.

Up to this date, the conventional treatment method is out of league and now a new method to treat POME is developed.

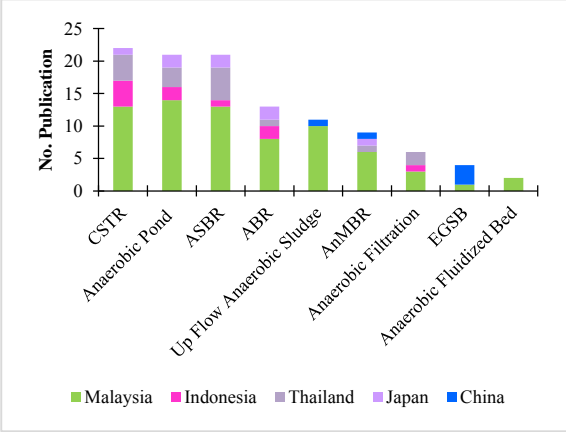

Figure 1: Treatment system for palm oil mill effluent (POME)

Figure 1 showing hybrid system studies conducted in the recent years. These systems were studied since it having lesser process time and higher efficiency. Continuous stirred tank reactor (CSTR), anaerobic sequencing batch reactor(ASBR), anaerobic baffled reactor (ABR), up flow anaerobic sludge fixed-film (UASFF), anaerobic membrane bioreactor (AnMBR), anaerobic filtration, expanded granular sludge blanket (EGSB) and anaerobic fluidized bed have been studied. These methods successfully reduced the hydraulic retention time (HRT) on a laboratory scale.

3. Prospective Treatment for POME

Anaerobic membrane bioreactor (AnMBR) is a hybrid process where membranes are integrated into anaerobic processes and comes with various advantages such as produces high quality effluent, less energy consumption with no aeration, less sludge production and bio-methane as by-product which can be used as energy (Jeong, Hermanowicz and Park, 2017).

Based on the previous research by Li *et al*. (2015), AnMBR removed almost 100% of soluble COD (S-COD) and about 80% of total COD. On the other hand, reactor without membrane only 70% of total COD was removed.

Hence, in the future research AnMBR system will be applied for the treatment of synthetic palm oil mill effluent. The AnMBR system are as can be seen in Figure 2. The AnMBR system will be assembled with hollow fiber membrane. However, main problem related to membrane system is membrane fouling but this can be encountered by injecting gas from the continuous stirred tank to the membrane console to remove attached material on the membrane to prevent the membrane fouling.

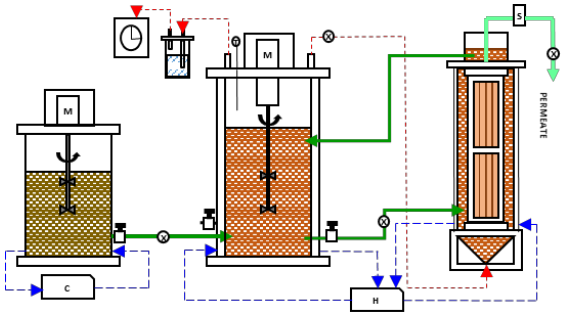

Figure 2: Schematic diagram of AnMBR for synthetic POME treatment

4. Conclusions

The palm oil industry has caused an undeniable source of pollution if it is not well treated. Wise action and regulations could counter this effect. As the demand increased, the palm oil industries in Malaysia are expanding, hence, the waste generation also increasing.

Despite there is anaerobic and aerobic treatment being used to treat POME, but, it is still not able to achieve the standard set by the authority. Furthermore, this method also having many disadvantages such as large area requirement and longer HRT. On the other hand, the gas releases from this treatment has causing greenhouse effect.

Although there were many studies has been conducted to treat POME, AnMBR seems to be a promising treatment method. AnMBR system possibly able to treat POME and resulting to low COD effluent and high biogas production

Optimization of cod removal of a full scale slaughterhouse wastewater treatment plant using a combination of uasb and activated sludge process

○Chaimaa Mribet [1], Jiang Wu [2], Hong Chen [2,3], Bo Jiang [2], Yu-You Li[1,2]

1Graduate School of Environmental Studies, Tohoku University, 6-6-06 Aoba, Sendai 980-8579, Japan.
2Department of Civil and Environmental Engineering, Graduate School of Engineering, Tohoku University, 6-6-06 Aza-Aoba, Aramaki, Aoba-ku, Sendai, Miyagi 980-8579, Japan.
3 Key Laboratory of Water-Sediment Sciences and Water Disaster Prevention of Hunan Province, School of Hydraulic Engineering, Changsha University of Science & Technology, Changsha, 410004, China.

*E-mail: eeling@utm.my

Abstract

In this case study, a wastewater treatment and biogas production plant performance was investigated. The influent wastewater comes mainly from a meat factory (50%), poultry feathers (30%) and other sources. The current treatment process consists of a Dissolved Air floatation unit, followed by an Upflow Anaerobic Sludge Blanket (UASB) and an activated sludge unit. The investigation involves the analysis and interpretation of the variations in the performance of the three main treatment units (DAF, UASB and Activated sludge), along with the treatment efficiency of the whole process. The main objective was to optimize the performance of the plant by increasing the removal efficiency of COD, SS and Nitrogen compounds, while reducing the plant energy costs.

The results indicate a fluctuation of the treatment efficiency in the different treatment units, mainly due to seasonal changes in temperature, as well as influent flow and composition. The Dissolved Air floatation unit has increased its performance considerably, reaching 81% of the total COD removal efficiency, while the UASB has proven to be best performant during summer time. The AS was considered to be the most efficient unit and has an average removal efficiency of 80%. The maximum biogas Yield obtained was 730 Nm3/day

Keywords: Dissolved-air flotation (DAF), Full-scale slaughterhouse wastewater, Upflow anaerobic sludge blanket (UASB) reactor, Activated Sludge, COD removal, Methane yield.

1. Introduction

Meat and poultry industries use a huge amount of water. The wastewater coming out of these factories is mainly composed of diluted blood, fat, suspended solids. The meat processing industry is one of the largest consumers of total freshwater used in the agricultural and livestock industry worldwide. It uses 24% of the total freshwater consumed by the food and beverage industry and up to 29% of that consumed by the agricultural sector worldwide (Mekonnen and Hoekstra, 2012; Gerbens-Leenes et al., 2013). And with the population increase, it is expected that the global consumption of meat will continue to rise in the future, resulting in a higher amount of wastewater coming from meat processing industries that needs to be treated before being discharged into the environment. With the high blood, proteins and organic matter concentrations, it is characterized as a high strength wastewater and is classified as one of the most detrimental industrial wastewaters to the environment by the United States Environmental Protection Agency (US EPA) and therefore needs special attention and requires meticulous treatment.

Anaerobic Digestion is a controlled biological degradation process, in which stabilization of organic substrates is achieved through the combined action of different microbial consortia, in the absence of oxygen. The main products of this process are biogas (a mixture of CH4, CO2 and other gases in traces) and digested sludge. The former can be used for energy applications and the latter to potentially improve soil fertility (Singh et al., 2010).

Among the different treatment systems, high rate anaerobic reactors have been proposed as good alternative and effective system because of its numerous advantages like low initial and operational costs, smaller space requirements, high organic removal efficiency and low sludge production, combined with a net energy benefit through the production of biogas (Banu et al., 2007; Behera et al., 2007; Juang and Chiou, 2007; Liu et al., 2010; Bicheldey and Latushkia, 2010; Karapidakis et al., 2010).

Our case study is a slaughterhouse wastewater treatment plant that uses both aerobic and anaerobic processes for the treatment. The objective is to optimize the treatment of the wastewater and reduce energy consumption, focusing on the performance of the UASB reactor operating conditions. The effects of the flow rate, the pH, temperature, and their interactions on the overall treatment efficiency as well as the biogas yield are studied.

2. Materials and Methods

The investigation involves the analysis and interpretation of the variations in the performance of the three main treatment units (DAF, UASB and Activated sludge), along with the treatment efficiency of the whole process. Monitoring involves temperature, pH, DO, ORP, biogas production, daily flow and pressure which are measured in-situ by a plant operator. COD, SS, VSS, MLSS, MLVSS, NH4+, NO2- and NO3- are analysed in the laboratory in a weekly basis. The data analysis from the plant is from

January 2017 to December 2017, while laboratory analysis period is from July 2017 to December 2017. CODCr measurements were carried out according to APHA Standard Methods, SS measurement were analysed according to 2540 D. The nitrogen compounds (NH4+-N, NO2−-N and NO3−-N) were analysed by capillary electrophoresis (Agilent 7100). Protein was analysed by Lowry method. Volatile fatty acids (VFA) were analysed by gas chromatography (Agilent 6890) and pH was measured by an Orion 370 PerpHecT meter (Thermo Fisher Scientific, USA). The biogas composition including CH4, CO2 and N2 was measured using a gas chromatograph (Shimaszu GC-8A, Japan) equipped with a thermal conductivity detector.

3. Results and Discussion

An important factor influencing the efficiency of the wastewater treatment process is the intensity and variability of inflows and their characteristics. All the results obtained and graphs have a linear correlation with the concentrations of the influent wastewater.

From a whole scale level, the plant's removal efficiency has got an average of 96%, where, 79% of the removal occurs in the activated sludge system that removes most of the COD, while the UASB's average removal rate is 52%. The dissolved air floatation system has an average efficiency of 40%. The latest data suggests a remarkable increase of the DAF efficiency and a decrease performance of the Activated Sludge unit.

The data shows a direct correlation between temperature and the performance of the plant. The unique weather of the region in which the plant is located contributes largely in the performance, affecting energy consumption that tends to rise during winter. the UASB is being operated under mesophilic conditions, and its treatment efficiency was at its best during summer time. Whereas in winter time, as the temperatures tend to decrease significantly, the TCOD removal rate decreased and biogas production rate was unstable. pH levels have also been affected, and dropped to less than 6.5. The period of April and May the COD appears to be easily removed by the UASB.

The results herein show the importance of primary treatment to decrease substantially the organic load to be treated in combined systems, and the role of dissolved air flotation in conjunction with anaerobic and aerobic processes for the treatment of meat industry wastewater in achieving low discharge parameters of organic persistent pollutants.

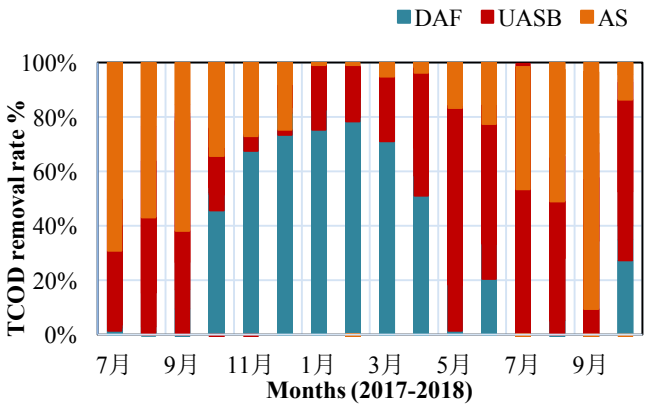

Figure 1: Total COD removal efficiency by the treatment process

Conclusions

The overall results suggest that due to seasonal changes, it is best to first alternate between the UASB unit and Activated Sludge unit depending on the temperature. During hot weather opt for an anaerobic treatment, and use aerobic treatment during cold weather. As the latest data indicates that more than 90% of the COD treatment occurs in both DAF and UASB units, it could be suggested to restraint the treatment to these two units; hence lowering energy consumption, and saving money which could be used in recovering the biogas that is still kept unexploited and released into the atmosphere. A further study on cost analysis of the WWTP could estimate the profitability and feasibility of this scenario, comparing it with the previous one where the treatment process was using the DAF unit and Activated Sludge unit.

4. References

Alvarez R, L. G. (2008). Semi-continuous co-digestion of solid slaughterhouse waste, manure, and fruit and vegetable waste. Renew Energy 33, 726-734.

Bustillo-Lecompte, C. F. (2015). Slaughterhouse wastewater characteristics, treatment, and management in the meat processing industry: A review on trends and advances. . Journal of Environmental Management , 161, 287–302.

Ciro Fernando Bustillo-Lecompte, M. M. (2017). , Treatment of actual slaughterhouse wastewater by combined anaerobic–aerobic processes for biogas generation and removal of organics and nutrients: An optimization study towards a cleaner production in the meat processing industry. Journal of Cleaner Production, Volume 141, 278-289.

D.A. Lovett, S. T. (1986). Dissolved air flotation for abattoir wastewater . Water Research, 20 , 421-426.

Ihsan Hamawand, A. G. (n.d.). A Critical Review on Processes and Energy Profile of the Australian Meat Processing Industry .

MIRANDA, L. A., HENRIQUES, J. A., & MONTEGGIA, L. O. (Dec. 2005). A full-scale UASB reactor for treatment of pig and cattle slaughterhouse wastewater with a high oil and grease content. Braz. J. Chem. Eng., São Paulo , v. 22, n. 4, 601-610.

Using Microbial Quantification for Water, Sanitation and Hygiene (WASH) Intervention Study in Rural Nepal

Sital UPRETY[1,3]*, Bipin DANGOL[2], Mohan AMRASIRI[3], Daisuke SANO[3,4] Thanh NGUYEN[1]
[1]Department of Civil and Environmental Engineering, University of Illinois at Urbana Champaign, Urbana, Illinois, USA
[2] Environment and Public Health Organization (ENPHO), Kathmandu, Nepal
[3] Department of Frontier Science for Advanced Environment, Tohoku University, Sendai, Japan
[4] Department of Civil and Environmental Engineering[2], Graduate School of Engineering, Tohoku University, Sendai, Japan
*E-mail: uprety2@illinois.edu

Abstract

Poor water quality and limited sanitation is responsible for approximately 3.5 billion diarrheal episodes and 1.87 million diarrhea-related deaths in children under five each year, mostly occurring in the developing world. Recent outbreaks of water-related diarrheal disease following extreme weather events such as those in Indonesia and Haiti in 2004 and 2010, respectively, demonstrate the interdependent relationship between climate change, water, and public health. Water, Sanitation and Hygiene (WASH) intervention in low-income countries is most common way to improve the water quality and sanitation in the household. This study focused on quantifying bacterial pathogen in water and surrounding environment. Two villages of similar climatic condition and similar socioeconomic condition but one going through extensive WASH intervention for next two years and one without any planned intervention, were selected for this study. We hypothesize that over the same study period, village with intervention will have a decreases pathogen load in water and household, while pathogen load will not change drastically in the village with no intervention. To test this hypothesis, twenty-four pathogens were selected and the assays were designed for the targeted pathogen using microfluidic quantitative polymerase chain reaction (mfqPCR). Results indicated the deteriorated sanitation practices in addition to contaminated drinking water.

Keywords: WASH, Intervention, Pathogen, microbial quantification, Nepal

1. Introduction

Waterborne diseases pose a major threat to human health risk all over the world causing 1.5 to 15 million deaths every year . Like several low- and middle – income countries, Nepal faces several problems in water, sanitation and hygiene from cities to villages. The objectives of this study were to identify and quantify pathogenic genes commonly associated with human intestinal infections in drinking water, cleaning water and environmental samples over three months in villages in Nepal. Water samples were collected from drinking water, drainage channels, and surface water in Dhading, Nepal from May 2017 to August 2017. Target genes commonly representative of pathogenic organisms were quantified over time at multiple water sources. To the best of our knowledge, this is the first study to longitudinally measure waterborne pathogen presence in multiple water source types in a developing region going under water, sanitation and hygiene intervention.

2. Materials and Methods

2.1 Location

SUAAHARA is a $63 million integrated program dedicated to improving the health and nutrition status of women and children in 40/75 districts of Nepal. One of the strategies to improve the nutrition in these targeted districts is by improving Water, Sanitation and Hygiene (WASH) behavior and practices in the household. This is being done by extensive community level WASH intervention through capacity building, water quality testing and monitoring and promotion and demonstration of WASH solutions. Dhading, one of the districts in the SUAAHARA project, was selected for the study. Ten households each from two villages were selected from Dhading district, one going through extensive WASH intervention (V1) and one village where no intervention activities are planned. Drinking water (DW), cleaning water (CW), handwash (HW) and swab samples were collected from each household. For swab samples, toilet handle (TH), utensil swabs(U) and water vessel (WV) swab samples were collected. Three rounds of sampling were conducted from June-July 2017 in these two villages of Dhading district.

2.2 Sampling protocol

Two-liter water samples (DW, CW and HW) were collected at each sampling site in sterile Whirl-pak® sampling bags and were processed within 24 h of collection. Thereafter, water samples were sequentially vacuum filtered through a 1.6-µm-pore glass fiber filter (Millipore, Ballerica, MA) followed by a 0.45-µm-pore nitrocellulose filter placed in a 47-mm filtration funnel. filtrate were sterilized prior to each sample filtration according to EPA guidelines . At UIUC, filters were

stored at -80°C until DNA extraction. BD Liquid Eswabs (El Paso, TX) were used for sampling toilet handles, utensils and water vessels and was stored at -20°C until DNA extraction.

2.3 Simultaneous quantification using Biomark:

24 pathogens of interest were selected for quantification based on diseases incidences in Nepal and validity of assays. Assay designs for all target genes were adapted from previous studies to detect *Enterococcus*, two genes of General *E. Coli*, Enteropathogenic *E. Coli*, two genes of Shiga-toxin producing *E. Coli*, two genes of *Shigella* spp, *Shigella flexneri*, two genes of *Camopylobacter jejuni*, *Campylobacter lari*, two genes of *Salmonella*, *Colostridium prefringes*, *Listeria monocytogenes*, two genes of *Vibrio cholerae*, Adenovirus Type 40/4, *Giardia lambia* and *Cryptosporidium parvum*. NH8B was used as Internal Amplification Control (IAC) in the experiment.
Forward, reverse primers and standards for all assays were obtained as Custom DNA Oligos (Integrated DNA Technologies, Coralville, IA). Probes were obtained from Universal Probe Library (UPL) (Rosche, Basel, Switzerland). Prior to enumeration by MFQPCR (Microfluidic Quantitative Polymerase Chain Reaction), all DNA samples and standard pool dilutions underwent standard target amplification (STA) PCR to increase template DNA yields. mfqPCR was performed in a Biomark HD Real-Time PCR (Fluidigm) using the following thermal conditions: 70°C for 30 min, 25°C for 10 min, 95°C for 1 min, followed by 35 cycles of 96°C for 5 sec and 60°C for 20 sec.

3. Results and Discussion

Figure 1 shows the quantification of pathogens in swab sample in copies/swab in three sampling period and Figure 2 shows the quantification of water samples in copies/L in the same sampling period.
Overall results showed high presence of several enteropathogenic bacteria. Presence was seen higher in swab samples compared to water samples. When swab samples were investigated in detail, utensil samples seemed to be of highest risk compared to water vessel sample and toilet handle samples indicating the need to wash utensils in a proper way between meals to avoid any potential enteric diseases. In water samples, drinking water samples were the cleanest but cleaning water samples and handwashing samples showed the potential of being of high. Handwash samples especially had multiple pathogen detected with higher concentrations, again indicating deteriorated sanitation practices in household. Better handwashing practices would be essential to avoid the risk of getting sick from diarrheal diseases.

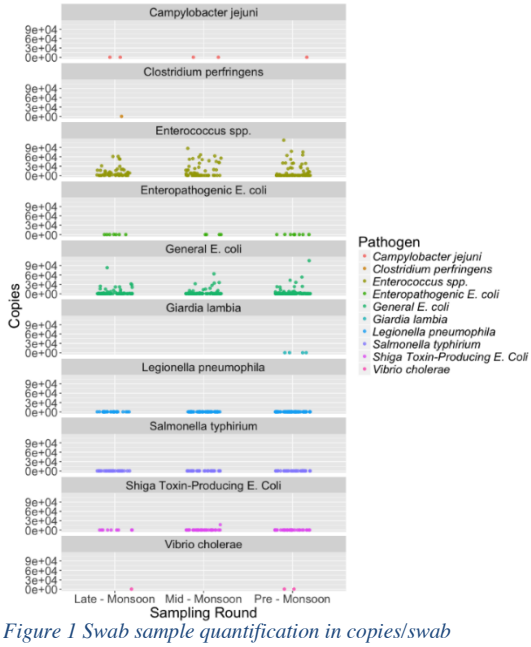

Figure 1 Swab sample quantification in copies/swab

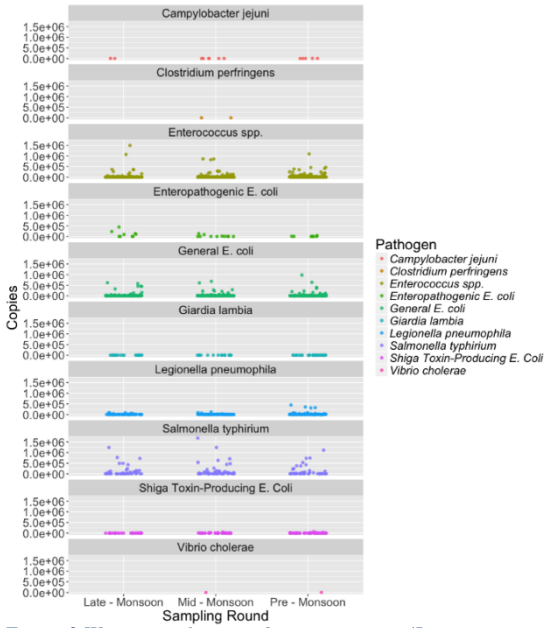

Figure 2 Water sample quantification in copies/L

4. Conclusions

(1) Several pathogenic bacteria detected with higher concentration like *Salmonella* and *Legionalla* which can be life threatening to individuals
(2) Swab samples showed higher detection and concentration indicating deteriorated sanitation conditions in the households.
(3) Intervention strategies targeting behavioral change in sanitation might be more impactful

5. Acknowledgments

The authors would like to thank National Science Foundation International Research Experience for Undergraduates (NSF-IRES) Grant and Japan Society for Promotion of Sciences (JSPS) Fellowship.

Nitrogen Removal Performance of an Anammox Membrane Reactor Operated at 25℃ with Increasing Sludge Loading Rate

○Ying Song[1,2], Shaohua Sun[1], Wei-kang Qi[1,2]*, Yu-You Li[2]*

[1] School of Chemical Engineering, Beijing University of Chemical Technology, Beijing, 100029, China
[2]Department of Civil and Environmental Engineering, Graduate School of Engineering, Tohoku University, 980-8579, Sendai, Japan
*E-mail: song.ying.q2@dc.tohoku.ac.jp

Abstract

An anaerobic ammonium oxidation (anammox) membrane bioreactor operated at 25 °C was used to investigate nitrogen removal under different sludge retention time (SRT) and nitrogen loading rate (NLR). Specific anammox activity (SAA) tests were performed to evaluate the effects of ammonium and nitrite on the anammox sludge. Over an SRT of 500 d, the content of volatile suspended solids (VSS) gradually increased from 125 mg/L to 5590 mg/L, and the maximum nitrogen removal rate (NRR) reached 1.18 kg N/m^3/d. When the SRT was decreased to 50 d, the sludge concentration declined gradually, which necessitated an increase in the sludge loading rate (SLR), and the maximum sludge nitrogen removal rate (SNRR) of 0.67 g total nitrogen (TN)/g VSS/d was achieved at this time.

Keywords: Anammox, membrane bioreactor, nitrogen removal, high sludge loading rate

1. Introduction

The anaerobic ammonium oxidation (anammox) process is a novel and cost-effective nitrogen removal biotechnology. The method is suitable for the treatment of low C/N wastewater and has low energy consumption levels, no requirements for an external carbon source, and negligible sludge production. Use of a membrane allows for complete separation of solids and liquids in the suspended sludge. Therefore, compared to other reactors, MBR is more suitable for retaining sludge and preventing sludge loss and the suspended sludge contributes greatly to the anammox activity. The optimum temperature for the anammox process is about 30–40°C. However, the temperature of wastewater is generally below 30 °C. Thusly, achieving the required effluent quality at temperatures of 10 °C to 25 °C represents one of the main current challenges towards realizing full-scale application of the technology.

In this study, a completely stirred anammox membrane bioreactor was used to investigate nitrogen removal at 25 °C. Low anammox sludge concentration (125mg-VSS/L) was seeded into the reactor to investigate the long-term anammox performance under different operation conditions. The stable and inhibited phases during the long-term process were investigated with increasing sludge loading rate. These results are expected to contribute to the development of strategies to maintain stable operations in anammox reactors at 25 °C.

2. Materials and Methods

2.1 Experimental setup and operating conditions

As shown in Fig. 1, a cylindrical anammox MBR with a working volume of 10 L was designed. A submerged hollow fiber membrane module with a pore size of 0.1 μm was used to retain all the bacterial biomass in the MBR. The reactor was operated over the course of 800 d with a hydraulic retention time (HRT) of 12 h. The pH and dissolved oxygen (DO) concentration in the reactor were controlled at 7.8– 8.2 and < 0.05 mg/L, respectively. The specific anammox activity (SAA) tests were carried out in 400 mL glass bottles with 200 mL biomass taken from the reactor. The batch test bottles were maintained at a temperature of 25 °C in a water bath. The initial total nitrogen (TN) concentration was 200 mg/L with a NO_2^--N to NH_4^+-N ratio of 1.32.

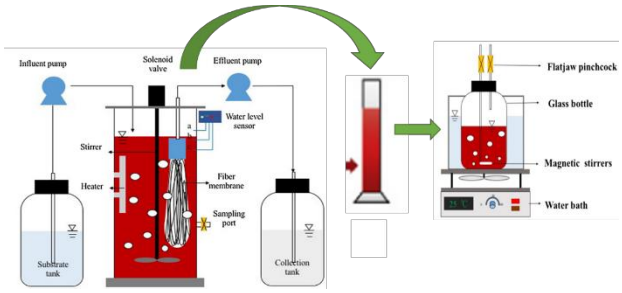

Figure 1 Schematic diagram of anammox MBR and batch test setup

2.2 Analyses

The concentrations NO_2^--N to NH_4^+-N and NO_3^--N were measured in accordance with APHA. The TN was calculated as the sum of the three kinds of nitrogen compounds. The measurement of suspended solid(SS) and volatile suspended solids (VSS) was according to APHA. The sludge nitrogen removal rate (SNRR) was calculated as an indicator of the anammox activity during long-term operations as shown in Eq. (1), in which NRR represents nitrogen removal rate.

$$SNRR = NRR/VSS \quad \text{Eq. (1)}$$

3. Results and Discussion

3.1 Reactor performance

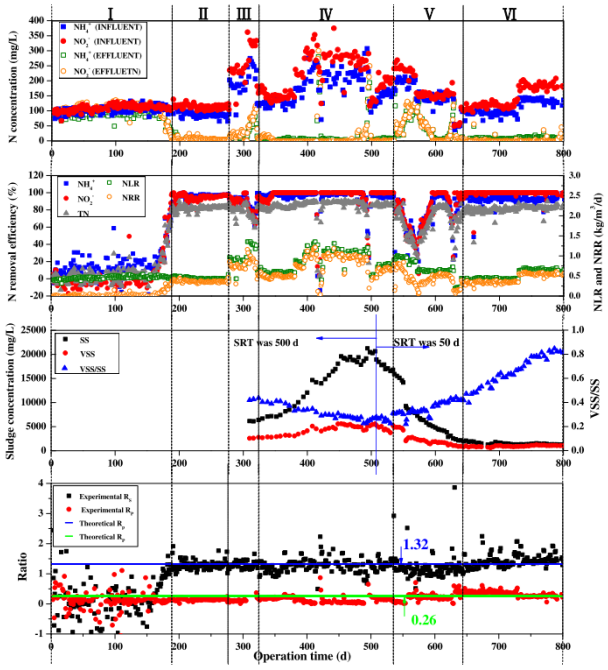

Figure 2 Long-term performance of the anammox MBR

From the beginning of the operations to the 160th day, the concentration of effluent NH_4^+-N and NO_2^--N fluctuated. R_S and R_P were highly unstable and irregular during this period. After the 161st day, the effluent NH_4^+-N and NO_2^--N concentrations decreased simultaneously, which was consistent with nitrate production. At the 190th day, the NH_4^+-N, NO_2^--N, and TN removal efficiency reached 90%, 100%, and 85%, respectively, which indicated that the start-up of the anammox MBR was successful. Starting on the 189th day, the influent ratio of NH_4^+-N and NO_2^--N was modified to the theoretical value of 1.32. The TN removal efficiency was over 80% and the ratio of consumptive NH_4^+-N and NO_2^--N was close to the theoretical value of 1.32. However, the productive NO_3^--N was less than theoretical value, which may have been the result of accompanying biological reactions like denitrification. Starting on the 278th day, the nitrogen loading rate (NLR) was increased from 0.45 kg N/m^3/d to 0.86 kg N/m^3/d and correspondingly the TN removal efficiency decreased slightly from 88.01% to 77.48%. However, when the NLR reached 1.14 kg N/m^3/d, the TN removal efficiency was only 70%, which is obvious indicative of substrate inhibition and then NLR was adjusted to 0.59 kg N/m^3/d according to capacity. From the 324th day to the 416th day, increasing the concentration of the influent TN from 300 mg/L to 600 mg/L led to a stepwise increase in the NLR from 0.6 kg N/m^3/d to 1.26 kg N/m^3/d, whereby the TN removal efficiency was maintained at 80%. Although the reactor experienced twice abnormal increase of the effluent concentration of NH_4^+-N and NO_2^--N, which led to forceful reduction of NLR to recover the performance. The high substrate concentration with low sludge concentration necessitated an increase in the sludge loading rate (SLR), which led to instability in the reactor. On 535th day, NLR was up to 0.9 kg N/m^3/d, the TN removal efficiency was dropped to 20%. The long-term inhibition without application of adjustment strategies was then investigated to document the sludge activity under a high SLR. However, the reactor performance still deteriorated with the increased SLR. Until the NRR decreased to a minimum of 25%, the NLR was gradually reduced to 0.22 kg N/m^3/d to recover the reactor performance. During this period, the abnormal phenomenon mentioned above appeared again. From the 640th day to the 729th day, the NLR was increased and the TN removal efficiency was maintained at 80% with an R_S and R_P of 1.379 and 0.380, respectively. From the 730th day to the 800th day, the influent concentration was continuously increased while the nitrogen removal rate remained at 80%.

3.2 Sludge characteristics

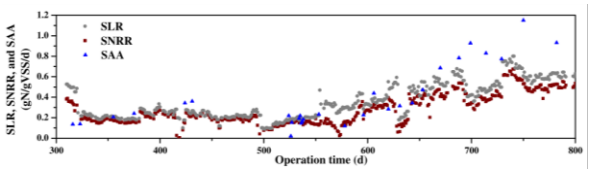

Figure 3 Long-term capacity of anammox sludge

The concentrations of VSS and SS in the anammox MBR at different periods were monitored continuously throughout the operating process from the 300th day onward, as shown in Figure 1. The maximum concentration of VSS was 5590 mg/L with an SS of 19,565 mg/L at the 453rd day causing a VSS/SS ratio of 0.28. From the 505th day onward, the SRT was shortened from 500 days to 50 days and the concentrations of VSS and SS decreased simultaneously and immediately. The VSS/SS increased from 0.3 to 0.8 with the short SRT, thus indicating that the amount of biomass in the total sludge increased when metabolites were discharged from the reactor. As shown in Figure 3, The SNRR was calculated as an indicator of the anammox activity over the long-term operation period, which was in accordance with the nitrogen removal efficiency, VSS and NLR. The highest SNRR of 0.67 g N/g VSS/d with an SLR of 0.8 g N/g VSS/d was obtained at the 740th day. For in-depth study of the anammox activity, batch tests were performed by using sludge samples from the reactor at different stages during the long-term process. the comparisons with SAA and SNRR provided more information and allowed us to adjust the influent concentration under different periods. For example, when the SAA was higher than SNRR, the potential removal capacity was higher than that demonstrated during the long-term operation, which could increase the NLR. When the SAA was lower than SNRR, the anammox reactor might have been in an over-loading state.

4. Conclusions

In this study, an anammox MBR was operated for 800 days, and the anammox process was successfully started up at 25℃ over a period of 180 days with a low seed sludge concentration of 125 mg VSS/L. The maximum NLR of 1.35 kg N/m^3/d corresponded to an NRR of 1.18 kg N/m^3/d, and the highest SLR of 0.80 g N/g VSS/d corresponded to an SNRR of 0.67 g N/g VSS/d. Several sudden increases of the effluent concentration over a period of a few days occurred during the long-term process, and this phenomenon requires further study in the future.

Successful Operation Performance of Partial Nitritation and Anammox Reactor Treating Low-Strength Ammonium Wastewater at Room Temperature

○Yujie Chen[1], Rong Chen[1,2], Yasuyuki Takemura[1], Jiayuan Ji[1], Yu-You Li[1]
[1]Department of Civil and Environmental Engineering, Tohoku University, Sendai, Miyagi 980-8579, Japan
[2]Xi'an University of Architecture and Technology, Xi'an, Shaanxi 710055, P.R.C.
*E-mail: gyokuyu.ri.a5@tohoku.ac.jp

Abstract
The treatment effect of low-strength ammonium wastewater at room temperature by the partial nitritation/anammox (PN/A) process is still far from satisfactory. This study realized the stable treatment performance of 50 mg/L ammonium wastewater with a granule-based PN/A reactor. In the long-term operation, the nitrogen removal efficiency of 71.8±9.9% was obtained stably under a relatively short hydraulic retention time (HRT) of 2 h. Most of the granules were in a size range of 265-536 μm according to the analysis on the physicochemical properties of the granules. The three-layer structure of the granules was found: the majority of the anammox bacteria agglomerated and created a granule kernel, and ammonium oxidizing bacteria (AOB) formed an outer thick rim and a little nitrite oxidizing bacteria (NOB) co-exist with AOB in the surface layer. The tests showed the activity of NOB was well limited through dissolved oxygen (DO) regulation.

Keywords: Anammox; AOB; partial nitritation; low-strength

1. Introduction
The nitrification-denitrification process in the conventional activated sludge system needs much energy mainly for the aeration to oxidize the ammonium. The discovery of anammox in 1990s makes it possible to save energy and reduce cost by autotrophic nitrogen removal. Furthermore, the application of PN/A process can further simplify the nitrogen removal procedure through the synergy between nitritation by AOB, oxidizing part of NH_4^+ to NO_2^-, and anaerobic ammonium oxidizing by anammox bacteria, which convert NH_4^+ and NO_2^- to nitrogen gas in the same reactor as the following equation.

$$NH_4^+ + 0.85O_2 \rightarrow 0.11NO_3^- + 0.445N_2 + 1.13H^+ + 1.43H_2O$$

However, the application of mainstream PN/A remains in slow progress, due to the unstable partial nitritation and inactivation of anammox bacteria resulting from low nitrogen concentrations, oxygen inhibition and temperatures lower than its optimum temperature of about 35°C. In addition, the long doubling time of bacteria makes it difficult to offset the run off of microorganisms, which can be solved by using the granulation of slow-growing anammox bacteria endowing excellent biomass retention and settleability. Additionally, studies about treating low-strength wastewater (nitrogen concentration < 100 mg/L) with the granules, whose size are smaller than 1 mm, are still scarce.

This study focused on the efficiencies of PN/A process with the co-immobilization of AOB-anammox bacteria for treating the low-strength ammonium wastewater by using a granule-based reactor at room temperature.

2. Materials and Methods
A lab-scale integrated reactor was developed to concurrently achieve PN/A, sedimentation and sludge circulation. As shown in Figure 1, an air-lift completely mixed zone with 2 L effective volume was used as reaction unit for PN/A, while an inclined-plate zone with 0.4 L of volume was employed to serve as sedimentation unit where the sediments can be returned to the reaction unit under the driving force of air lift. The temperature in the reactor was maintained at 25°C with a water jacket and pH was 7.6 ± 0.3 during the entire operation.

As Figure 2 shows, the experiment was operated continuously for 250 days, which can be divided into three stages in different conditions: the start-up period (Stage I), the hydraulic retention time (HRT) decreasing period (Stage II), and the stable operation period (Stage III).

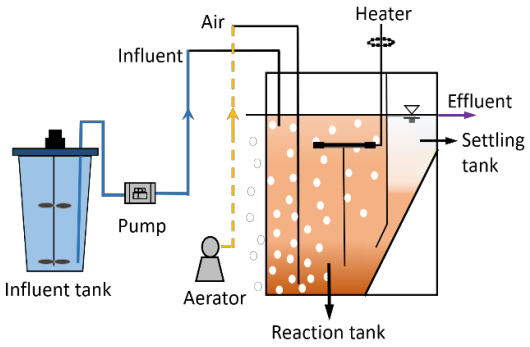

Figure 1 Diagram of PN/A process

3. Results and Discussion
3.1 Operation Performance
During the start-up period, the influent was 100 mg NH_4^+-N /L at a HRT of 6 h to provide an adaptive phase for the seed sludge.

In Stage II, the NH_4^+-N concentration in the influent was reduced to 50 mg/L and the HRT was shortened stepwise to 3h, 2h and 1 h, resulting the increase of NLR from 0.8 up to 2.4 g N/L/d. As Fig. 2A shows, aeration rates of 0.3 L/min at an HRT of 3 h, and 0.35 L/min at an HRT of 2 h resulted in

a DO range of 0.06-0.17 mg/L and 0.06-0.21 mg/L respectively. At the two HRTs, more NO_3^--N was found than NH_4^+-N in the effluent with little NO_2^-N remaining (Fig. 2B). As a result, the average total nitrogen (TN) concentration in the effluent was 13.5 mg/L and average nitrogen removal efficiency was 72.5%. The stable performance was disrupted when the HRT was decreased to an extremely short HRT of 1 h. Firstly, a lot of NH_4^+ was not consumed and remained in the effluent. Then the aeration rate was stepwise increased to 0.4 and finally to 0.6 L/min to enhance the oxidization of NH_4^+, and the DO increased accordingly, gradually approaching 0.6 mg/L. Therefore, the NH_4^+ was reduced significantly in the effluent with the augment of NO_3^- at the same time, which reached more than 30 mg/L in the later period of HRT 1 h. Therefore, TN in the effluent increased to an average of 36.1 mg/L and the nitrogen removal efficiencies were down to an almost 29.3%.

In Stage III, the HRT was returned to 2 h and the aeration rate was lowered to 0.35 L/min, causing an average DO concentration of 0.13 mg/L. As a consequence, the TN in the effluent decreased to approximately 15.9 mg/L and remained stable from the 167th day on and the nitrogen removal efficiency of 71.8±9.9% was gotten for over 80 days. Finally, the NH_4^+-N, NO_2^--N and NO_3^--N concentrations in the effluent averaged 5.65, 0.72 and 7.61 mg/L, respectively, which indicated a stable performance.

In conclusion, according to the performance at the HRT of 1h, the activity of anammox bacteria was deemed to be inhibited when the DO concentration was more than 0.5 mg/L. Furthermore, the relatively high DO content could boost NOB overgrowth which outcompeted anammox bacteria by consuming NO_2^-. In addition, a large portion of the granules was easy to be washed out from the reactor when the HRT was extremely short, which resulted in the further deterioration of the reactor performance.

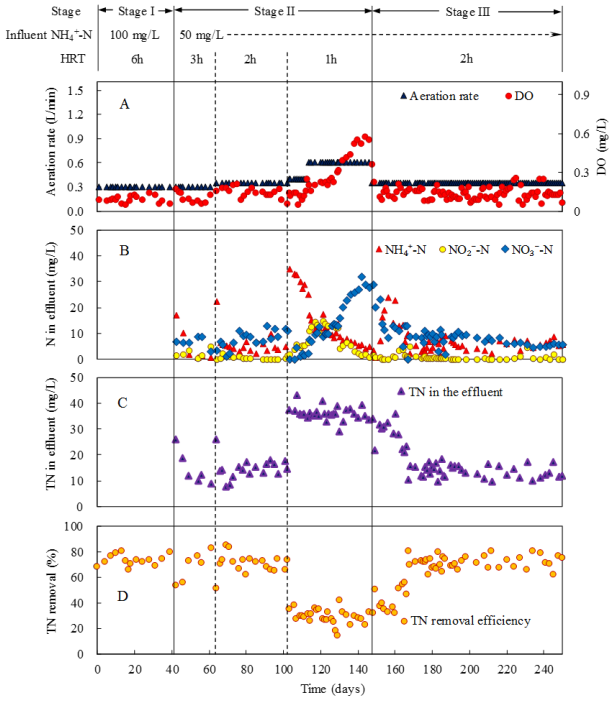

Fig. 2 Reactor performance

3.2 Physicochemical Properties

According the results of physicochemical properties test, most granules are elliptical with clear outlines and bright red. The mean size and median size of the granules were respective to be 338.3 μm and 388 μm, which were much smaller than those formed in many fixation-growth granule reactors. In addition, more than 50% of the micro granules were in size range of 265-536 μm.

3.3 Spatial AOB-anammox association

The spatial distribution of AOB and Anammox bacteria in the granules was visualized by Fluorescent in situ hybridization (FISH). Four images are shown in Figure 3. In these pictures, all of the bacteria are shown in blue, while the specific anammox and AOB population are respectively indicated in red and green. Fig. 3A and B show the images of the granule clusters, and Fig.3C and D shows the images of one granule. It can be concluded that anammox bacteria and AOB were the two most dominant bacteria in the granules and anammox bacteria accounted for an average 37.7% of the total bacteria, while AOB accounted for 34.7%. Furthermore, the FISH test illustration unveiled the spatially syntrophic co-immobilization of the two most important bacteria, anammox bacteria and AOB, within the granules: a majority of the anammox bacteria agglomerated and created a kernel of the granule with AOB and a little NOB formed an outer thick rim, which established a three-layer structure.

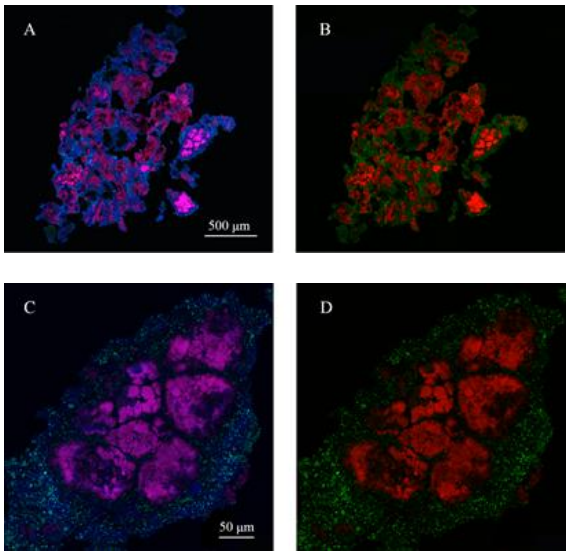

Fig. 3 FISH analysis of AOB and anammox bacteria in granules

4. Conclusions

The results of this study were concluded as below:

1) The PN/A reactor successfully achieved the treatment of low-strength ammonia wastewater with nitrogen removal efficiencies of 71.8±9.9% at a short HRT of 2 h.

2) The size of the granules formed in the reactor were measured and the mean size was 338.3 μm.

3) The special structure of AOB and anammox bacteria could be revealed by FISH illustration.

Effective post treatment of methane fermentation effluent by using two-stages system combined with BOD oxidation and anammox.

○Chenglei XIE[1*], Yu QIN[1], Yan GUO[1] & Yu-You Li[1]

[1]Department of Civil and Environmental Engineering, Graduate School of Engineering, Tohoku University, 6-6-06 Aramaki Aza Aoba, Aoba-ku, Sendai, Miyagi, 980-8579, Japan

*E-mail: xie.chenglei.q6@dc.tohoku.ac.jp

Abstract

Owing to biogas plant is an effective measure to manage food waste and recover energy, its number in operation is increasing yearly all over Japan. During the biogas fermentation process, volatile fatty acids and alcohols often accumulate in the digestive liquid. Also the concentration of ammonia nitrogen in digestive liquid is about 1000-40000mg/L. The accumulation of volatile fatty acids will inhibit methane production amount. And nitrogen should be removed from the discharged water. In order to analyze the influence of volatile fatty acids on the fermentation process, a biogas plant located in Sendai was chosen to study. A set of pilot scale experiment device combines BOD oxidation and anammox was installed in the downstream of the drainage port of the plant's sewage treatment facility. The aim of this device is to remove the organics and nitrogen from the methane fermentation effluent. Biogas samples from each tanks and digestive liquid samples in this plant and the pilot scale experiment device were taken regularly. Then these samples were analyzed in our laboratory. The results show both fermentation tank No. 2 and No. 4 were acidulated. The pH average of these two tanks were 5.42 and 4.99 respectively. While pH average of tank No. 1 and No. 3 were 7.85 and 7.66 respectively. As a result of acidification, the biogas produced by tank No. 2 and No. 4 contained approximately 8% hydrogen. The average methane content of all tanks below 50%. The average ammonia nitrogen concentration of these four tanks were 4124, 2772, 3089, and 2379 mg/L respectively.

Keywords: Methane fermentation, sewage effluent, BOD oxidation, anammox

1. Introduction

Although the amount of food waste generated in Japan rises to approximately 20 million tons per year, the recycling rate is as low as about 27.0%. Due to measures to promote recycling of food waste such as the Food Recycling Law and the Feed-in tariff Law, the number of biogas plants in operation is increasing yearly. During the decade from 2000 to 2009, more than one hundred plants had been built. As of 2015, the total number of biogas plants is about 150.

During the biogas fermentation process, volatile fatty acids and alcohols often accumulate in the digestive liquid. The accumulation of volatile fatty acids will inhibit methane production amount. In order to analyze the influence of volatile fatty acids on the fermentation process, a biogas plant located in Sendai was chosen to study.

The concentration of ammonia nitrogen in food waste fermentation plant's digestive liquid is about 1000-40000mg/L generally. This nitrogen should be removed from the discharged water. The anammox bacteria use nitrite as the electron acceptor and ammonium as the electron donor to allow for the removal of ammonium from wastewater in the absence of oxygen and organic matters. Since the anaerobic and autotrophic nature of anammox bacteria permits significant reductions in energy consumption and organic carbon investments for biological nitrogen removal, the application potential of the anammox process has been attracted more attention in recent years. By operation in laboratory, many facts such as substrate, organic matter, sulfide, salinity, and other nutrient salts can have negative effects on anammox bacteria activity have been concluded. Among the inhibitors, the substrate with too high concentration is the most common and important factor. More and more cases combining laboratory conclusions with industrial applications are burgeoning around the earth.

In addition to analyzing this plant operation condition, we conduct a pilot scale experiment to remove nitrogen by using two-stages system combined with BOD oxidation and anammox in this plant. Because the anammox bacteria are highly sensitive to environmental conditions, we use the BOD acidification tank of this device to remove as many inhibitors as possible, so that anammox tank can receive a stable water supply quality.

Since the pilot scale experiment is still in its initial stage, this study mainly focuses on the operation of the methane fermentation plant at present.

2. Materials and Methods

2.1 Brief introduction of biogas plant

The target biogas plant is called J-Nex Corporation (abbreviated as JNEX), which is located in the northern part of Sendai city. It processes food waste collected as industrial waste with processing capacity around 48 tons per day. Input materials consist of various kinds of food wastes discharged from restaurants, hotels, and food factories. Typically, wastes discharged from the former include vegetables, fruit scraps and leftovers; while the latter contains animal and vegetable residues, waste drinks and dairy products. It needs to be pointed out that waste sludge and grease trap sludge discharged from food factories were treated as sludge. The biogas produced in this plant was used to generate electric energy, while dehydrated sludge was made into organic fertilizer.

This plant consists of four methane fermentation tanks, a digestive liquid tank. While the pilot scale experiment device

consists of raw water tank, BOD oxidation tank, post treatment water tank and anammox tank. The inlet of raw water tank is located in the downstream of the waste water treatment facility of this plant.

2.2 Samples collection and analysis

Samples were collected in Monday, Wednesday and Friday of per week. Among them, biogas samples were collected by using a gas pump blowing gas into air bags from the tank No. 2, No. 3 and No. 4. Digestive liquid samples were collected from the top, the middle and the bottom of each methane fermentation tank. Since blockage accidents had happened to the bottom sampling nozzles of tank No. 1 and No. 3, corresponding samples were absent.

All samples were brought to our laboratory in less than 3 hours after they were collected. Biogas samples were analyzed by two Gas Chromatograph (GC-8A Series, SHIMADZU, JAPAN). Digestive liquid samples were analyzed to obtain pH, alkalinity and concentration of ammonia nitrogen.

3. Results and Discussion

Figure 1 shows the pH trend of each fermentation tank. From the results, we can know fermentation tank No. 2 and No. 4 were acidulated. Among them, tank No. 2 seems to be going to further deteriorate. Figure 2 shows the biogas composition variation trends of each fermentation tank over time.

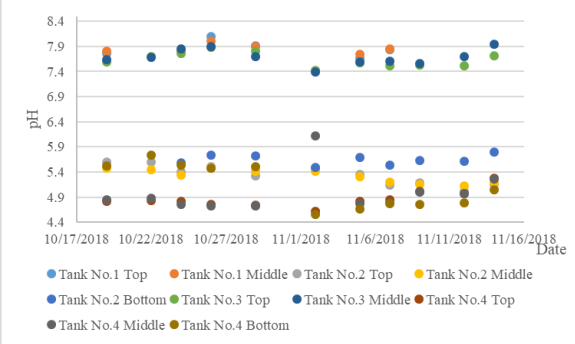

Figure 1: Trend of pH in each fermentation tank

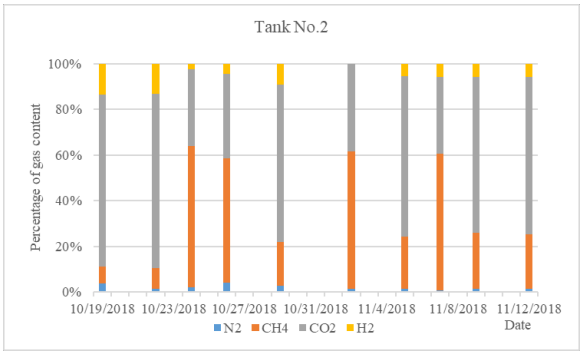

(a)

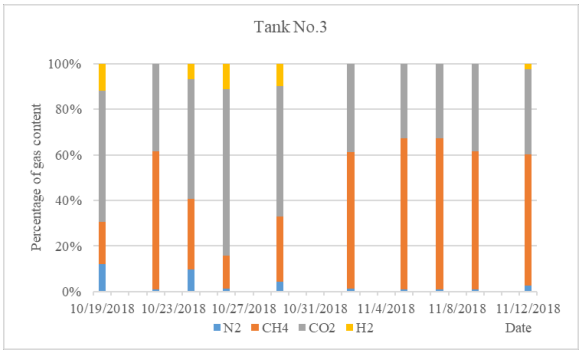

(b)

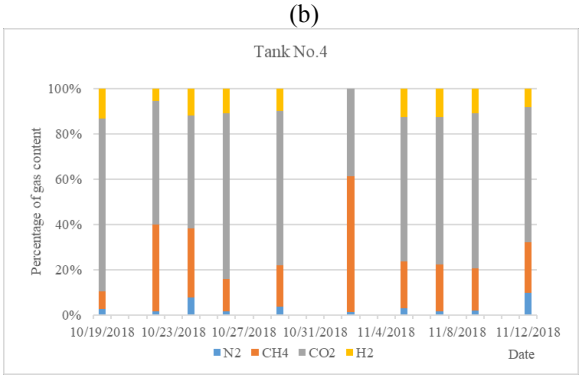

(c)

Figure 2: Biogas composition of each fermentation tank

The average pH, average content of methane, hydrogen and ammonia nitrogen of these four methane fermentation tanks were as shown in Table 1.

Table 1: Average pH, content of methane, hydrogen and ammonia nitrogen in each tank

Tank No. / Average value	1	2	3	4
pH	7.85	5.42	7.66	4.99
CH_4(%)		34.34	46.36	25.18
H_2(%)		6.47	4.22	9.59
NH_4-N(mg/L)	4124	2772	3089	2379

From table above, we can know methane content of biogas produced in these two tanks decreased greatly compared to a normally operating tank and hydrogen content approximately to be 8%. Since hydrogen has bad impact on the generator boilers during its combustion process, this plant's power generation facility has to suspend operation. It is suggested that alkaline substance such as caustic soda be added into fermentation tank No. 2 and No. 4.

4. Conclusions

(1) Fermentation tank No. 2 and No. 4 were acidulated and alkaline substance should be added into them.

(2) Methane content of biogas produced in this plant's three tanks significantly lower than normally operating methane fermentation tank, which will do great harm to generator biogas combustion boiler.

Simultaneous Nitrogen and Phosphorus Recovery using an Anammox Expanded Bed Reactor at Low Temperature

○Yuanfan ZHANG[1]*, Haiyuan MA[1], Yi XUE[2], Yu-You LI[1]

[1]Department of Civil and Environmental Engineering, Graduate School of Engineering, Tohoku University, Sendai, Miyagi 980-8579, Japan.

[2]Graduate School of Environmental Studies, Tohoku University, Sendai, Miyagi 980-8579, Japan.

*E-mail: zhang.yuanfan.s1@dc.tohoku.ac.jp

Abstract

High concentrations of nitrogen and phosphorus treatment contained in the digester liquids becomes a big issue in recent years. In this study, the concept of crystallization reactor used for side-stream phosphorus recovery was borrowed to be integrated with anammox reactor. This study was aimed at the performance of simultaneous nitrogen removal and phosphorus recovery in an anammox expanded granular sludge bed at 15°C and detected the sludge characteristics variation according to operation condition and granule structure in this new process.

Keywords: Anammox, Phosphorus recovery, HAP, Granular sludge

1. Introduction

The extensive use of fertilizers in modern agriculture has increased world crop yields, making it possible for the global population to exceed 7.4 billion. However, the nitrogen and phosphorus consumed in food typically exceed nutrient requirements, and the remainder leaches into waterbodies, leading to eutrophication and other concomitant environmental problems. In addition, an estimated 40 million tons of phosphorus rock is used for fertilizer each year for food crops and at the present population growth rate phosphorus reserves are estimated to be depleted by 2090. Phosphorus recovery at WWTPs can have a significant impact on extending the life of phosphorus reserves and fertilizer cost. An obvious way to reduce risks to water quality and resource exhaustion is to remove phosphorus and nitrogen from wastewater and recover phosphorus in the form of valuable products.

Anammox have been made over the approximately last 30 years as an innovative and sustainable nitrogen removal process. The Anammox process is a biological mediated reaction in which ammonia is oxidized to nitrogen gas using nitrite as the electron acceptor under anaerobic conditions. In a partial nitritation-anammox process, the operation cost is reduced due to the lower aeration energy and because no organic carbon is required.

In this study, a simultaneous nitrogen and phosphorus recovery process at low temperature was developed. And discussed the effects of nitrogen load and phosphorus loading on processing performance and sludge properties of this process.

2. Materials and Methods

2.1 Inoculum

The reactor was initially inoculated with a mixture of activated sludge and anaerobic digestion sludge taken from a municipal wastewater treatment plant in Sendai, Japan. The initial suspended solids (SS) and volatile suspended solids (VSS) were 19.64 g/L and 11.64 g/L, respectively.

2.2 Reactor set-up

An AAFEB reactor with a 5 L working volume was used in this study shown in Fig.1. The operational temperature was run at 35 °C at start-up period and then controlled at 15 °C. Effluent recirculation was applied to dilute the substrate concentration and to maintain fluidization condition in the AAFEB reactor. Diluted sulfuric acid (2–5%) was continuously fed into the recirculation water to adjust the operational pH to around 8.5 for both the anammox process and HAP crystallization. The synthetic wastewater simulating the composition of effluent from a previous partial nitritation reactor treating anaerobic digestion effluent consist of (NH4)2SO4 0.67 g/L, NaNO2 0.84 g/L, KH2PO4 0.057 g/L, CaCl2·2H2O 0.3 g/L, NaHCO3 0.5 g/L, KCl 0.57 g/L, MgSO4·7H2O 0.2 g/L and trace elements. The reactor was operated for more than 250 days.

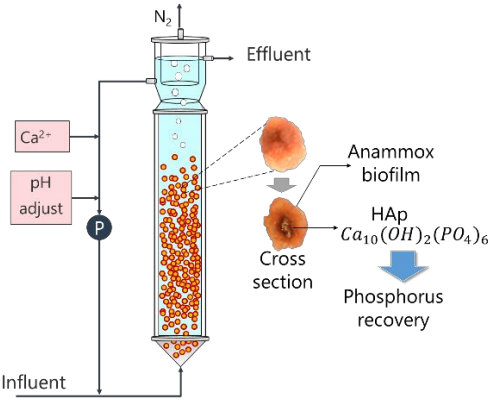

Figure 1. Reactor configuration used in this study

2.3 Sampling and analysis

Influent and effluent samples were collected from the reactor every two days, filtered by 0.45-μm-pore-diam membrane filter and stored in a refrigerator at 4 °C before analysis. Nitrogen components of NH4+-N, NO2−-N and NO3−-N were analyzed by an Agilent 7100 capillary electrophoresis (CE) system (Agilent Technologies, Wilmington, USA). Total phosphorus and other inorganic

elements were analyzed by an Agilent 720 inductively coupled plasma optical emission spectroscopy (ICP-OES) system (Agilent Technologies, Wilmington, USA). pH was monitored by a pH meter (TOA, HM-30V).

2.4 Sludge analysis

Sludge samples were taken from different heights (reactor heights of 23 cm, 43 cm, 63 cm) of the reactor for sludge analysis. The VSS (volatile suspended solid) and SS (suspended solid) were analyzed according to APHA standard methods.

A fluorescence in situ hybridization (FISH) analysis was conducted on microtome section of typical composite granule in the reactor obtained from the end of the operation period to reveal the microbe distribution. Fixation and FISH with fluorescently monolabeled oligonucleotide probes was conducted according to standard FISH protocol provided by the SILVA database (Llobet-Brossa et al., 1998, Manz et al., 1992).

3. Results and Discussion

Table 1 shows the summary of the operation performance in this expanded bed reactor reactor.

Table 1 Performance summary of this study

Phase	TN removal eff. (%)	NRR (gN/L/d)	Eff. TP conc. (mg/L)	TP removal eff. (%)	PRR (gP/L/d)
0	84.8±4.1	8.48±0.41	6.84±1.26	70.0±5.5	0.25±0.02
1	86.9±1.7	2.17±0.04	6.54±1.99	71.3±8.7	0.06±0.01
2	87.6±3.4	3.07±0.12	8.58±3.56	62.4±15.6	0.06±0.01
3	89.1±2.1	4.46±0.10	9.40±1.95	58.8±8.5	0.05±0.01
4	88.9±2.3	6.67±0.18	12.67±1.55	44.4±6.8	0.05±0.01
5	88.3±1.8	8.83±0.18	15.66±1.97	31.3±8.6	0.05±0.01
6	86.6±2.8	8.66±0.28	7.88±1.22	84.2±2.4	0.30±0.01
7	84.5±4.9	8.45±0.49	8.36±3.25	91.2±3.7	0.63±0.06

During the operation period, an average TN removal efficiency of 87.4 % was obtained while the NLR range from 2.5 to 10 gN/L/d. The average TP removal efficiency was 67.6 % with an influent TP concentration of 22.8 mgP/L in period 1-5. However, the TP removal efficiency was decreased with shorter HRT. Ca^{2+} was added into the recirculation system in phase 6 and 7. The increasing of TP removal efficiency indicated that Ca^{2+} can obviously increase P recovery efficiency.

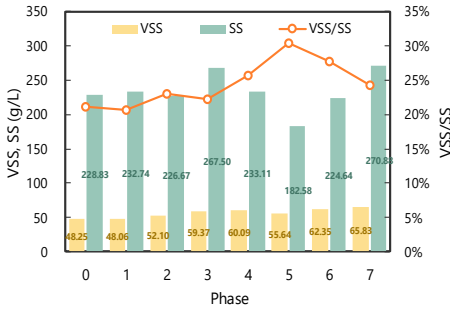

Figure 2. Sludge characteristics

The VSS concentration was gradually increased during this process and up to 65.83g/L in phase 7. A very high SS concentration was observed in this reactor rose from 228.83g/L in Phase 1 to 270.88 g/L in Phase 7 mainly due to the mineral precipitation of calcium and phosphorus. The VSS/SS proportion increased with NLR/PLR but decreased to 25% due to Ca^{2+} input and increase of phosphorus load from Phase 6 and Phase7.

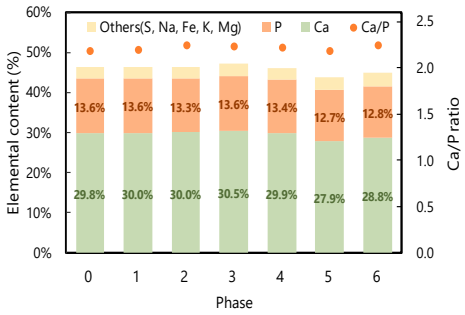

Fig. 3 Elemental content of sludge

The results of the content of P and Ca indicated that granule sludge in this process contains high Ca and P concentrations. More than 40% of the sludge is composed of $Ca_x(PO4)_y$. The proportion of Ca/P contained in the sludge was within the range of 2.1- 2.3, showing a composition close to 2.15 of HAP.

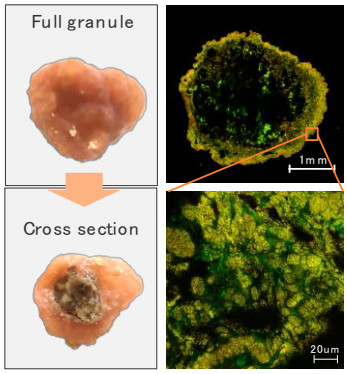

Fig. 4 Fluorescence in situ hybridization analysis for full granule and cross section. (Yellow for "Ca. Kuenenia stuttgartiensis" and "Ca. Brocadia anammoxidans"; green for most of the bacteria.)

The FISH image results indicated that anammox bacteria mainly distributed in the outer layer of the granule and anammox bacteria predominated in the most bacteria. The fluorescence intensity in the inner part was obviously lower than that of the outer layer, which showed the low microbial density in the core of composite granules. The results of the Anammox bacteria mainly distributed in the outer side of granules. Anammox predominated in most bacteria.

4. Conclusions

(1) Simultaneous nitrogen removal and phosphorus recovery is realized in an anammox expanded granular sludge bed reactor operated at 15 °C.

(2) Nitrogen removal efficiency of 85-89% at nitrogen loading rate of 10 gN/L/d was obtained.

(3) TP removal efficiency of 84.2% at 50 mg-TP/L and 91.2% at 100 mg-TP/L were obtained with proper Ca/P ratio and pH control.

(4) Two-layer structure of anammox biofilm attached to calcium phosphate inner core was demonstrated.

Beach Nourishment as an Adaptation to Future Beach Loss due to Sea Level Rise in Thailand

○Chatuphorn Somphong[1*], Keiko Udo[2], Sompratana Ritphring[3], Hiroaki Shirakawa[4] and So Kazama[2]
[1]Graduate School of Engineering, Tohoku University, Sendai 980-8579, Japan
[2]Graduate School of Environmental Studies, Tohoku University, Sendai 980-8579, Japan
[3]Faculty of Engineering, Kasetsart University, Bangkok 10900, Thailand
[4]Graduate School of Environmental Studies, Nagoya University, Nagoya 464-8601, Japan

*E-mail: Chatuphorn.Somphong.p1@dc.tohoku.ac.jp

Abstract
A recent study suggested that in the future (2081-2100), Thailand sandy beach areas were projected to be lost approximately 46%-72% of its current condition due to sea level rise (SLR) based on Intergovernmental Panel on Climate Change's (IPCC) projection of SLR. This study proposes a framework and provides preliminary results of sand volume and costs required for beach nourishment for each coastal zone in Thailand by using Yoshida method. The results indicate that it would require a minimum of 1,062 million USD (RCP2.6) to a maximum of 3,190 million USD (RCP8.5) to keep all the beaches at present width. The results of this study can be used as an overview and will be useful for decision makers to develop more feasible adaptations plan in Thailand.

Keywords: Beach nourishment, Sea level rise, Beach loss

1. Introduction
The global sea level rise and climate change can result in coastal erosion and cause a serious problem for the population at the low-laying coastal area [1)]. The IPCC 5th assessment reports also showed that the projection of regional sea level rise along Thailand's coastlines ranges between about 0.39-0.61 m. Recently, Ritphring et al. [2)] has projected the sandy beach loss by the future sea level rise for entire Thailand's coastlines based on 4 Representative Concentration Pathway (RCP) scenarios and indicated, by 2081-2100, Thailand possibly loss 46-72% of the present beach areas.

The sea level rise may cause the physical and socio-economic damages to the coastal regions. Since Sandy beach is one of the most important coastal resources as tourism areas or environmental preservations function. Therefore, it is important to preserve the beach areas. Yoshida et al.[3)] proposed a framework for beach nourishment as an adaptation to beach erosion induced by sea level rise for the entire Japanese's coastlines and it aims to specify venerable beach areas and estimates the sand volume and costs to maintain beach width in terms of different beach functions. Since there is no adaptation plans to deal with the future sea level rise in Thailand. This study aims to develop a framework for a proper beach nourishment and estimate the sand volume and costs by using Yoshida method.

2. Method
Thailand's coastlines are located nearby the South China Sea (Fig. 1) and covers approximately 3,148 km including 2,055 km in the Gulf of Thailand (GOT) and 1,053 km in the Andaman Sea. The Department of Coastal and Marine Resources (DMCR) of Thailand have categorized beaches into 64 zones based on the physical characteristics of beaches, where 51 zones are composed of sandy beaches. Generally, sandy beaches in Thailand has a small beach width with entirely-averaged of 34.8 m. The sand particle size is averagely 0.3 mm and the beach slopes range between 1-14 degrees [2)].

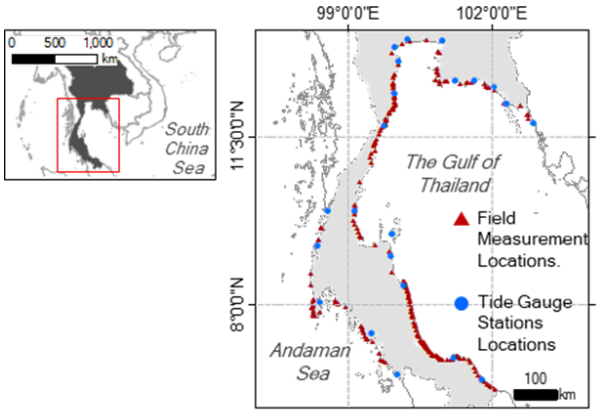

Fig. 1 Study Area

The beach nourishment volume estimation in present study followed Yoshida's method [3)] in which the optimal nourishment volume was determined based on the concept of the Bruun rule [4)].

The concept of beach nourishment for keeping beach for a design width (Y_*) is shown in Fig. 2. The profile increases by adding sand with the amount of B. After the nourishment, the shoreline would retreat due to sea level rise. The nourishment can maintain the future beach width to larger or equal to Y_*.

The beach model was based on the assumption of the equilibrium profile concept [5]. When sea level rise occurs, to maintain the equilibrium profile, the beach profile needs to be raised vertically to compensate the amount of sea level rise. Based on this assumption, the sand volume can be calculated by equation (1).

$$V_p = BY_0 + \int_0^{W_*} \left(Ay^{2/3} + B\right) dy - \int_0^{W_*} \left(Ay^{2/3}\right) dy \quad (1)$$

where Vp is the profile change volume (m^3/m), Y_0 is the dry beach width, A is scaling parameter, B is the height of beach nourishment, i.e. the amount of vertical increase of equilibrium profile, to maintain the beach width to be protected, Y_*, and W_* is the cross-shore distance to closure the depth h_*. The amount of vertical increase of equilibrium profile B can be described in equation (2) which is modified from the Bruun equation [4].

$$B = S - \left(\frac{h_* + B_h}{W_*}\right)(Y_0 - Y_*) \quad (2)$$

where S is the sea level rise, h_* is the closure depth and B_h is the berm height. The amount of sea level rise after beach nourishment causes an allowable retreat (Y_0 -Y_*) after the profile increases the amount of B. The beach data set used in this study are from Ritphring et al.'s study including sea level rise data, sediment size, and beach slope. It should be noted that this study assumes that the native sediment size and the filling sediment size are same and the design width (Y_*) is the beach width at present condition of each coastal zone.

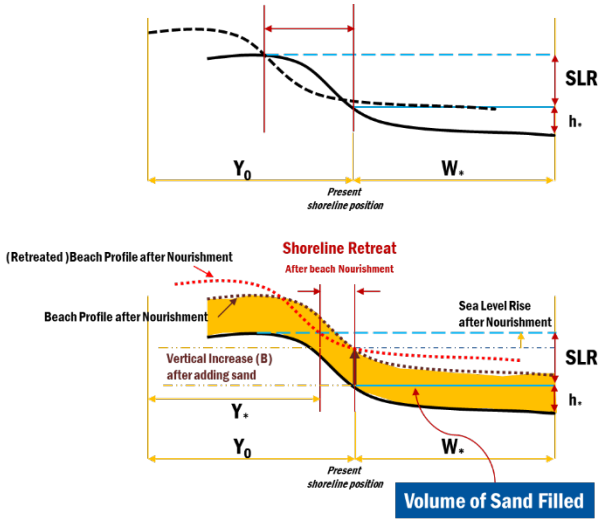

Fig. 2 The concept of beach nourishment for keeping beach width for each option

3. Results

This study calculated the beach nourishment volume and the costs for each Thailand sandy beach zone. Fig. 3 shows the sand volume required for the nourishment of each RCP scenarios and indicated that it would need a minimum of 193 million m^3 (RCP2.6) to a maximum of 303 million m^3 (RCP8.5) to preserve the existing shorelines. According to the Thai government's coastal engineering's project reports, a cubic meter of sand costs approximately 5.5-10.5 USD. Hence, the costs of beach nourishment could reach the minimum of 1,062 million USD to the maximum of 3,190 million USD to keep the shorelines at the present position for all sandy beach zone as shown in Fig. 4.

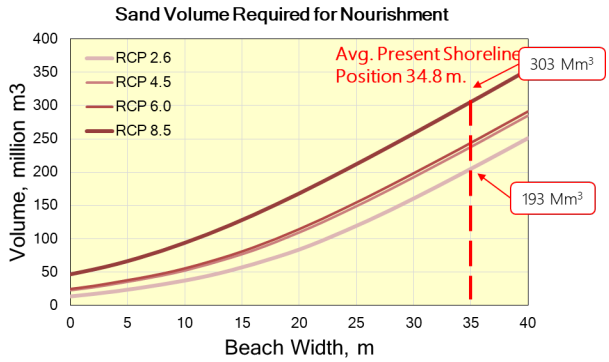

Fig. 3 Total sand volume required for beach nourishment for 4 RCP scenarios.

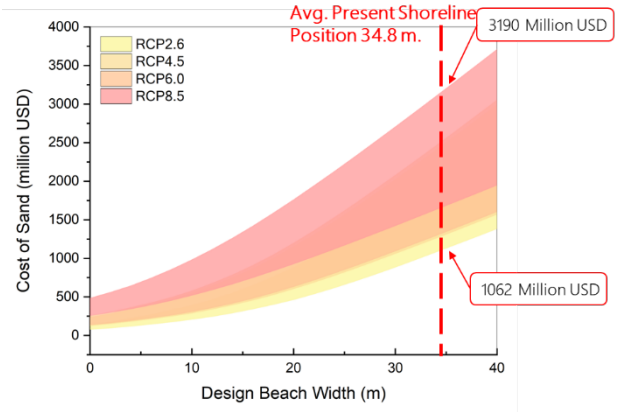

Fig. 4 Costs of sands required for entire coastlines for 4 RCP scenarios.

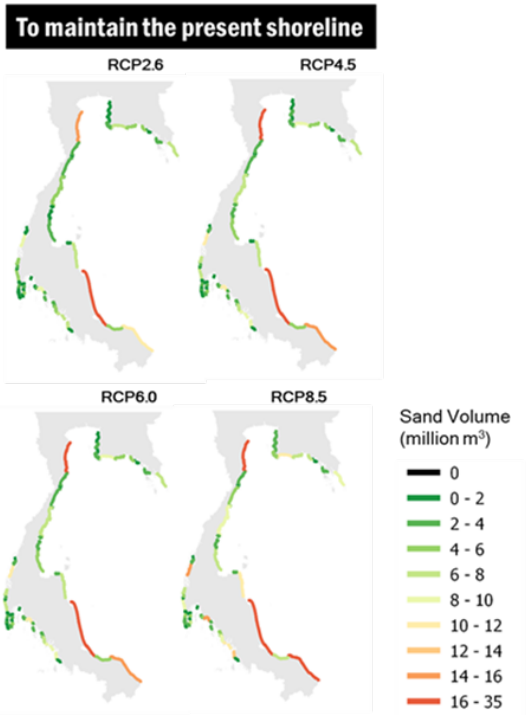

Fig. 5 The volume of sand for beach nourishment for each sandy beach zone

This study also shows the zonal beach nourishment volume and its costs in Fig 5 for each beach zone. By overall, to preserve the present beach width, sandy beach zones in the lower Gulf of Thailand need larger amounts of sand than the other part. This is because of the beach width in those areas are larger compared to the upper Gulf of Thailand and the Andaman Sea.

4. Conclusions

This study provides preliminary results of sand volume and costs required for beach nourishment for each coastal zone in Thailand for keeping beach width in present condition. However, this is only one-time nourishment (to a future period, 2081-2100) and this study only considered beach the impact of Sea-Level Rise and the beach replishment time interval should be assessed in future work. The benefit of the beach is needed to be evaluated to determine optimum beach widths and further cost-benefit analysis is required for realistic nourishment in design practice.

References

1) Roshanka Ranasinghe, David Callaghan, Marcel J. F. Stive : Estimating coastal recession due to sea level rise: beyond the Bruun rule. Climatic Change, 110, 561–574, 2012.
2) Sompratana Ritphring, Chatuphorn Somphong, Keiko udo, So kazama : Projections of future beach loss due to sea level rise for sandy beaches along Thailand's coastlines, Proceedings from the International Coastal Symposium (ICS) 2018 (Busan, Republic of Korea). Journal of Coastal Research, Special Issue No. 85, 16–20, 2018.
3) Jun yoshida, Keiko udo, Yuriko takeda, Akira mano : Framework for proper beach nourishment as an adaptation to beach erosion due to sea level rise. In: Green, A.N. and Cooper, J.A.G. (eds.), Proceedings 13th International Coastal Symposium (Durban, South Africa), Journal of Coastal Research, Special Issue No. 70, 467-472, 2014.
4) Per Bruun : Sea-Level rise as a cause of shore erosion, Journal Waterways, and Habors Division. ASCE, 88, 117-132, 1962.
5) Robert G. Dean: Equilibrium beach Profiles: characteristics and applications. Journal of Coastal Research, 7(1), 53-84, 1991.

The impact of spatial discretization scale on urban hydrological modeling performance and prediction

○Qing Chang[1*], Yoshiya Touge[1], So Kazama[1]
[1]Graduate School of Engineering, Tohoku University, Sendai 980-8579, Japan

*E-mail: chang.qing.q3@dc.tohoku.ac.jp

Abstract
Model subdivision is used to capture spatial heterogeneity in input parameters and it is well-established that spatial resolution (i.e., degree of aggregation) affects model output. However, a general consensus about the effect does not exist. The objective of this study was to investigate the effects of spatial resolution on model predictions in an urban catchment, and to understand the mechanism(s) responsible for the scale effect. The general approach is to develop models at various spatial resolutions, perform simulations, and compare the predictions of total outflow volume and peak flow. Models were developed on the basis of actual drainage networks, urban parcels and specific land use. Simulations were performed by using the EPA Storm Water Management Model (SWMM), and model output was compared for 50 storms. There was very little difference in the total annual outflow volumes predicted by the different resolutions. However, peak flows showed a dual scale effect. Peak flow reduced with model aggregation, which can be explained by differences in infiltration. The result of independent calibration, all the models showed good performances. The performance of the calibrated models were equal to or better than the high resolution model which meant that calibration could completely compensate models' scale effect. The consideration of EIA (effective impervious area) as a calibration parameter increased performance of calibration period but decreased performance in validation period which indicated the importance of detailed EIA identification.

Keywords: Spatial resolution, Model performance, Automatic calibration, EIA (effective impervious area)

1. Introduction
Urbanization had significantly altered the land cover and geomorphology characteristics of natural catchment. Consequently the hydrological processes in urbanized area are quite different and more complex compared with natural state. The large proportion of impervious area decreased infiltration capacity and increased catchment response time, meanwhile manmade structures like roofs, roads and channels largely impacted overland flow and runoff routing process. Thus it is essential to make an accurate representation or characterization of urbanized catchment for hydrological modeling.

Modeling urban hydrological process at proper scale is not a trivial issue. However, increasing the modeling detail and reducing model uncertainty are naturally two contrary targets. Thus, practically speaking, a compromise or tradeoff should be find between these targets (Pertrucci, 2014). In recent 10 years, the computational capacity and availability of high resolution distributed data had increased in a large degree. As a consequence, more and more researchers build up their model in high resolutions and using detailed methods. Schubert et al. (2012) emphasized importance of the rooftop footprints extraction and found that the rooftop representation in model could improve the model performance. Chang et al. (2015) explored the interactions between 1d sewer flow and 2d surface flow and different rooftop drainage physics. Leandro et al. (2016) had pointed out the importance of identify heterogeneity urban key features (roof type and land surfaces) in successful urban flood modeling. Most recent efforts in this category focused on the impact of collecting inlets modeling in urban flood simulation (Chang et al, 2018; Jang et al, 2018). Both studies claimed the necessity of inclusion of inlets for accurate flood extent and duration estimation because these inlets mean a more realistic representation of the actual drainage capacity between surface and sewer system.

All these research modeled urban hydrological processes at very fine scales (single rooftop or urban blocks), and this called for a lot of tedious work in delineating and data processing. Recent development, however, posed a possibility to overcome this problem. The public available database like the Open Street Map, can provide information like roof top footprint and detailed surface land use distribution which can be directly transferred to objects in GIS tools. On the other hand, (semi)automatic surface delineation tools had been developed and it can largely alleviate the model building work. Sanzana et al. (2016) presented a semi-automatic tool Geo-PUMMA which can generate well-shaped vector meshes or Urban Hydrological Elements (UHEs). In order to avoid the tedious task of building the SWMM model, Warsta et al. (2017) developed a tool called GisToSWMM5 that can automatic generate raster based sub-catchments as well as their parameters that can be directly used in model. A more recent work is using deep learning technology to identify the buildings or rooftops footprints all over the America.

Although it is an irreversible trend to model urban hydrology at higher resolution and in more detailed method,

the benefit and drawbacks of doing so should be further discussed. One of the concerns was that the high resolution may lead to the increase of uncertainty or over-parameterization (Pertrucci, 2014). The other concern is the existence of effective parameters. These effective parameters can representing a global hydrological behavior, and some of them cannot be directly measured or linked to geographical data. This means that some low resolution can have same performance with more detailed model and can save more resources. What is more, although the high resolution model can provide simulate more detailed hydrological processes, most of the current calibration technology are focused on fitting the hydrograph data of one or few points. This raise an issue called equifinality which means that the different parameter sets may produce equal model performance. This also reduced the fidelity of the simulated results at the local scale of a distributed model.

Therefore, the scale issue of distributed model is an important question to be understood. It is also a naturally concomitant problem in urban hydrology. The research of scale or resolution issues in urban hydrology had a long history. One of the earliest studies was conducted by Zaghloul (1981), who studied the effect of surface discretization on simulated runoff applying SWMM to one hypothetical and four real urban catchments in the United States, Australia and Canada. Stephenson (1989) studied the dependency of model parameter values on the level of surface discretization for a 0.74 ha residential catchment in South Africa. Park et al. (2008) studied the effects of spatial resolution on simulated runoff and pollutant loads using SWMM for an urban catchment in South Korea. Elliott et al. (2009) studied the effect of aggregation of stormwater control devices for a small medium-density catchment in New Zealand (0.83 km2) with primarily residential land-use using the dynamic stormwater model MUSIC. Ghosh and Hellweger (2012) evaluated the effects of spatial resolution on simulated runoff using SWMM and both real and artificial networks in a 3.7 km2 catchment dominated by residential housing. While both Ghosh and Hellweger (2012) and Park et al. (2008) reported that the simulated runoff volume was not affected by perturbations in spatial resolution, Stephenson (1989) observed a reduction of simulated runoff volume with increasing sub catchment aggregation. In terms of runoff peaks, simulations were clearly affected by variations in spatial resolution in this study. Whereas Stephenson (1989) and Elliott et al. (2009) reported similar observations with increasing sub-catchment aggregation, Ghosh and Hellweger (2012) and Zaghloul (1981) reported both increase and decrease of peak flow for lower catchment resolutions. While the variation reported in Ghosh and Hellweger (2012) were found for the same catchment but different storms, Zaghloul (1981) found these results for same storms but different catchments. However, these research are always lack of a detailed description of how the parameters values were determined during the change of scale. One exception was G.krebs et al. (2014), who used the method of area weight average to determine the parameters across different resolutions. However, the value of one important parameter EIA (effective impervious area) was not maintained during the sub-catchment upscale process. What is more, most of these previous studies neglect a calibration process. Those who conducted calibration did not or failed to calibrate each model with different resolutions to assess how calibration can compensate the scale non-linearity of the model.

The objective of the present study is to evaluate the effects of horizontal spatial discretization on performance of urban hydrology model. The EPA Storm Water Management Model was used in this study because this model is one of the most popular model in urban hydrology simulation. Three questions were attempted to be answered in this research:

(1) What is the impact of spatial resolution change on model performance?

(2) If calibration can compensate the scale effect and how the calibrated parameters will change?

(3) If the calibrated parameters have the same performance at smaller local scale?

The evaluation is performed using model fit and performance criteria. The improvement of model performance obtained with an automatic calibration process is also investigated. The results of this study can help modelers define the horizontal spatial discretization for their models by better perceiving its influence on model performance and model prediction uncertainties.

2. Method

Study site description

We chose the Kunimigaoka area (KA) in Sendai City, Japan for the case study. KA is located in the north-western part of the uptown of Sendai City, which covers approximately 50 hector with a medium gradient slope topography. KA is featured with a temperate monsoon climate and the annual average rainfall and temperature are 1254 mm and 12.4C, respectively. KA is an old uptown where urbanization degree is rather complete and the land use shows little change after 2000. The urban land use accounts for over 90% of the total in this region. The storm water was firstly drained to a regulating pond and then to a downstream river. The drainage system of KA can be divided into two parts, one being the sewer network in the Northern part of KA which accounted for most of the drainage areas; the other is a located in the southern part beside the regulating pond. The whole catchment can be divided into two independently drained sub area: a larger one in the North part accounting for around 45 hector and a small one in the South with an area of 5 hector. Those 2 sub areas drained to the pond by circular pipes with diameters of 2400 mm and 450 mm.

Data preparation

The DEM of KA was available in the form of a high-resolution (5x5m) elevation data set, which was provided and quality controlled by the Land and Resources Department of Japan. In order to represent the blockage effect of buildings on surface flows, the building profiles were distinguished using the planar graph and Google satellite image.

The underground pipeline data were obtained from Sewer Administration Office of Sendai City which contained geographic and geometric information of more than 400 pipelines and manholes. Most of the pipes were circular with diameters ranging from 0.3 to 2.4 m, while some pipes were rectangular whose widths and heights varied from 0.4 to 0.8 m. The pipe slopes showed a wide range, varying from 0.5 to 38%.

The rainfall was collected by two tipping-bucket rain gauges within the catchment. The record resolution of the

rain gauge was 0.2 mm and 1minute. Since these rain gauge had not yet collected enough data, some additional rainfall data were got from the Japan Metrological Agency. These rainfall data was collected by a metrological station at Sendai city which was around 4.2 km to the study site.
At the outlet, flow rate is calculated from water level measurements at 5 min intervals obtained by two field cameras and velocity measurements at different levels. The water level–flow rate relationship is obtained from a previous measurement campaign. There are some very small dry weather flow rate, may be due to ground water exfiltration, is subtracted from records in order to obtain the storm water flow rate. Continuous measurements used for this study cover the period from the 26th of February to the 29rd of June 2018.

The Storm Water Management Model (SWMM)

The EPA Stormwater management model (SWMM) was selected as the modelling platform for this study. SWMM was primarily developed for urban areas and allows short- and long-term simulations for both water quantity and quality (Huber and Dickinson, 1988; Rossman, 2010). Conceptually, catchments in SWMM are treated as nonlinear reservoirs, which receive inflows from precipitation and adjacent catchments and generate different components of outflows and losses including surface runoff, infiltration, and evaporation. The surface storage available through ponding, surface wetting, and interception determines the capacity of these reservoirs. This capacity is defined in SWMM through the depression storage parameter and surface runoff is only generated when the catchment water depth exceeds the designated storage depth, at which the outflow is computed using the Manning's equation. Catchments may be subdivided into a pervious and an impervious sub-area (defined by the imperviousness parameter) with individual parameters (such as the depression storage or Manning's n for overland flow) assigned for either sub-area. While available surface water over the entire catchment is subject to evaporation, infiltration occurs only for water on the pervious fraction of the catchment (Rossman, 2010). In this study, flow routing computations used the dynamic wave theory and infiltration from pervious areas was based on the GREEN_AMPT method (Rawls et al., 1992).

References

1) Chang, T. J., Wang, C. H., & Chen, A. S. (2015). A novel approach to model dynamic flow interactions between storm sewer system and overland surface for different land covers in urban areas. Journal of Hydrology, 524, 662-679.
2) Chang, T. J., Wang, C. H., Chen, A. S., & Djordjević, S. (2018). The effect of inclusion of inlets in dual drainage modelling. Journal of Hydrology, 559, 541-555.
3) Elliott, A. H., Trowsdale, S. A., and Wadhwa, S. (2009). "Effect of aggregation of on-site storm-water control devices in an urban catchment model." J. Hydrol. Eng., 14(9), 975–983
4) Ghosh, I., Hellweger, F. L., and Fritch, T. G. (2006). "Fractal generation of artificial sewer networks for hydrologic simulations." Proc., 2006 ESRI International User Conf., Environmental Systems Research Institute (ESRI), Redlands, CA.
5) Huber, W.C., Dickinson, R.E., 1988. Storm Water Management Model Manual, Version 4: User's Manual, EPA/600/3-88/001a. US EPA, Athens, Georgia, USA.
6) Jang, J. H., Chang, T. H., & Chen, W. B. (2018). Effect of inlet modelling on surface drainage in coupled urban flood simulation. Journal of Hydrology, 562, 168-180.
7) Krebs, G., Kokkonen, T., Valtanen, M., Setälä, H., & Koivusalo, H. (2014). Spatial resolution considerations for urban hydrological modelling. Journal of hydrology, 512, 482-497.
8) Leandro, J., Schumann, A., & Pfister, A. (2016). A step towards considering the spatial heterogeneity of urban key features in urban hydrology flood modelling. Journal of Hydrology, 535, 356-365.
9) Park, S. Y., Lee, K. W., Park, I. H., and Ha, S. R. (2008). "Effect of the aggregation level of surface runoff fields and sewer network for a SWMM simulation." Desalination, 226(1–3), 328–337.
10) Petrucci, G., & Bonhomme, C. (2014). The dilemma of spatial representation for urban hydrology semi-distributed modelling: Trade-offs among complexity, calibration and geographical data. Journal of Hydrology, 517, 997-1007.
11) Rawls, W.J., Ahuja, L.R., Brakensiek, D.L., Shirmohammadi, A., 1992. Infiltration and soil water movement. In: Maidment, D.R. (Ed.), Handbook of Hydrology. McGraw-Hill, New York, USA, pp. 5.1–5.51.
12) Rossman, L.A., 2010. Storm Water Management Model User's Manual Version 5.0, EPA/600/R-05/040, US EPA National Risk Management Research Laboratory, Cincinnati, Ohio, USA.
13) Sanzana, P., Gironás, J., Braud, I., Branger, F., Rodriguez, F., Vargas, X., ... & Jankowfsky, S. (2017). A GIS-based urban and peri-urban landscape representation toolbox for hydrological distributed modeling. Environmental Modelling & Software, 91, 168-185.
14) Schubert, J. E., & Sanders, B. F. (2012). Building treatments for urban flood inundation models and implications for predictive skill and modeling efficiency. Advances in Water Resources, 41, 49-64.
15) Stephenson, D. (1989). "Selection of stormwater model parameters." J. Environ. Eng., 115(1), 210–220.
16) Warsta, L., Niemi, T. J., Taka, M., Krebs, G., Haahti, K., Koivusalo, H., & Kokkonen, T. (2017). Development and application of an automated subcatchment generator for SWMM using open data. Urban water journal, 14(9), 954-963.
17) Zaghoul, N. A. (1981). "SWMM model and level of discretization." J. Hydraul. Div., 107(11), 1535–1545.

Using MODIS to detect crop type changes in the Aral Sea Basin in the 21st Century

○Mbugua Jacqueline Muthoni*[1], Yoshiya Touge [1], So Kazama[1]

[1]Graduate School of Engineering, Tohoku University, Sendai 980-8579, Japan

*E-mail: mbugua.jacqueline.muthoni.s8@dc.tohoku.ac.jp

Abstract

The Aral Sea Basin in Central Asia is a region plagued by a severe water crisis. The Union of Soviet Socialist Republics (USSR); installed a massive scale irrigation project here. This led to a rapid expansion of irrigation in the region from the late 19th century until the collapse of the USSR in 1991. Extensive irrigation in the Aral Sea Basin has resulted in some emerging environmental problems. Central Asia is not only a region plagued by excessive water loss through low irrigation efficiency but is also faced with increasing soil salinity problems. This necessitates the cropping pattern to continuously change in order to allow crop growth. The main objective of this research is to clarify the local farming situation. The study assesses the crop type focusing on wheat and cotton which changes annually due to climate variability and as a strategy for farmers to adapt to irrigation induced problems such as increasing salinity levels. Crop type was identified through GPS drive recorder and camera data and the NDVI based phenology was assessed and checked against cropping calendar to identify representative phenology for crop type detection in a wider area. Some points located in regions that are heavily affected by salt in Uzbekistan showed great changes in the crop type suggesting local adaptation measures undertaken by farmers in place to mitigate the salinity.

Key words: Remote sensing, Irrigated crop type identification, MODIS

1 Introduction

Agriculture is the main water consuming sector in Central Asia and is responsible for approximately 90 percent of the total consumptive water use (Hoekstra, Chapagain, Aldaya, & Mekonnen, 2009). The main crops under irrigation are cotton, and cereal which includes wheat and rice, however, wheat is the most dominant crop in the region (Frenken, 2012). Cereals account for 49 percent of the total harvested irrigated crops in the Central Asia region. Of this figure, wheat alone represents 39 percent of the total. Cotton is the second most harvested crop accounting for 23 percent average of the total harvested irrigated crops in the region from 2005 to 2011.

Cropping pattern; which refers to the proportion of area under different crops at a particular period of time is decided before the start of the irrigation season. A spatial-temporal analysis of the annual variability in the cropping pattern will not only help us to identify a dry year period or a drought period but also assess farmers' decision and judgment in the implementation of irrigation management practices at the farm scale.

Some studies using NDVI in the detection of crop type include: Yorozu et al, 2005 who uses seasonal change of n-NDVI which is normalized NDVI to prepare global 1-degree crop type dataset. This dataset is however fixed for all years. Kotsuki &

Tanaka, (2014) use seasonal NDVI to prepare a crop calendar for use in a hydrological model. These two studies use the GLCC dataset to divide irrigated and non-irrigated areas.

2 Study area

Analysis for the identification of crop type was carried out in Uzbekistan. One of the main challenges in crop type identification and mapping is the lack of quality data (Shao, Y., Lunetta, R.S., Ediriwickrema, J. and Iiames, 2010). The reason why Uzbekistan was selected is that this region has a larger availability of local data on irrigation and hydrology (collected from field based observations carried out between 2011 and 2017 excluding the year 2016) than the other Central Asia nations. Verification data was also readily available from FAO's AQUASTAT. Recently the cropping pattern in Uzbekistan has been changing drastically due to increasing salinity.

3 Methodology

3.1 Drive recorder and camera data assessment

A large amount of data in the form of pictures and video recordings with GPS information taken during previous visits to the study area were available. This data contained a record of various activities relating to irrigation and hydrology in the basin. Firstly, the drive recorder and camera data were assessed.

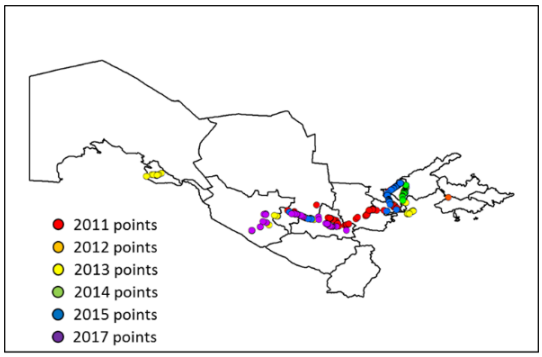

Figure 3.1 Distribution of total crop type data 2011-2017

This data was enlisted and used to pick out pictures and videos where the crop type could be identified. Information about the type of crop and the longitude and latitude coordinates were retrieved. The total number of crop type points retrieved from 2011 to 2017 was 482. Of this, more than 90 percent was dominated by cotton and wheat. See **Figure *3.1*** above.

3.2 NDVI phenology retrieval and analysis

Longitude and latitude coordinates obtained were then used to locate the individual points in a gridded Sinusoidal projection for the retrieval of NDVI data from MODIS. To retrieve NDVI based phenology for the different crops types identified in each year, MOD13Q1 product was employed. In order to reduce noise in the NDVI time series data, Best Index Slope Extraction (BISE) method was applied (Viovy, Arino, & Belward, 1992). Noise is the resultant impact to NDVI values due to cloud contamination, atmospheric variability and bidirectional effect.

3.3 Selection of representative phenology for different crop types

Quality data is a key requirement in order to produce representative phenology for different crops. Therefore, crop types which had insufficient representation were eliminated from further analysis. In this case, all crop types except cotton (61 percent), wheat (30 percent) and rice (4 percent) were removed from further analysis. The eliminated crop types are also not dominant in the Central Asia region. NDVI time series data was then plotted for each year for all the remaining points.

The resultant phenology data for each point was then referenced with the crop calendar information for that crop type. This was done in order to isolate noisy points which did not correspond to the crop calendar information provided. One of the major drawbacks of MODIS data is that the sensor has a course resolution. This may in turn cause the resultant phenology to have mixed pixels, especially when carrying out analysis in relatively small fields.

In order to obtain representative points, homogenous data is required. Therefore, points which exhibited mixed pixel properties were eliminated. This was done using an intelligent selection approach based on local knowledge (Zheng, Myint, Thenkabail, & Aggarwal, 2015). Crop types usually have unique NDVI signals which can be used for visual interpretation (Shao, Y.,

Lunetta, R.S., Ediriwickrema, J. and Iiames, 2010; Wardlow & Egbert, 2008). Visual analysis of NDVI signature has been utilized in a number of studies for land cover classification and crop type identification (Carrão, Gonçalves, & Caetano, 2008; Conrad, Colditz, Dech, Klein, & Vlek, 2011). ***Figure 3.2*** below shows the representative phenology derived after checking each point. After removing points with mixed pixel effect only wheat and cotton had enough points left to identify a trend and therefore pick representative phenology related to the cropping calendar.

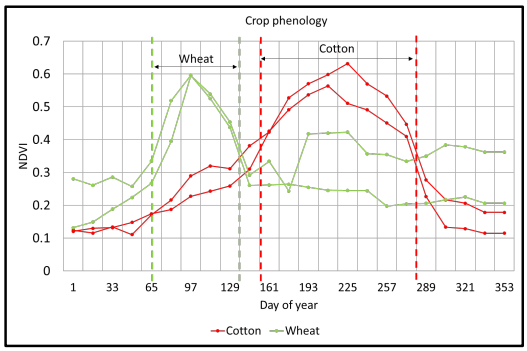

Figure 3.2 Representative phenology for wheat and cotton

3.4 Crop type identification in Uzbekistan region

To identify crop type, an algorithm was created based on observation of the phenology in the representative points. Different thresholds were set for the identification of crop type in a wider temporal and spatial scale. GLCC dataset was then employed to isolate irrigated cropland.

An evaluation of the crop type variability from 2001 to 2017 showed a temporal change in the crop type in majority of the farms in the study area. Due to the problems with irrigation infrastructure, farmers try to adopt to the situation using strategies such as switching to drought- or salt resistant crops (Bucknall et al., 2003) **Figure 3.3** below shows some points with changing crop type. This can be seen through changes in the NDVI based phenology evaluated from 2001 to 2010. These two points are located in some of the most salt affected regions in Uzbekistan; Khorezm and the Zeravshan river basin. Changes in the cropping pattern suggest the adaptation measures that the farmers could be undertaking to mitigate the salinity effect.

A

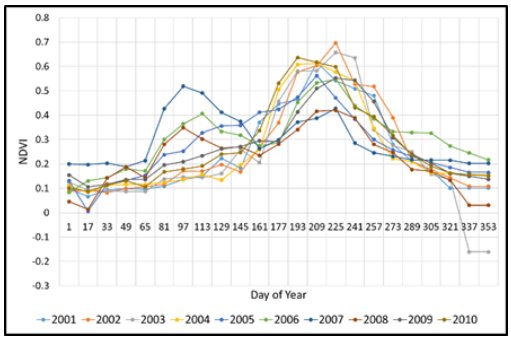

NDVI phenology 2001-2010 in a farm in Khorezm region Uzbekistan

B

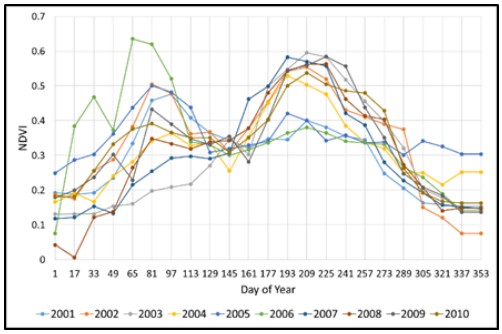

NDVI phenology from 2001-2010 in a farm in Zeravshan river basin Uzbekistan

Figure 3.3 NDVI phenology showing changes in crop type

4 Conclusion

The study found that majority of the points analyzed in the basin from 2001 to 2010 showed a variability in crop types. Some of the points are located in regions that are heavily affected by salt in Uzbekistan. Changes in the cropping pattern could suggest local adaptation measures undertaken by farmers to mitigate the salinity problem.

5 Acknowledgement

This paper is based on achievements of the collaborative research program (29G-11) of the Disaster Prevention Research Institute of Kyoto University.

6 Reference

Bucknall, J., Klytchnikova, I., Lampietti, J., Lundell, M., Scatasta, M., & Thurman, M. (2003). Irrigation in Central Asia. Social, economic and environmental considerations. *Europe and Central Asia Region*, (February), 104. Retrieved from www.worldbank.org/eca/environment

Carrão, H., Gonçalves, P., & Caetano, M. (2008). Contribution of multispectral and multitemporal information from MODIS images to land cover classification. *Remote Sensing of Environment*, *112*(3), 986–997.

Conrad, C., Colditz, R. R., Dech, S., Klein, D., & Vlek, P. L. G. (2011). Temporal segmentation of MODIS time series for improving crop classification in Central Asian irrigation systems. *International Journal of Remote Sensing*, *32*(23), 8763–8778. http://doi.org/10.1080/01431161.2010.550647

Frenken, K. (FAO). (2012). *Irrigation in Central Asia in figures. AQUASTAT Survey-2012. Irrigation in Central Asia in figures. AQUASTAT Survey-2012* (Vol. 39). Retrieved from http://doi.wiley.com/10.1111/j.1467-6346.2007.00685.x

Hoekstra, A. Y., Chapagain, A. K., Aldaya, M. M., & Mekonnen, M. M. (2009). Water Footprint Manual State of the Art 2009. *Water Footprint Network*, (november), 131. Retrieved from http://waterfootprint.org/media/downloads/WaterFootprintManual2009.pdf

Kotsuki, S., & Tanaka, K. (2014). Improvement of Global Crop Calendar Product using Satellite-Sensed Vegetation Indexes. *Journal of Japan Society of Civil Engineers, Ser. B1 (Hydraulic Engineering)*, *70*.

Shao, Y., Lunetta, R.S., Ediriwickrema, J. and Iiames, J. (2010). Mapping Cropland and Major Crop Types across the Great Lakes Basin using MODIS-NDVI Data. *Photogrammetric Engineering and Remote Sensing*, *75*(1), 73–84. http://doi.org/10.14358/PERS.76.1.73

Viovy, N., Arino, O., & Belward, A. S. (1992). The Best Index Slope Extraction (BISE): A method for reducing noise in NDVI time-series. *International Journal of Remote Sensing*, *13*(8), 1585–1590.

Wardlow, B. D., & Egbert, S. L. (2008). Large-area crop mapping using time-series MODIS 250 m NDVI data: An assessment for the U.S. Central Great Plains. *Remote Sensing of Environment*, *112*(3), 1096–1116. http://doi.org/10.1016/j.rse.2007.07.019

Yorozu, K., Tanaka, K., & Ikebuchi, S. (2005). Creating a global 1- degree dataset of crop type and cropping calendar through timeseries analysis of NDVI for GSWP simulation considering irrigation effect. In *85th AMS Annual Meeting, 19th conference of Hydrology* (p. Vol.6).

Zheng, B., Myint, S. W., Thenkabail, P. S., & Aggarwal, R. M. (2015). A support vector machine to identify irrigated crop types using time-series Landsat NDVI data. *International Journal of Applied Earth Observation and Geoinformation*, *34*(2015), 103–112.

Remote estimation of rice crop yield using MODIS Vegetation Indices data: A case study of Solo river basin rice field, Indonesia

○Vempi Satriya Adi Hendrawan[1], Daisuke Komori[1]
[1]Graduate School of Environmental Studies, Tohoku University, Sendai 980-8579, Japan

*E-mail: vempi@dc.tohoku.ac.jp

Abstract

Food security for half of the entire world's population relies on the rice supply. As one of the largest rice producer country in the world, Indonesia has faced a challenge to ensure the sustainability of rice production every year. Predicting the crop yield is one of the critical issues for the country that requires technical skill utilizing various methods and datasets. As one of the widely applied approaches, this study was done to develop a regression model for rice crop yield estimation using remote sensing imagery data. We applied the approach for a case study in the Solo river basin as one of the largest rice crops plain in the country. We employed Moderate Resolution Imaging Spectroradiometer (MODIS) Normalized Difference Vegetation Indices (NDVI) and Enhanced Vegetation Indices (EVI) as predictors and annual average yield data on a city scale as the dependent variable. We processed it in three main steps: (1) rice crop field masking, (2) extracting raw NDVI and EVI value averaged in each city for selected years, and (3) establishing regression crop yield model. We selected the year of 2007 and 2008 as samples. The results showed that the adjusted coefficient of the determination (R^2_{adj}) of both models are 0.215 and 0.238 respectively. From the result, it indicates a low correlation between yield and VI for the expected ripening period (November-December) for the October-January rice crops. Some factors were revealed presumably as a subject of uncertainty in this study. First, there was a lack of the quality of raw grid value due to atmospheric contamination and other optical noises. Second, there was an inconsistent use of yield data as a predictor. We used an annual average yield data on a city scale to build a model while the predictor is the vegetation phenology information from one crop season which is October-January rice crop. Therefore, a further analysis is absolutely needed to deal with the above issues in order to improve the model for estimating the crop yield.

Keywords: NDVI, EVI, Rice, Crop, Yield

1. Introduction

Food security for half of the entire world's population relies on the rice supply (FAO, 2004a). Rice production plays an important role in the economy of Asian countries, especially Southeast Asian countries (Timmer, 2009; Evenson and Rosegrant, 2003), as a region that annually produces approximately 150 million tons of rice grain or 25% of global rice production (Raitzer, 2009). Rice production has fallen short of consumption since 2000, while the global rice trade increased by more than 30% from 1995 to 2005 as the world's population growing at 1.1% annually (FAO, 2004b; OECD-FAO 2006). Furthermore, the impacts of climate such as temperature increases, rising seas, and changes in rainfall patterns, could lead to decreased crop production. The reduction of rice production in major rice-producing countries may trigger increases in rice prices, consequently causing food security issues (Son, 2013).

As one of the largest rice-producing country in the world (MoA, 2015), Indonesia has faced a challenge to ensure the sustainability of rice production every year. Predicting the crop yield is one of the critical issues for the country that requires technical skill utilizing various methods and datasets. Thus, timely and accurate prediction of rice crop yield at the country could allow for a more precise assessment of food production and better crop management strategies to provide solutions to food challenges.

Remote estimation of crop yield has been getting attention by many researchers since remote sensing technology allows in an advance way to capture any geo-parameters remotely in higher spatio-temporal resolution. Estimating yield using remote sensing technique is considered as an inexpensive and fast way as it is publicly available. It is also considered as a promising complement to the survey yield assessment that cannot be neglected to do as well (Lopestri, 2015).

Estimating crop yield using remote sensing data has been widely investigated since the early 1980s. Vegetation Indices (VI) has been recognized for its ability to monitor crops and as an estimator of crop yield by both using a single image or a time-series image (Lobell, 2013; Son, 2014; Sakamoto, 2014; Johnson, 2016). Previous studies proved that yield estimation using data from a single image at the peak of crop development showed good result. It encompassed the critical period for grain production. Moreover, yield estimation could be also done by extracting time-series VI value to phenology information as the estimation parameters. Both methods can be applied in any crop including rice in any area of interest.

As there is no physical correlation between VI value retrieved from optical sensor and yield in the real field, an

empirical model has been proposed as a commonly used model of crop yield estimation using remote sensing data. The empirical model has been often preferred because it requires fewer data and is simple to implement at a local or regional scale. Many researchers have coupled remote sensing data with crop models or agrometeorological models (Doraiswamy, 2004; Moriondo, 2007; Yuping, 2008). Crop growth simulation models are probably more accurate to estimate yield, but they require numerous specific inputs that are not always available (e.g. soil characteristics, management practices, agrometeorological data, and crop parameters). Therefore, the empirical model using without incorporating such kind of data seems more applicable since the approach is applied in a developing country where such data are challenging to be collected.

Among all of the available remote sensing products, The Moderate Resolution Imaging Spectroradiometer (MODIS) was selected to be used in this study. The reason to choose MODIS data are: (1) its fair spatial and temporal resolution that allows to monitor and mapping the vegetation at local or regional level, (2) having cloud-free images due to the high revisit frequency of the sensor (per one or two days), and (3) no cost and publicly available on the website. Thus, based on above several merits, we used MODIS as a predictor to establish crop yield estimation model in this study.

The main objective of this research is to remotely estimate rice crop yield using MODIS VI data for a case study in the selected major rice field in Indonesia. This paper discusses the applicability and capability of MODIS for assessing crop yield using simple linear regression using raw VI value. The robustness of the established models was evaluated by comparisons between the predicted yields and crop yield statistics in a city scale.

2. Method

2.1. Case study

Solo river basin was selected as a case study to estimate rice crop yield. Solo river basin is the largest river basin in Java island Indonesia with approximately 16,100 km2 of the total area and 600 km total length of the main river. As shown in Figure 1, the downstream of the river basin is characterized by a plain area which is suitable for crop cultivation. There are approximately 526,000 ha rice crop cultivated in the basin, or 26% of the total basin area. Total rice field area in this basin accounts 28% of the total rice field area in East Java which has a significant amount of production in Java and even in the national scale. There are mainly two rice-crop pattern system in the river basin (Shresta, 2016): (1) western part of basin rice cultivation pattern in October-January and February-June and (2) eastern part- rice cultivation pattern in December-April and April-June. It is varying spatially and temporarily based on local farmer's practice and climate condition.

The annual average precipitation is around 1,800-2,100 mm/year whose climate is dominated by a maritime monsoon climate (Iwami, 2017). There are two main seasons: (1) dry season during May-October and (2) wet season during November-March. Heavy rains usually occurred in December-February inducing flood causing damage to property and destruction of crops in the basin annually.

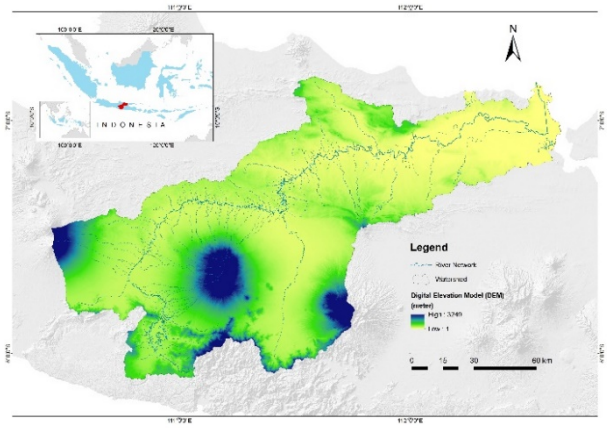

Figure 1 Solo River Basin

2.2. Data

In this study, three types of data were used.

1. MODIS surface reflectance data

Moderate Resolution Imaging Spectroradiometer (MODIS) 250-meter 16-day Vegetation Indices (VI) average value provided by the Land Processes Distributed Active Archive Centre (LP DAAC) were used to evaluate surface vegetation color condition. The Earth Observing System (EOS) Terra and Aqua MODIS surface reflectance MOD13Q1 and MYD13Q1 Version 6 products provide a VI value at a per pixel basis. There are two vegetation layers were used in this study. The first is the Normalized Difference Vegetation Index (NDVI) and the second vegetation layer is the Enhanced Vegetation Index (EVI), which has improved sensitivity over high biomass regions. The formulas for obtained NDVI and EVI are as follows:

$$NDVI = \frac{Rnir - Rred}{Rnir + Rred}$$

$$EVI = 2.5 \times \frac{Rnir - Rred}{Rnir + 6 \times Rred - 7.5 \times Rblue + 1}$$

where R_{Nir}, R_{Red} and R_{Blue} refer to near-infrared, red and blue bands of surface reflectance imagery images.

2. Land use layer map

The national land cover/land use database was provided by the Geospatial Information Agency (BIG). The vector layer of land use was obtained using Landsat Imagery map classification in 2010. Although it might be changing from year to year, we found that there were no big changes in the crop field area between 2007 and 2010. Therefore, we used that same crop field layer in this study.

3. City-level crop statistics

Agricultural data were provided by the Central Bureau of Statistic (BPS). BPS collect annual city level agricultural information across East Java and Central Java Province covering Solo river basin. Yield data (t/ha) for rice in 2007 and 2008 were obtained. Land use map was used for masking Vegetation Indices raster map. The Vegetation Indices from

MODIS surface reflectance data and the yield statistic were then employed to develop a regression model.

2.3. Methodology

We employed Normalized Difference Vegetation Indices (NDVI) and Enhanced Vegetation Indices (EVI) as predictors and annual average yield data on a city scale as the dependent variable. We processed it in three main steps: (1) image processing and data analysis, (2) rice crop field masking, and (3) establishing regression crop yield model.

1. Image Processing and Data Analysis

Two MOD13Q1 scenes (h28-v09 and h29-v09) were used covering the study area. Then a mosaic was done for each date within the month of November-December where a ripening stage was taken in place for October-January crop based on the crop calendar for the year of 2007 and 2008 as samples. GIS software was used to extract NDVI and EVI information of each date.

2. Rice Crop Field Masking

Based on field layer map, NDVI and EVI mask for each city crop field was obtained to isolate the disruption signal from another land use surface reflectance (Freund, 2005). The average of NDVI and EVI values per city mask was calculated. This was considered to represent the intercepted signal within the city mask when the yield value is an annual yield for each city.

3. Establishing Regression Crop Yield Model

Vegetation indices and agricultural data statistic were used to develop an empirical model to estimate crop yield. A number study as reviewed by Funk (2009) documented a close relationship between NDVI and EVI. Most of the studies showed the capability of a linear regression equation to model crop yield by various advance pre-processing and remote-sensing based approach. However, as a preliminary analysis, in this study, we used the raw value of Vegetation Index (VI) value of several dates in the ripening stage of October-January crop.

The regression model derived in this study as follows:

$$y = \sum_{i=1}^{m} \sum_{j=c}^{n} a_{ij} \times x_{ij} + b_0$$

where y is the crop yield, x is vegetation indices (NDVI and/ EVI), i represents the vegetation indices index, j represents the targeted month from c ton (12 months), a is regression slopes and b_0 is the model intercept.

3. Results and Discussion

In this paper, a crop yield model for the river basin scale was obtained based on the city-based mask of averaged NDVI and EVI value and the annual average rice yield data on a city scale. The yield model equation is shown in Table 1. From the adjusted coefficient of determination (R^2_{adj}) of both equations, it can be seen that there is no high correlation enough between yield and NDVI and EVI in the month of November and December by R^2_{adj} = 0.215 and R^2_{adj} = 0.238 for 2007 and 2008 model respectively. Figure 2 and Table 2 shows the actual yield from statistic data and the model estimation. Table 2 shows the percent error between actual and modeled city average yield.

Table 1 Yield Regression Model

Year	Regression Equation	R^2_{adj}
2007	Y = 6.226 – 4.103*NDVInov + 2.834*EVIdec	0.215
2008	Y = 6.565 – 2.789*NDVInov – 6.19*EVInov + 6.005*NDVIdec	0.238

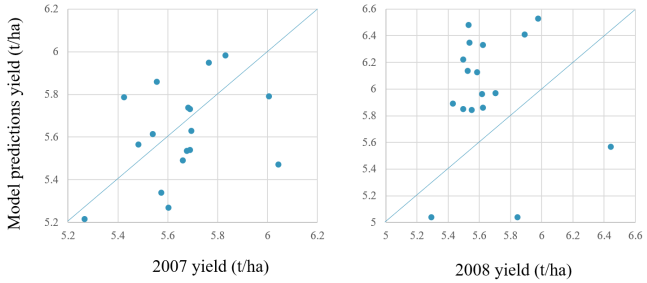

Figure 2 Actual and modeled yield

Table 2 Actual and modeled yield

City	2007			2008		
	Model (t/ha)	Data (t/ha)	Percent error	Model (t/ha)	Data (t/ha)	Percent error
Blora	5.27	5.10	3.35%	5.29	5.04	5.11%
Bojonegoro	5.57	5.34	4.32%	5.55	5.84	4.94%
Boyolali	5.48	5.57	1.50%	5.62	5.86	3.94%
Gresik	6.01	5.79	3.73%	5.89	6.41	8.05%
Karanganyar	5.68	5.74	1.01%	5.62	5.96	5.71%
Klaten	5.54	5.61	1.32%	5.71	5.97	4.36%
Kota Madiun	5.69	5.73	0.70%	5.63	6.33	11.10%
Surakarta	5.60	5.27	6.30%	5.58	4.83	15.38%
Lamongan	5.83	5.98	2.52%	5.98	6.52	8.40%
Madiun	5.69	5.54	2.71%	5.59	6.13	8.79%
Magetan	5.76	5.95	3.16%	5.53	6.48	14.65%
Ngawi	5.66	5.49	3.13%	5.43	5.89	7.81%
Pacitan	5.60	3.91	43.21%	5.37	4.65	15.43%
Ponorogo	5.56	5.86	5.15%	5.54	6.35	12.68%
Semarang	5.26	5.22	0.94%	5.84	5.04	16.03%
Sragen	5.68	5.53	2.61%	5.50	5.85	5.94%
Sukoharjo	5.42	5.79	6.32%	5.50	6.22	11.58%
Tuban	5.69	5.63	1.09%	5.52	6.14	9.98%

City	2007			2008		
	Model (t/ha)	Data (t/ha)	Percent error	Model (t/ha)	Data (t/ha)	Percent error
Wonogiri	6.04	5.47	10.41%	6.44	5.56	15.85%

From the result, it indicates a low correlation between yield and VI for the expected ripening period (November-December) for the October-January rice crops. Some factors were revealed presumably as a subject of uncertainty in this study.

1) Lack of the quality of raw grid value due to atmospheric contamination and other optical noises.
2) An inconsistent use of yield data as a predictor. We used an annual average yield data on a city scale to build a model while the predictor is the vegetation phenology information from one crop season which is October-January rice crop.

Another factor can also be assumed as a source of uncertainty as within one of crop field mask and among city-based mask could be contain mixed different crop type or crop system showing the different stage of reflectance of Vegetation Indices.

Therefore, a further analysis is absolutely needed to deal with above issues in order to improve the model for estimating the crop yield such as a time-series smoothing of vegetation indices approach that has been widely applied in remote sensing studies to remove such noises.

References

1) FAO. 2004a. Global Climate Changes and Rice Food Security. Rome: FAO.
2) FAO. 2004b. The State of Food Insecurity in the World. Rome: FAO.
3) OECD-FAO. 2006. “Agricultural Outlook 2006–2015.” In Organisation for Economic Co-operation and Development. Paris: OECD.
4) Timmer, C. P. 2009. A World without Agriculture: The Structural Transformation in Historical Perspective. Washington, DC: American Enterprise Institute.
5) Evenson, R. E., and M. Rosegrant. 2003. “The Economic Consequences of Crop Genetic Improvement Programmes.” In Crop Variety Improvement and Its Effects on Productivity: The Impact of International Agricultural Research, edited by Robert E. Evenson and Douglas Gollin. Wallingford: CABI Publishing.
6) Raitzer, D. A., J. Roseboom, M. K. Maredia, Z. Huelgas, and M. I. Ferino. 2009. Prioritizing the Agricultural Research Agenda for Southeast Asia: Refocusing Investments to Benefit the Poor. Bangkok: Asia Pacific Association of Agricultural Research Institutions.
7) N. T. Son , C. F. Chen , C. R. Chen , L. Y. Chang , H. N. Duc & L. D. Nguyen. 2013. Prediction of rice crop yield using MODIS EVI−LAI data in the Mekong Delta, Vietnam. International Journal of Remote Sensing.
8) MoA (Ministry of Agriculture). 2015. Rencana Strategi Kementrian Pertanian Tahun 2015-2019. Kementrian Pertanian Republik Indonesia. (Website: http://www.pertanian.go.id/file/ RENSTRA_2015-2019.pdf, citation on 11 November 2017).
9) Lopresti, M.F., Di Bella, C.M. and Degioanni, A.J., 2015. Relationship between MODIS-NDVI data and wheat yield: A case study in Northern Buenos Aires province, Argentina. Information Processing in Agriculture, 2(2), pp.73-84.
10) Lobell, D.B., 2013. The use of satellite data for crop yield gap analysis. Field Crops Research, 143, pp.56-64.
11) Son, N.T., Chen, C.F., Chen, C.R., Minh, V.Q. and Trung, N.H., 2014. A comparative analysis of multitemporal MODIS EVI and NDVI data for large-scale rice yield estimation. Agricultural and Forest Meteorology, 197, pp.52-64.
12) Sakamoto, T., Gitelson, A.A. and Arkebauer, T.J., 2014. Near real-time prediction of US corn yields based on time-series MODIS data. Remote Sensing of Environment, 147, pp.219-231.
13) Johnson, D.M., 2016. A comprehensive assessment of the correlations between field crop yields and commonly used MODIS products. International Journal of Applied Earth Observation and Geoinformation, 52, pp.65-81.
14) Moriondo M, Maselli F, Bindi M. A simple model of regional wheat yield based on NDVI data. Eur J Agron 2007; 26(3):266–74.
15) Doraiswamy PC, Hatfield JL, Jackson TJ, Akhmedov B, Prueger J, Stern A. Crop condition and yield simulations using Landsat and MODIS. Remote Sens Environ 2004; 92(4):548–59.
16) Yuping M, Shili W, Li Z, Yingyu H, Liwei Z, Yanbo H, et al. Monitoring winter wheat growth in North China by combining a crop model and remote sensing data. Int J Appl Earth Obs Geoinf 2008; 10(4):426–37.
17) Shrestha, B.B., Sawano, H. and Kuribayashi, D., 2007. Assessment of Disaster Damage due to Flood Hazard in the Solo River Basin of Indonesia.
18) Iwami, Y., Hasegawa, A., Miyamoto, M., Kudo, S., Yamazaki, Y., Ushiyama, T. and Koike, T., 2017. Comparative study on climate change impact on precipitation and floods in Asian river basins. Hydrological Research Letters, 11(1), pp.24-30.
19) Fruend, J. (2005). Estimating Crop Production in Kenya: A Multi-Temporal Remote Sensing Approach. Master’s Thesis (59 p.). Santa Barbara: University of California [December 2005].
20) Funk, C. and Budde, M.E., 2009. Phenologically-tuned MODIS NDVI-based production anomaly estimates for Zimbabwe. Remote Sensing of Environment, 113(1), pp.115-125.

Preliminary study of grape farmers' perception to changing climate in Takahata city, Yamagata prefecture, Japan

○ Sopha Soliya[1*], Daisuke Komori [1], Shinsuke Furuno[2], Eisuke Adachi[2], Noriko Kaneda[2]
[1]Graduate School of Environmental Studies, Tohoku University, Sendai 980-8579, Japan
[2]Yamagata Prefectural Government, Agriculture, Forestry and Fisheries Horticulture Promotion Division, Japan
[*]Email: sopha.soliya.r6@dc.tohoku.ac.jp

Abstract
This study examined the influence of climatic conditions toward grape cultivation in Takahata city, Yamagata prefecture. To do so, the historical of grape yields and climate data have been collected during the last 38 years. Then We have classified the yields of each year into two groups namely high and low yields years, and we have analyzed the climate data including monthly and seasonally of rainfall and temperature by applying the Principle Component Analysis (PCA). The results showed that in high yield years' have found the warm temperature and less rainfall in berry development and maturity phases. However, in low yield years' have appeared the cold temperature and heavy rainfall during those phases. In addition, this study investigated the grape farmers' perception to changing climates. The qualitative data has been conducted by using structure questionnaire forms and face to face interview by interviewing the farmers. The results showed that farmers' have perceived that the climatic factors including heavy rainfall and cold climate have negatively influenced to grape cultivation.

Keywords: Changing climate, Perception, Grape farmers

1. Introduction
Agricultural productions have been affected by changing climate (Adger et al.2007). In Japan, the annual precipitation and temperature have been confirmed of changes during the last decades (JMA., 2011). The changes are likely to affect fruit trees, vegetables and rice cultivation (Sugiura et al. 2012). Especially, grape berry has been impacted by temperature and sunlight on the skin coloration in last decade (Shinomina et al., 2015; Sugiura et al., 2017). The extremely events of changing climates and its responses are challenges for the farmers (Adger et al. 2007; Belliveau et al.2006). And, farmers' perception to changing climate is not well understood (Bradshaw et al., 2004). Most of the studies have been discussed aboutå the perception, adaptation and influenced climate to grape cultivation separately.

Hence, by understanding the influences of climatic conditions and farmers' perception to the changes, it would be provided us the preliminary fundamental data for developing adaptation strategy and it would lead to make the effective accountabilities and implementation of agricultural cultivation. Therefore, the objectives of this study are to examine the climatic conditions influencing grape cultivations and to investigate the grape farmers' perception to changing climate in Takahata city, which is located in Yamagata prefecture as a case study.

2. Study areas
Takahata city is selected as the study area, because it is ranked as the largest area of grape cultivation in the Tohoku region (MAFF 2016), and the grape cultivation is the first main source of income, following by rice, soba and etc. The total areas of grape farming are 268 hectares and the total number of grape farmers are 461 people (Takahata Town Hall Agriculture, 2018).

Grape growing areas in Takahata city, Yamagata prefecture, Japan

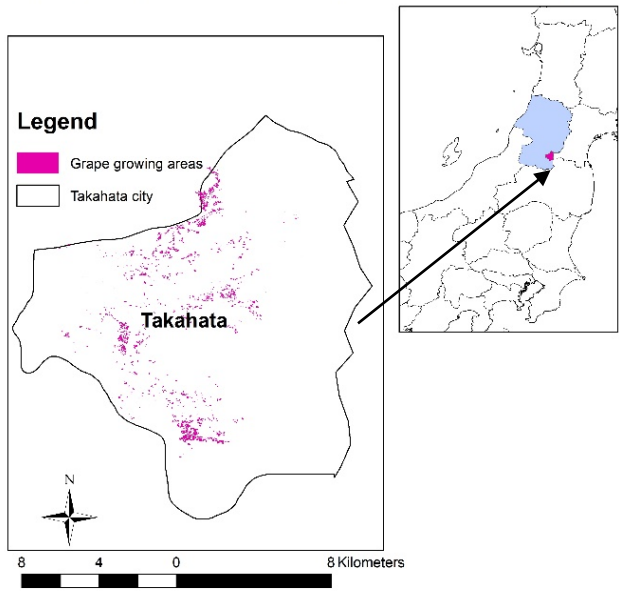

Figure 1: Location of study area

3. Methodology
1. Data collection: the data has been collected from the primary and secondary data sources, which is included qualitative and quantitative data as following examination:

Primary data: The qualitative data has been conducted by face to face interview by interviewing the farmers who have major income from grape cultivation. The questionnaire included multiple choices and open-and close-ended

questions. In addition, we also have discussed with key informants namely agricultural officers and field observation.

Secondary data: the quantitative data has been collected the historical of grape yields and climate data during the last 38years (1977-2015). The climate data obtained including daily, monthly and seasonally rainfall and temperature.

2. Data analysis

Quantitative data analysis: grape yields data has been classified into two groups namely high and low yields years. The climatic observation data has been classified into 26 variables based on the grape planting seasons (A.Kobayashi et al 1968; santos et al 2011) including total rainfall and monthly mean temperature in April, May, June, July, August, September and October; seasonal mean temperature, day and night time temperature and total rainfall in shooting and flowering (April-May), berry development (June-July) and maturity (August, September, October). Then to select the high correlation of dependent variables as grape yields and independent variables as climate, we used the linear model and Variance Inflation Factors (VIF) to remove the collinearity (or multi-collinearity), the model has been rounded 16 times to get the final results of VIF which is less than 2.5. Therefore, finally, we obtained 10 variables of climate parameters namely mean temperature in April, May, June, July, August; total rainfall in April, May, July, September and October. The set of data have been analyzed and compared the different climate of high and low yields years by applying the Principle Component Analysis (PCA).

Qualitative data analysis: the exploratory and descriptive methods have been used to analyze and explain the qualitative data.

4. Results

Principle Components Analysis (PCA) of climatic variables in high and low yields

The results show that the standard deviation is greater than 1 and cumulative proportion is exceeded 79%. The details of principle component for high yields years shows in Table 1, in the first principle component (PC1) has a high negative correlation with rainfall in July and September (berry development and maturity phases). This mean that there was less rainfall in those months. In the PC2 has a high positive correlation with mean temperature in May and July, and also shows a high negative correlation with rainfall in May and July. Therefore, we conclude that there was warm temperature and less rainfall in May and July. In the PC3 has a positive correlation with mean temperature in June and high negative correlation with mean temperature in April. This determines about there was still cold climate in April and warmer climate in June.

For Table 2 shows the principle component in low yields, the first principle component (PC1) has a negative correlation with mean temperature in April and May (shooting and flowering phases), and it has a positive correlation with rainfall of those months. We conclude that there was high rainfall and cold temperature in both months. In the PC2 has a positive correlation with mean temperature in August and rainfall in July and September. That mean it was warm climate in August and heavy rainfall in July and September. Meanwhile, in the PC3 has the highest positive correlation with mean temperature in June, which concludes about warm climate.

Table 1: Principle component for high yields

climatic parameters (factors loading)	PC1	PC2	PC3
mean. temp. Apr	-0.41	-0.02	-0.32
mean. temp. May	-0.41	0.12	-0.2
mean. temp. June	-0.20	-0.19	0.66
mean. temp. Jul	-0.06	0.4	0.23
mean. temp. Aug	-0.007	0.44	0.28
rainfall. Apr	0.4	-0.17	0.26
rainfall. May	0.33	-0.21	-0.38
rainfall. Jul	-0.15	0.42	0.02
rainfall. Sep	-0.11	0.36	-0.11
rainfall. Oct	-0.30	-0.35	0.19

Table 2: Principle component for low yield

climatic parameters (factors loading)	PC1	PC2	PC3
mean. temp. Apr	-0.24	0.04	-0.60
mean. temp. May	-0.24	0.43	-0.11
mean. temp. June	0.17	-0.01	0.64
mean. temp. Jul	0.2	0.44	0.16
mean. temp. Aug	-0.11	0.30	-0.05
rainfall. Apr	-0.34	0.14	0.2
rainfall. May	0.1	-0.47	-0.25
rainfall. Jul	-0.37	-0.36	0.11
rainfall. Sep	-0.42	-0.06	-0.19
rainfall. Oct	0.26	0.34	-0.04

Farmers' perception of climatic conditions

After the preliminary field survey, we summarized the farmers' perception of climatic conditions shows in the Table 3. Farmers perceived that in some years they got the low and high yields, which they considered that climatic factors have influenced to grape yields such as heavy rainfall and snow. For example, in low yields year as in 2018, there was heavy snow and humidity in April. In 2008, 2012, 2013 and 2015, farmers noted that there was heavy rainfall and they got low yields, in those years there was high amount of rainfall in July and September, which was between 315 to 627mm/month (JMA, 2017). Besides, there also had low temperature in April, which was about -2.58 to -4.17 °C (JMA, 2017). In addition, farmers perceived that in some years namely 2007, 2010, 2014, they got high yields. In those years, the amount of rainfall in July and September was between 134 to 219

mm/month (JMA, 2017); and the temperature in April was among -1.82 to 2 °C (JMA, 2017). Therefore, in high yields years, farmers mentioned that there was less rainfall in summer and warm climate in April. Thus, we conclude that farmers' perception and scientific observation data have been similarly consequences. Farmers' perceived as heavy rain and low climate occurrence in low yield years. At those years, the scientific observation was showed higher amount of rainfall and lower climate than other years.

Furthermore, famers mentioned that the greater amount and late melting of snow in winter have impacted in the first stage of growing season in April. Besides, farmers have understood that heavy rainfall in summer has affected the grape berry, especially for the berry size, color and berry cracking, which are important factors for the markets' requirement.

Table 3: Farmers' perception of climatic conditions

Discussion

Descriptions	Farmer' perception 1	Farmer' perception 2	Farmer's perception 3
Low yield	Year: 2018 Heavy snow and humidity	Years: 2008, 2013, 2015 Heavy rainfall	Years: 2012 Heavy rainfall
High yields	Year: 2014 Less rainfall	Years: 2007, 2010 Less snow	Year: 2014 Less rainfall

The principle component analysis results demonstrate the different climatic conditions between high and low yields years. The high yields years (Table 1) is represented the less rainfall in July and September (berry development and maturity phases). In addition, it is appeared the warm climate in May and July. However, in the low yields years (Table 2), is represented the cold temperature in April and May, and it is indicated the heavy rainfall in May, July and September. These results are accurate with the farmers' perception and scientific observation data of each year, which found that in low yields years there was heavy rainfall in July and September, and there was cold climate in April. That mean humid conditions have the trend to slow down the berry development and promote diseases (Morinaga et al., 2005). Oppositely, in high yield years there was less rainfall in July and September and warm climate in April, which determines that warm temperature has made the benefits to grape yields later than cold temperature (Santos et al., 2011). Furthermore, another relevant factors namely occurring diseases (Kenny et al., 1992) and decreasing in soil moisture (Malheiro et al., 2005) would lead the significant effects to yields in the future.

Conclusion

The PCA results illustrated that the high yields years had less rainfall and warmer temperature in berry development and maturity phases. And the low yields years had lower temperature and high rainfall during those phases. These results are precise with the farmers' perception and scientific observation data, which found that heavy rainfall and cold temperature in low yields years. Oppositely, there was less rainfall and warm climate in high yield years.

This preliminary study can conclude that farmers' perception, climatic observation data and PCA results, are similarly consequences. The results would be the baseline data for further study about farmers' adaptation, adoption of innovation and its diffusion to the changing climate in the future.

References

1) Adger WN. Agrawala S., et al., 2007. Assessment of adaptation practices, options constraints and capacity. Cambridge University Press, Cambridge, 717–743.
2) Belliveau S, Smit B, Bradshaw B., 2006. Multiple exposures and dynamic vulnerability: evidence from the grape industry in the Okanagan Valley, Canada. Glob Environ Change 16:364–378
3) Bradshaw B, Dolan H, Smit B., 2004. Farm-level adaptation to climatic variability and change: crop diversification in the Canadian prairies. Climate Change 67:119–141.
4) Fujisawa M, Kobayashi K., 2015. Shifting from apple to peach farming in Kazuno, northern Japan: perceptions of and responses to climatic and non-climaticimpacts. Reg Environ Change. 13(6):1211–1222.
5) Japan Meteorological Agency (JMA), 2017. Statistic of climatic information, http://www.data.jma.go.jp/gmd/risk/obsdl/#!table.
6) Kobashi et al., 1968. Favorable day and night temperature combination for the fruit growth of Delaware grape and Satsuma oranges. Division of Pomology, Kyoto Uni.
7) Morinaga et al., 2005. Grape production in Japan. Persimmon and Grape Research center, National Institute of Fruit Tree Science, MAFF.
8) Santos J.A., Malheiro A.C., et al., 2011. Statistical modelling of grapevine yield in the Port Wine region under present and future climate conditions. Int. J. Biometeorol.55, 119-131.
9) Shinomiya et al., 2015. Impact of temperature and sunlight on skin coloration of Kyoho table grape. Fukuoka Agricultural and forest research center. Scientia Horticulture 193: 77-83.
10) Statistics of Agriculture, Forestry and Fisheries (2016) Ministry of Agriculture, Forestry and Fisheries.http://www.maff.go.jp/j/tokei/kouhyou/sakumotu/sakkyou_kazyu/index.html
11) Sugiura et al., 2012. Overview of recent effects of global warming on agriculture production in Japan. JARQ 46 (1), 7-13.

Yamada et al., 2016. Advances in table grape breeding in Japan. NARO Institute of fruit tree science. Breeding Science 66: 34-45.1

Estimation of woody debris recruitment by landslides: A Case study of Typhoon Lionrock in Iwaizumi, Japan

Thapthai Chaithong[1], Yuto Sukegawa[2], Satoshi Anzai[2], ○Akihiro Ichiba[1*], Daisuke Komori[1]
[1]Graduate School of Environmental Studies, Tohoku University, Sendai 980-8579, Japan
[2]Graduate School of Engineering, Tohoku University, Sendai 980-8579, Japan

*E-mail: akihiro.ichiba.r2@dc.tohoku.ac.jp

Abstract

A landslide can produce large amounts of debris in the form of boulders, cobbles, soil, sand and log or wood. The woody debris produced by a landslide flows into a downstream river or village. It can form obstructions in the stream and make the stream flow over. In this study, we aimed to develop a procedure for estimation of woody debris recruitment by landslides. Understanding the volume of woody debris can help predict and prevent hazards from this debris. The proposed procedure combines a shallow landslide model, tree density data, and observational data flowing landslide occurrence. The study site is a sub-watershed of the Omoto River watershed in Iwaizumi town, Iwate Prefecture. This town got a big damage from Typhoon No.8, Typhoon Lionrock. This typhoon delivered over 200mm rainfall per a day and induced many landslides. Based on field surveys, we found that about 520m^3 of woody debris gathered in a narrow section under a railway bridge. Moreover, about 180m^3 of woody debris compose natural woody debris dam in the stream channel of the target watershed. Using the proposed protocol, we estimate that woody debris recruitment to the stream was approximately 638m^3.

Keywords: Woody debris, Lionrock, Landslide, Woody debris dam,

1. Introduction

Japan has been damaged by typhoon for a long time. Typhoons cause not only direct damage by their strong wind and heavy rain, but also indirect damage by landslides. Landslides produce a lot of woody debris. Our target, Typhoon No.8 in 2016 is without exception. On 30, August, 2016, Typhoon Lionrock struck the Pacific coast of north-eastern Japan. The typhoon caused flash flooding, landslides, and debris flows in the north part of Japan, destroying houses and infrastructure.

Although there are a lot of studies about how woody debris or drift woods flow in the river, there are not many case studies about how woody debris can be produced. However, the estimation of the amount of woody debris is important. Woody debris are mainly produced by landslides in the mountain and river-side forests. The mechanism of landslides of mountain area are stated as follows. Rainwater infiltrates into a sloping surface of forest area. Therefore, the groundwater level go up, or pore water pressure increases. These factors reduce the effective stress of soil and the soil can be easily sheared by its own weight[1)].

Although how the several standing on saturated soil trees fall down can be explained by distinct element method[2)], it is not so efficient to the estimation of estimation of woody debris recruitment over the watershed. In this paper, we aim to use data collected after a landslide to develop a method of estimation of woody debris recruitment.

2. Methods and targets

2.1 Targets

We focused our target on Omoto river water disaster caused by Typhoon Lionrock. The total area of the study site is approximately 0.87km^2 and the total length of the stream is approximately 3.75km.

2.2 Methods and dataset

The proposed procedure can be divided into four steps.

2.2.1 First step: hillslope hydrology model and Infinite stability model

The first step involves simulating the unstable area with an analytical shallow land slide model that describes the source of woody debris recruitment to watershed. This model makes two major assumptions: (1) the landslides characteristics are based on an infinite slope and (2) the hydrological conditions are based on steady state subsurface flow and infiltration. The model is analytical and simulates the physical process of slope destabilization caused by an increase in ground water.

The hillslope hydrology model used in this study consists of two parts. One part simulates the saturated subsurface flow and the other part simulates rainfall infiltration into sloping surface. The equation of saturated surface flow is based on Darcy's low and the equation of rainfall infiltration into the sloping surface is based on the modified Green-Ampt equation [3)]. From the water balance equation and Darcy's law, the following expression can be obtained:

$$\mathbf{I \cdot A = \eta \cdot m \cdot b \cdot k \cdot \sin\beta} \ldots (1)$$

I: rainwater infiltration, A: catchment area, η: the porosity of the soil, m: steady water table height, b: width of the topographic elements, k: saturated hydraulic conductivity, β: slope angle
Equation 1 can be translated as follows.

$$\mathbf{m} = \frac{\boldsymbol{I \cdot A}}{\boldsymbol{b \cdot k \cdot \eta \cdot \sin\beta}} \ldots (2)$$

The Green-Ampt equation is simplified mathematical expression that represents the infiltration process. The rate of infiltration for the sloping surface and the cumulative infiltration are as follows:

$$\mathbf{i = k[\cos\beta + \frac{(\psi \cdot \Delta\theta)}{I(t)}]} \ldots (3)$$

$$\mathbf{I(t) - \frac{(\psi \cdot \Delta\theta)}{\cos\beta} \cdot \ln\left[1 + \frac{I(t) \cdot \cos\beta}{(\psi \cdot \Delta\theta)}\right] = k \cdot t} \ldots (4)$$

i: infiltration rate at time, I(t): cumulative infiltration at time, Δθ: volumetric water content deficit, ψ: the suction at wetting front, t: time.

Based on field observation, a slip-type landslide occurred and was parallel to the slope surface. Thus, the infinite slope stability model can be used to analyze the stability of the slope based on the factor of safety (FS). The shear strength of soil used in this study is based on the Mohr-Couloms failure criterion and can be expressed as follows:

$$\boldsymbol{\tau_f = c + \sigma \tan\phi} \ldots (5)$$

τ_f : shear strength of soil, c: the total soil cohesion, σ: the normal stress, φ: total friction angle.

Effective normal stress resists downslope movement and can be expressed as follows:

$$\boldsymbol{\sigma = [(m \cdot \gamma_{sat}) + (D - m) \cdot \gamma_t] \cdot \cos^2\beta} \ldots (6)$$

D: depth of soil, γ_{sat}: saturated soil unit weight, γ_t: the submerged soil unit weight.

The mobilized shear force and therefore the FS can be expressed as follows:

$$\boldsymbol{\tau_d = [(m \cdot \gamma_{sat} + (D - m)\gamma_t] \cdot \sin\beta + \gamma_w \cdot m \cdot \sin\beta} \ldots (7)$$

$$\mathbf{FS} = \frac{\boldsymbol{c + m[\gamma_{sat} + (D-1) \cdot \gamma_t] \cdot \cos^2\beta \cdot \sin\beta}}{\boldsymbol{m \cdot [\gamma_{sat} \cdot \gamma_w + (D-1)\gamma_t] \cdot \cos\beta \cdot \sin\beta}} \ldots (8)$$

τ_d : mobilized shear force, γ_w: water unit weight

In addition, elevation data can be obtained from ASTER Global Digital Elevation Model (GDEM) by National Aeronautics and Space Administration (NASA) of the U.S. and Ministry of Economy, Trade, and Industry of Japan. From the source, we can calculate β using ArcGIS. The soil parameters at this site are in Table 1. For the rainfall dataset, we adopted Inverse distance weighted method (IDW) and determined the distribution of rainfall using the data of 5 rain gauges in Iwaizumi town.

Parameters	Unit	Value
Total soil cohesion (c)	kPa	10.8
Total friction angle (φ)	Degree	29.7
Saturated soil unit weight (γ_{sat})	kN/m^3	16.7
Water unit weight (γ_w)	kN/m^3	9.81
Saturated hydraulic conductivity (k)	cm/hr	2.99
The porosity of the soil (η)	-	0.437
The suction at wetting front (ψ)	cm	6.13
Volumetric water content deficit (Δθ)	-	0.27

2.2.2 Second step: Forest analysis

By a field survey of the height, diameter of trees and tree density and global tree density dataset, we analyzed the forest.

To determine the volume of downed woody debris in this study, we used Huber's formula (9). Then we modified this formula as (10).

$$\mathbf{V = L \cdot A_m} \ldots (9)$$

$$\mathbf{V = H \cdot A_{(DHB)}} \ldots (10)$$

V: volume of standing trees, L: the length of a downed woody debris piece, A_m: the cross-sectional area at longitudinal midpoint, H: height of the trees, $A_{(DHB)}$: the cross-sectional area at breast height.

Tree density is important, and we obtained tree density data from the global scale tree map by Crowther[4] (2015) (Fig 1).

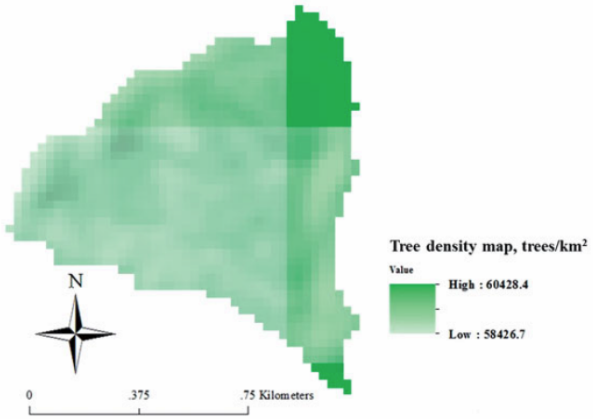

Fig. 1: Tree Density map of the study site from the global man of tree density

Tree height data are found to be normally distributed (P=0.461) and diameter shows a right-skewed distribution (P-0.183). Mean of the height is 15.09m (Coefficient Variation is 0.39) and that of diameter is 0.30m (CV: 0.52)

By Monte Carlo method, the peak of volume of standing is calculated. The volume peak is 0.75m^3.

2.2.3 Third step: Active stream channel identification

We use satellite images and aerial photography of Google Earth and Geospatial Information Authority of Japan to determine the active stream channel zone.

2.2.4 Final step: Estimation of woody debris recruitment

From 1st step, we can gain the FS map for August 30, Iwaizumi, 2016 (Fig. 2). I this figure red zone means unstable area, that is, area of FS<1. Unstable areas are located on steep hillslope (>30°), which is consistent with results of field survey. The field surveys showed that slope failures occurred along the channel banks and in high elevation areas with steep slopes. Compared to the actual landslide scars from aerial photograph, the GIS-Based Shallow model overestimated the unstable areas, maybe because the spatial variance of soil parameters was limited; in addition, access to the study site was difficult. Moreover, determining land slide scars from aerial photos may be mistaken because the effect of tree cover and shadow. In this study, the unstable area was estimated as 0.42km^2.

As mentioned previously, woody debris recruitment was calculated based on the values stated above (2.2.1). In addition, by field survey, we checked that woody debris dams exist along the stream channel and slopes. We estimates that the total the total volume of woody debris dams in the site was approximately 668.5m^3 (including void, soil, sand and rocks), and those in the stream was 178m^3.

The volume of woody debris deposited downstream was 524m^3 and that of woody debris dam in the stream channel was 178m^3 from the survey, so the total volume with this typhoon may be 702m^3 in total. However, on our analysis, the calculated value of woody debris recruitment is 638m^3, so we are sorry to conclude that this study underestimated the woody debris entrained downstream by 9.1%.

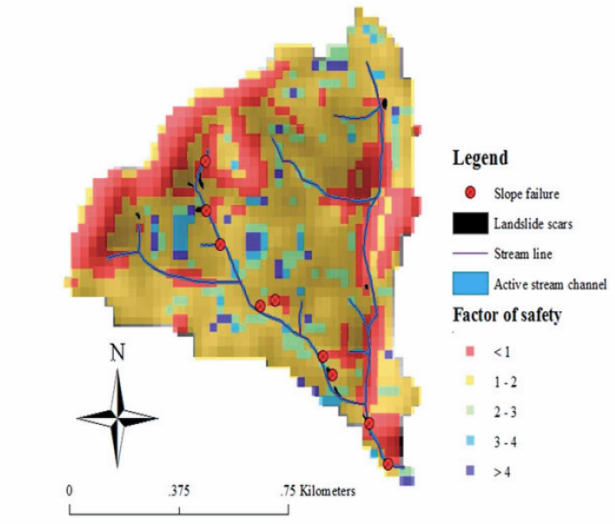

Fig. 2 Map of the FS, the locations of shallow landslides and the active stream channel

3. Conclusions

In our study, we improved a procedure to analyze the amount of woody debris that could be transported downstream. From the formulas and equations, we can estimate the woody debris recruitment over a watershed. However, FS value overestimates the actual landslides. Moreover, we found that our procedure underestimates this amount compared to field-based measurements. However, our results was able to demonstrate that the landslide or slope failures are significant, procedure of woody debris in the catchment area, which was confirmed by field surveys following the landslides.

References

1) Youichi Ohkura,:Fluidization mechanism of landslides and prediction of the travel distance, Bulletin of the Forestry and Forest Products Research Institute, 3(2), p109-164, 2004
2) Hitoshi Gotoh, Eiji Harada and Tetsuo Sakai: Effect of fallen trees on landslides at mountain stream, Annual Journal of Hydraulic Engineering, 45, p721-726, 2001
3) Chen L, Yong MH: Green-Ampt infiltration model for sloping surfaces, Water Resources 42, p1-9,2006
4) Crowther TW, Glick HB, Covey KR et al: Mapping tree density at a global scale, Nature, 525, p201-205, 2015.

Evaluation and sensitivity analysis for surface and bottom snowmelt process by runoff analysis

○Koji Sakamoto[1*], So Kazama[1]

[1] Graduate School of Engineering, Tohoku University, Sendai 980-8579, Japan

*E-mail: koji.sakamoto.r5@dc.tohoku.ac.jp

Abstract

Bottom snow melting is affected by groundwater and bottom soil type, and bottom snowmelt amount varies within the year even at the same spot. Runoff analysis was conducted to validate the accuracy of bottom snowmelt processes proposed by Saito et al. (2017) using laboratory snowmelt experiments and a one-dimensional advection diffusion model. In addition, sensitivity analysis of meteorological data was conducted to identify the cause of error in the runoff analysis. A Nash-Sutcliffe (NS) coefficient of 0.70 was obtained from the runoff analysis. Months when bottom snowmelt is dominant had little influence in lowering the NS coefficient, but months when surface snowmelt is dominant needs further consideration. Also, lack of sufficient meteorological data of the basin can be a cause of low accuracy, and sensitivity analysis showed that water vapor pressure has high sensitivity on the runoff analysis in winter.

Keywords: Bottom snow melting, Heat balance method, Lorentz curve, Gini coefficient, Water vapor pressure

1. Introduction

Japan is one of the world's heaviest snowfall countries, and more than 50% of the area is designated as a heavy snowfall area that accumulated snow accumulation value of 50 meters or more in a year. For that reason, long-term and spatial grasp of snow cover on basin scale is important for flood control and water use. Therefore, the purpose of this research is to examine the validity of calculation of bottom snowmelt amount by runoff analysis and consider the accuracy of the whole snowmelt model. In addition, we will clarify the cause of the error in the outflow analysis.

2. Study basin and data

The study basin is the Yoneshiro River Basin located in the northern part of Akita Prefecture (Fig-1). Yoneshiro River is a first-class river, and catchment area is 4,100 km 2 and trunk line extension is 136 km. The calculation period is from September 1, 2014 to May 31, 2016, and the analysis period is from September 1, 2015 to May 31, 2016. Table-1 summarizes the data required for calculation of snow accumulation model, snowmelt model, hydrological model and its data source.

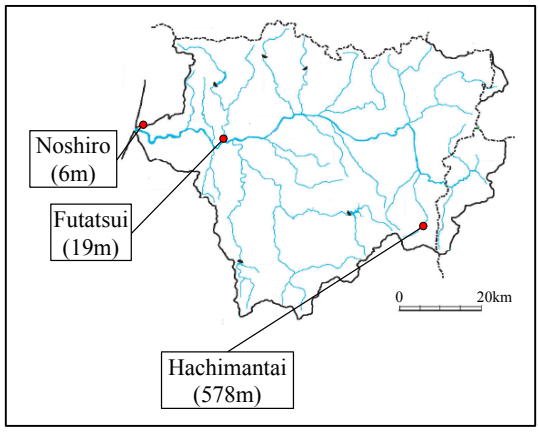

Fig-1 Study basin

Table-1 Data details

Data	Source
elevation	National Land Numeral Information
climate	AMeDAS
streamflow	Hydrology water quality database

3. Models and methods

3.1 Snow accumulation model

The SWE (Snow Water Equivalent) model of Kazama et al. [1] was used to estimate the distribution of SWE in the basin. The time change of SWE is expressed by the following equation.

$$\frac{d(SWE)}{dt} = SF - SM \qquad (1)$$

where, SWE is snow water equivalent (m), SF is snowfall (m/s), SM is snowmelt (m/s).

3.2 Snowmelt model

The amount of snowmelt was calculated by the sum of surface snowmelt amount and bottom snowmelt amount, the surface snowmelt amount was obtained by the heat balance equation, and the bottom snowmelt amount was obtained by equation (3)[2]. The calculation formula of snowmelt amount is shown below.

$$Q_M = (1 - ref)S^{\downarrow} + L_d - L_u - H - lE + Q_R \qquad (2)$$

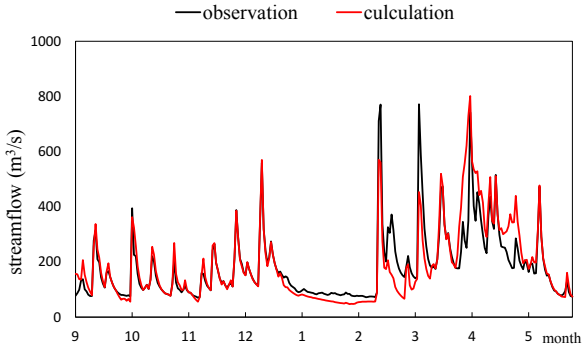

Fig-2 Streamflow in Futatsui

$$SM_b = a - 0.378\log_{10}(b) \quad (3)$$

$$SM = \frac{Q_M}{l_F \times \rho_w} + \frac{SM_b}{24} \quad (4)$$

where, Q_M is the amount of heat used for surface snowmelt (W/m^2), ref is albedo, $S^{\downarrow}$ is the shortwave radiation amount (W/m^2), L_d is the downward long-wave radiation amount from the Earth's atmosphere (W/m^2), L_u is the upward long-wave radiation amount from the snow cover surface (W/m^2), H is the sensible heat transport amount (W/m^2), lE is the latent heat transport amount (W/m^2), Q_R is the rainfall heat amount (W/m^2), l_F is the latent heat of fusion (= 3.33×10^5 J/kg), ρ_w is the density of water (=1.00×10^3kg/m^3), a is the parameter given for each land use,(a=4.5767 in building land and truck transportation land, a=4.0767 in the field, agricultural land, and golf course, a=3.5767 in the forest and wasteland), b is the time since the start of snow cover (h).

3.2 Runoff model

The amount of runoff was estimated based on the continuous equation and the Manning equation in the ground surface and the riverway part, and the storage function method in the ground. The calculation formula of snowmelt amount is shown below.

$$\frac{\partial A}{\partial t} + \frac{\partial Q}{\partial x} = \left(R + SM - R_{in} - E_p\right)B \quad (5)$$

$$Q = \frac{1}{n}Bh^{5/3}I^{1/2} \quad (6)$$

$$\frac{\partial s}{\partial t} = R_{in} - q_b \quad (7)$$

$$s = kq_b^p \quad (8)$$

where, A is the flow cross-sectional area (m^2), B is the mesh width (m), Q is the outflow flow rate (m^3/s), t is the time (s), x is the distance in the downward flow direction (m), I is a slope gradient, R_{in} is the permeation amount (m/s), E_p is the evapotranspiration amount (m/s), s is the storage height (m), q_b is the baseline flow outflow rate (m/s), and k and p are the model parameter (k=120.0, p =0.5)[3].

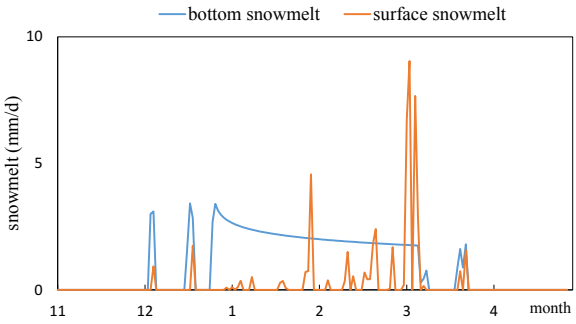

Fig-3(i) Snowmelt in Noshiro

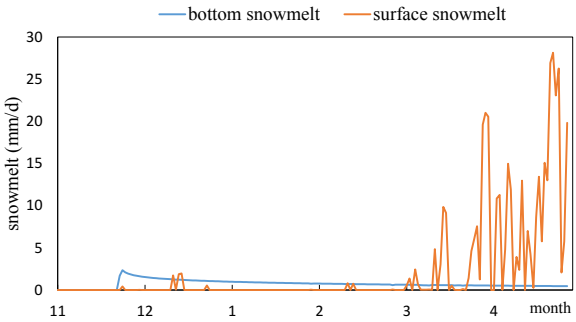

Fig-3(ii) Snowmelt in Hachimantai

3.3 Method of sensitivity analysis

Due to the lack of observatory in the basin, atmospheric pressure data, water vapor data and total solar insolation amount data were obtained only at one point. For this reason, sensitivity analysis was performed on these data to assess the impact of these data on runoff analysis. First, the maximum observation value and the minimum observation value of each data were obtained. Then, the interval between the minimum value and the maximum value was equally divided into 10, 10 types of input values were created, and the runoff analysis was performed. The input values were named rank 1, rank 2 ... rank 10 from low value.

3.4 Evaluation index of analysis

Nash-Sutcliffe efficiency coefficient was used as an evaluation index of runoff analysis. The following formula was used for the Nash-Sutcliffe efficiency coefficient equation.

$$NS = 1.0 - \frac{\sum_{i=1}^{N}(Q_{obsi} - Q_{cali})^2}{\sum_{i=1}^{N}(Q_{obsi} - \overline{Q_{obs}})^2} \quad (9)$$

where, Q_{obsi} is the observation river flow rate at timestep i (m^3/s), Q_{cali} is the calculated river flow rate at timestep i (m^3/s), N is the number of hours analyzed, NS is the Nash-Sutcliffe efficiency coefficient. Accuracy was defined as very good at 0.75 <NS≤1.00, good at 0.65 <NS≤0.75, normal at 0.50 <NS≤0.65 and bad at NS≤0.50.And, Gini coefficient was used as an evaluation index of sensitivity analysis. The calculation formula of Gini coefficient is shown below.

$$Gini = 2\int_0^1 \left(x - L(x)\right)dx \quad (14)$$

where, $L(x)$ is the Lorenz curve, and x is the level of the streamflow.

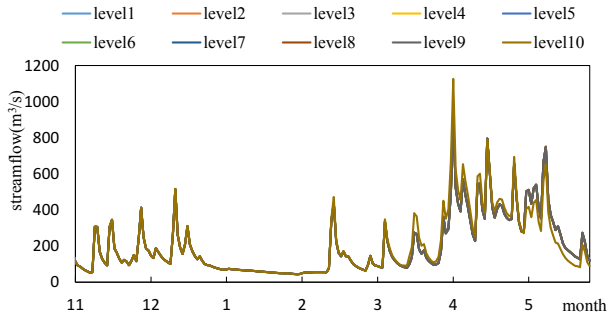

Fig-5(ⅰ) Sensitivity of solar insolation

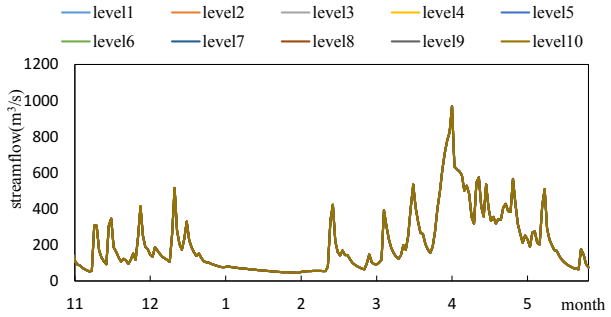

Fig-5(ⅱ) Sensitivity of atmospheric pressure

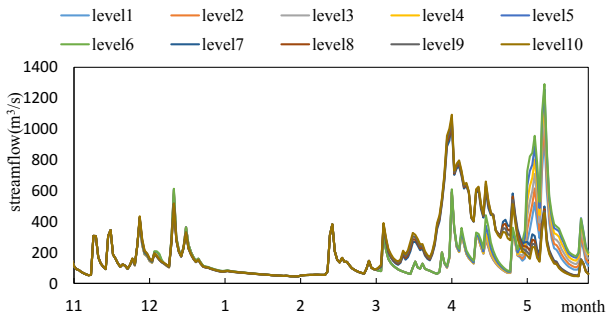

Fig-5(ⅲ) Sensitivity of water vapor

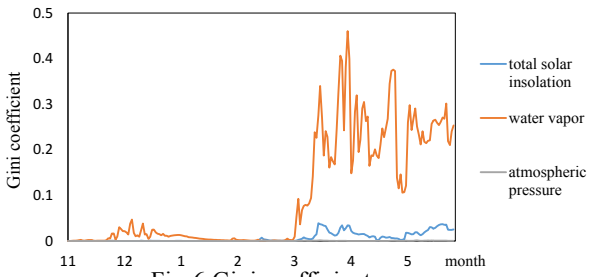

Fig-6 Gini coefficient

4. Results and discussions

4.1 Runoff analysis

Fig-2 shows the calculation results of the river flow rate at the Futatsui flow rate observation station. The NS coefficient was 0.70, which was judged to be good as the set precision. However, it underestimates the flow rate from the middle of December to the beginning of February and from the middle of February to the end of March. In addition, the flow rate was overestimated from the beginning of April to the snow disappearance in early May, and although the observation value is increasing, the calculated value is decreasing. Although the reproducibility up to the start of snowfall was high, errors in winter were noticeable.

Fig-3(i) ~ (ii) show the bottom snowmelt amount and surface snowmelt calculation results at Noshiro AMeDAS Observatory and Hachimantai AMeDAS Observatory from November to April. On both points, it can be seen that snow melting on the bottom is dominant from December to mid-February. In addition, it is only a few days in late February that surface snow melting is predominant at Noshiro AMeDAS Observatory, and it can be seen that the snowmelt was snowed almost by bottom snowmelt. However, at Hachimantai AMeDAS Observatory, there is almost no snow melting until the end of February compared with Noshiro AMeDAS Observatory, and from the beginning of March there has been a large amount of snow melting due to surface snowmelt. That's why it is thought that the cause of the error of the flow rate is the underestimation of snowmelt amount from the end of February to the beginning of March in the mountainous area and the excessive snowmelt estimation after the beginning of April.

4.2 Sensitivity analysis

Fig-4(i) ~ (iii) shows the outflow analysis results obtained by changing the atmospheric pressure, vapor pressure, and solar radiation amount data at the Futatsui flow rate observation station, and the time series change of the Gini coefficient is shown in Fig-5. As shown in Fig-4, large fluctuations are observed in runoff analysis with steam pressure data changed. It can be seen that the top 5 and bottom 5 rankings show different behaviors than in early March. The top five was the maximum flow rate in early April and the bottom 5th was the maximum flow rate in early May. As for atmospheric pressure, there is little disparity in runoff analysis. Regarding the amount of solar radiation, although there are some disparities in peak flow rate, there is no variation as much as vapor pressure. Regarding the Gini coefficient, from Fig-5, it is early March that the Gini coefficient fluctuates greatly, which is consistent with the time when the surface snowmelt begins to dominate. In other words, the surface snowmelt amount calculation shows a large influence on the error of the runoff analysis. In addition, the maximum value of the Gini coefficient of the solar radiation amount and the atmospheric pressure is both 0.10 or less, while the Gini coefficient of the vapor pressure is a large value of 0.46. From the above, it is concluded that the cause of the error in the outflow analysis is the vapor pressure data.

5. Conclusions

1) It was suggested that the cause of the error in the runoff analysis is the calculation of snowmelt amount.
2) It was found that the vapor pressure data greatly influences the calculation of snowmelt amount.

References

1) Kazama S, Izumi H, Sarukkalige R P, Nasu T, Sawamoto M: Estimating snow distribution over a large area and its application for water resources, Hydrological processes, Vol.22, pp.2315-2324, 2008.
2) Masato Saito, So Kazama, Syunsuke Aita: Evaluation of mutual effect of the storage of the subsurface water and snow in basin areas, technical presentation meeting of Tohoku branch of the Japan Society of Civil Engineers, 2017.

Estimation of nutrient distribution in Mekong river floodplain using satellite images

○Keitaro Yamada[1], So Kazama[1]

[1]1Graduate School of Engineering, Tohoku University

*E-mail: keitaro.yamada.r4@dc.tohoku.ac.jp

Abstract

Estimation of the total phosphorus concentration distribution using satellite images on the Mekong River floodplain was carried out. Partial least squares regression analysis was applied to satellite images of rainy season and dry season, and chlorophyll a concentration was obtained. Past studies about for relational expression between chlorophyll a and total phosphorus were examined, and the total phosphorus concentration was also determined from the concentration of chlorophyll a. From the regression equation in the rainy season the concentration distributions in the rainy season and the dry season were estimated. From the regression equation in the dry season, the concentration distributions in the rainy season and dry season were estimated. The correlation coefficient between the estimated value of the rainy season and the observation value by the regression equation of the rainy season was 0.97, and the correlation coefficient in the dry season was 0.070. The correlation coefficient in the dry season by the regression equation of the dry season was 0.66, whereas the correlation coefficient in the rainy season was -0.49. It is understood that the regression equation cannot be applied to different seasons and it was found that it is necessary to obtain a regression equation on suitable season for more accurate estimation.

Keywords: *remote sensing, Cambodia, chlorophyll, total phosphorus*

1. Introduction

It is said that the floodplain is important for agriculture and ecosystem. In the downstream of the Mekong river, the longest river in Southeast Asia, especially Cambodia, Rice cultivation using the floodplain is done. For Cambodia, where the main industry is agriculture, the floodplain brings significant benefits and it is necessary to evaluate the influence of this flood on agriculture recently. Hiraga estimated nutrient distribution using nutrient transportation model[1)]. However, although this model contains observation information by onsite observation, it is information at several points, not in wide area. Therefore we thought it would be possible to estimate more accurately by using satellite images. This estimation is thought to lead to the assessment of the influence of flood on agriculture. Based on the above, the purpose of this research is to estimate the nutrient distribution of flooded water using satellite images.

2. Study Area

The study area is a 140km×110km area (fig.1). There is Phnom Penh in the center of this area. In this area, water overflows from the Mekong river during the rainy season and spreads to the downstream area. In the floodplain, rice cultivation using nutrient-rich soil is done. In addition, the floodplain is not only an agriculture land, it also becomes a habitat for fish. The study area belongs to the tropical monsoon climate, the rainy season from May to October and the dry season from November to April. The rainfall is the highest in September, and the depth of the Mekong river is the largest in October.

Fig.1 Study area

3. Dataset and Method

Since the limiting factor in this area is phosphorus, we treat only phosphorus in this study. Moreover, it is difficult to directly estimate phosphorus present in various forms in water from satellite images. Therefore, according to the past case, the concentration of chlorophyll a which was estimated from the satellite image is first obtained. By clarifying the spectral reflection characteristics of chlorophyll a which is the observation target, its amount can be estimated from the satellite image. We tried to estimate total phosphorus concentration from chlorophyll a concentration.

(1) Dataset

In this study, Landsat data was used as satellite images. Landsat is an earth observation satellite aiming at observing the global environment by optical observation at multiple wavelengths. It has seven bands between 33 mm and 2300 mm, and the DN value is measured from the reflectance of the lights of each wavelength. The data used are satellite images of Landsat-8 / OLI in September 2017 and February 2018.

(2) Conversion to reflectance

The conversion equation for obtaining the reflectance from the DN value is shown in equation (1).

$$\rho\lambda_i = \frac{M_\rho Q_{cal_i} + A_\rho}{sin\theta_{SE}} \quad (1)$$

where $\rho\lambda_i$: reflectance of band$_i$(%), Q_{cal_i} : DN value of band$_i$, M_ρ : multiplicative rescaling factor, A_ρ : additive rescaling factor, θ_{SE} : local sun elevation angle.

(3) Estimation of chlorophyll a concentration

PLS analysis was performed using chlorophyll a concentrations of flood water at 14 sites in the rainy season and 12 dry seasons obtained by site observation as objective variables, and 7 DN values of Landsat data at the same point as explanatory variables. The equation of estimation is equation (2)

$$chla = x_0 + x_1\times\rho\lambda_1 + x_2\times\rho\lambda_2 + x_3\times\rho\lambda_3 + x_4\times\rho\lambda_4 + x_5\times\rho\lambda_5 + x_6\times\rho\lambda_6 + x_7\times\rho\lambda_7 \quad (2)$$

Where $chla$: chlorophyll concentration (μg/l), x_0 : intercept, $x_1 \sim x_7$: regression coefficient.

(4)Estimation of nutrient contribution

We examined whether the equation of the past study [2)~4)] can also be used in this area. Equation (3) shows these relational equation.

(Sakamoto, 1966)

$$\log_{10}[chla] = 1.53\log_{10}[P] - 1.13 \quad (3a)$$

(Dillon *et al* 1974)

$$\log_{10}[chla] = 1.45\log_{10}[P] - 1.13 \quad (3b)$$

(Carlson, 1977)

$$\log_{10}[chla] = 1.45\log_{10}[P] - 1.06 \quad (3c)$$

Where $chla$: chlorophyll concentration (mg/l), TP : total phosphorus concentration (mg/l).

Table.1 Result of PLS

	rainy season	dry season
x0	8.48	12.5
x1	-690	37.5
x2	177	63.9
x3	2290	125
x4	-2130	94.6
x5	2350	-44.2
x6	-1630	-35.1
x7	-1020	-14.7

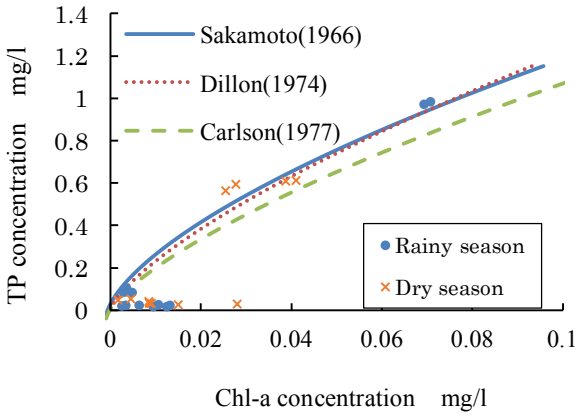

Fig. 2 TP and Chlorophyll concentration

4. Result and Discussion

(1) Conversion to reflectance

Table 1 shows the results of PLS analysis for rainy season and dry season, respectively. The concentration of chlorophyll a was estimated using this equation. And we calculate only in the water area extracted by normalized difference water index.

(2) Estimation of nutrient concentration

As a result of calculating the square sum of the difference between the estimated value and the observation value, the equation by Dillon was minimized. (Fig.2).

(3) Distribution of TP concentration

Chlorophyll-a concentration was estimated using a PLS equation, and the total phosphorus concentration was estimated using Dillon's equation. The concentration distribution map of total phosphorus in the rainy season and the dry season was prepared by the regression equation obtained from the observation information of the rainy season, and the concentration distribution map of the rainy season and the dry season was similarly prepared by the regression equation of the dry season (Fig. 3 ~ Fig. 6). The correlation coefficient between the estimated total phosphorus concentration obtained by two regression equations and the total phosphorus concentration obtained by field observation was obtained. The correlation coefficient between the estimated concentration in the rainy season estimated from the observation information of the rainy season and the observation value is 0.97 and the correlation coefficient between the estimated concentration in the dry

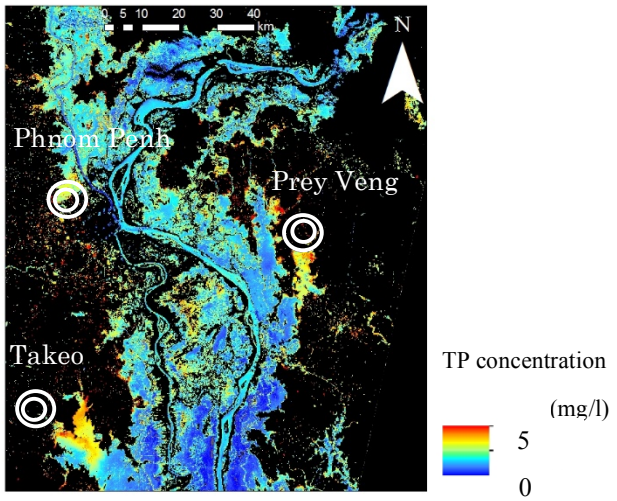

Fig.3 TP concentration in rainy season
(rainy season PLS equation)

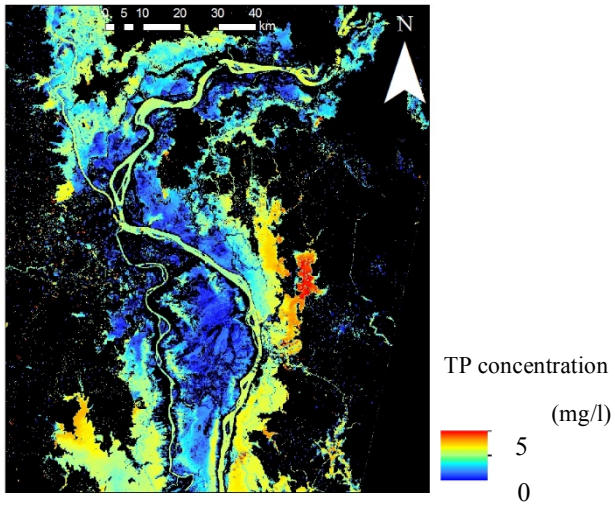

Fig.4 TP concentration in rainy season
(dry season PLS equation)

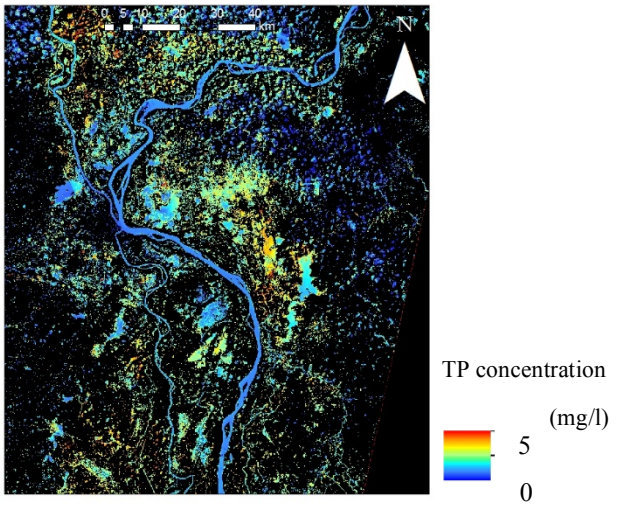

Fig.5 TP concentration in dry season
(rainy season PLS equation)

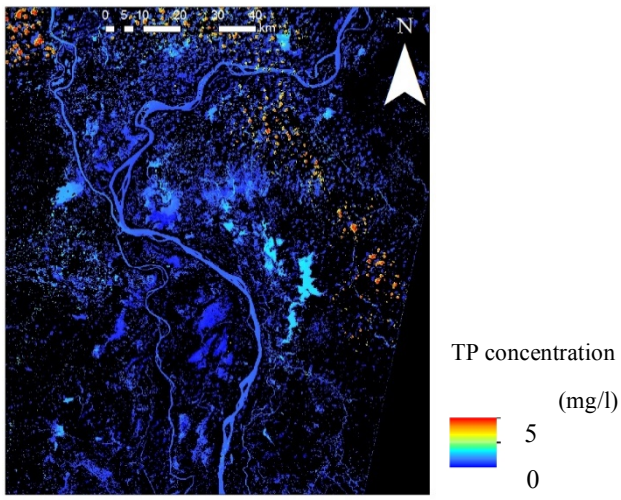

Fig.6 TP concentration in dry season
(dry season PLS equation)

season and the observation value by the regression equation obtained from observation information in the dry season is 0.66. While the correlation coefficient between the estimated concentration in the dry season and the observation by the regression equation in the rainy season is 0.07, the correlation coefficient between the estimated concentration in the rainy season and the observation value by the regression equation in the dry season is as low as -0.49 Value. It was shown that the regression equation obtained from observation information of rainy season and dry season cannot be used for estimating the concentration of different seasons.

5. Conclusion

In this research, the TP concentration in the rainy season was calculated based on the observation information of the rainy season and dry season. The concentration in dry season was also estimated. It was shown that the concentration increases in the edge of the flood plain and around the urban area. However, the regression equation obtained from observation information of rainy season and dry season cannot be used for estimating the concentration of different seasons. By conducting PLS analysis for each season, more accurate concentration estimation is possible.

References

1) 平賀優介，風間聡，峠嘉哉：メコン河氾濫原の干拓が周辺環境に及ぼす影響評価，土木学会論文集 B1（水工学），第 73 巻，第 4 号，pp283-288，2017
2) Sakamoto, M: Primary production by phytoplankton community in some Japanese lakes and its dependence on lake depth. Arch. Hydrobiol. 62: 1-28, 1966.
3) Dillon, P. J. & Rigler, F. H.: The phosphorus-chlorophyll relationship in lakes. Limnol. Oceanogr. 19，p.767－773，1974.
4) Carlson, R. E.: A trophic state index for lakes. Limnol. Oceanogr. 22: 361–369, 1977.

Long-term change and spatial anomaly of precipitation in Osaka, Japan

○Ryosuke Inomata[1*], Daisuke Komori[2], So Kazama[1]
[1]Graduate School of Engineering, Tohoku University, Sendai 980-8579, Japan
[2]Graduate School of Environmental Studies, Tohoku University, Sendai 980-8579, Japan
*E-mail: ryosuke.inomata.p4@dc.tohoku.ac.jp

Abstract

In this study, we statistically analyzed the spatial deviation of the precipitation and rainfall frequency distribution in the urban area of Osaka and its surrounding areas using the radar AMeDAS precipitation data for 23 years (1993 to 2015). As a result, the following findings were obtained. (1) In western part of the urban areas, precipitation, frequency of rain, frequency of heavy rain (precipitation (mm/hour) ≧5mm) was greater than that in the surrounding area, especially during the time zone during afternoon. (2) In northwestern part of the urban areas, the tendency that precipitation and frequency of rain was greater than that of the surrounding areas has been expanded over time (3) In the southwestern part of the urban areas, the tendency of precipitation and frequency of rain was lower than that of the surrounding areas has been expanded over time. From the above, we clarified that the impact of cities on weather is different inside the city.

Keywords: Precipitation, Spatial deviation, Interpolation, Radar AMeDAS

1. Introduction

As one of the influences of cities on weather, there is a change in precipitation. Many studies have pointed out that rainfall phenomena in urban areas is different from surrounding areas[1)2)3)4)]. Fujibe[5)] calculated spatial deviation of precipitation in the urban area and its surrounding areas and statistically analyzed precipitation and precipitation frequency distribution in urban areas. However, Fujibe's studies have used AMeDAS data observed at fixed point, which was established at about 1/17 km (pieces/km^2) in Japan, so challenges remain in spatial representation. Therefore, in this research, we will clarify the spatial deviation of the precipitation and rainfall frequency distribution in the urban area of Osaka and its surrounding areas, using radar AMeDAS analytical precipitation data that synthesized surface observation by rainfall radar and AMeDAS stationary observation.

2. Methodology

Fig. 1 shows the study area, the "urban area" (yellow mesh) and "surrounding area" (green mesh) in this study. In this research, 4 meshes which are occupied by populated areas of high - rise buildings and densely low - rise buildings were regarded as "urban areas" from the land use map of Osaka. The size of the mesh is 5 km square, and it matches the spatial resolution of the radar AMeDAS analytical precipitation. The "surrounding area" was 20 mesh outside of 2 mesh from the "urban area" mesh. Note that land use in meshes in the "surrounding area" is different from "urban area", and low rise buildings occupy a large proportion. The study period is the period from June to August of 1993 to 2015 when radar AMeDAS analysis precipitation data is available at the present time. The reason for targeting the period from June to August is that it seems that there is a biggest difference in rainfall between urban areas and their surrounding areas.

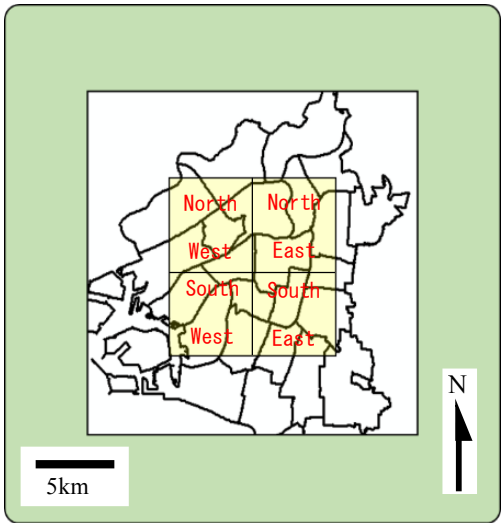

Fig.1 Study area

The flow chart of the research is shown in Fig 2. For analyzing the precipitation phenomenon in the target area, precipitation amount (mm), rainfall amount ≧ 1 mm hour number as an index of rainfall frequency, rainfall amount ≧ 5 mm hour number as index of heavy rainfall frequency was used as an analysis index. For each mesh, we calculate the average value of the 30-day precipitation and the 30-day integration of the number of precipitation amount ≥ 1 mm, and the precipitation ≥ 5 mm hour (hereafter referred as p_j (j represents each mesh). Interpolation value (pi) in urban area was calculated from p_j in the surrounding area by using least squares method defining quadratic surface based on Fujibe [1)]. A quadratic surface expression defined as an interpolation formula is optimized by the least squares condition to determine each coefficient b_1 to b_6 of the quadratic surface

$$f(x,y) = b_1x^2 + b_2y^2 + b_3xy + b_4x + b_5y + b_6 \quad \cdots(1)$$

$$\sum_j^J [p_j - f(x_j, y_j)]^2 \quad \cdots(2)$$

x_j, y_j represents the latitude and longitude of each mesh, and J represents the total number of meshes (= 20) in the surrounding area. The spatial deviation of rainfall and rainfall frequency (hereinafter referred as r_i) in urban areas and surrounding areas was defined as equation (3).

$$r_i = \frac{p_i}{\overline{p_i}} \quad \cdots(3)$$

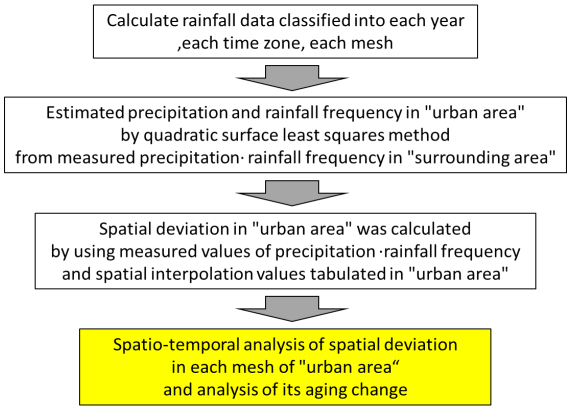

Fig 2 Flowchart

3. Result and discussion

Spatial deviation for the convenience of the paper, Fig. 3, 4 and 5 show only the diurnal change of r_i for each index in the northwestern part of the urban area where the most prominent trend in the spatiotemporal analysis in the June to August period was observed. The error bars show standard deviations. The day was classified into three time zones from sunrise to noon (4 to 11 o'clock), noon to sunset (12 to 19 o'clock), sunset to sunrise (20 o'clock to 3 o'clock, and we analyzed. In ri's space-time analysis, in the western part of the urban area, r_i of precipitation, rainfall frequency, heavy rainfall frequency was large during the noon to afternoon. In the northwestern part of the urban area which is the upwind side of the westerly wind, the trend of the r_i of the precipitation, frequency of rainfall ,frequency of heavy rainfall to increase becomes consistent with the findings [1) 2) 5)] of domestic and overseas studies. The finding that r_i of rainfall frequency also showed a trend to increase in the noon to afternoon time is a new finding obtained by enhancing the spatial representation of precipitation data by using the radar AMeDAS analysis precipitation. In the analysis of aging of r_i, it became clear that r_i tends to increase over time in the northwestern part of urban area. It became clear that the time zone during which ri gets larger spreads over a wider time zone. On the other hand, in the southwestern part of the urban area, r_i of rainfall tended to decrease with age. That is, we clarified that the influence of the city on weather is different inside the city. This is a new finding obtained in this research by analyzing urban areas divided by 5 km resolution.

4. Conclusions

1) In western part of the urban areas, precipitation, frequency of rain , frequency of heavy rain was greater than that in the surrounding area, especially during the time zone during afternoon
2) In northwestern part of the urban areas, the tendency that precipitation and frequency of rain was greater than that of the surrounding areas has been expanded over time

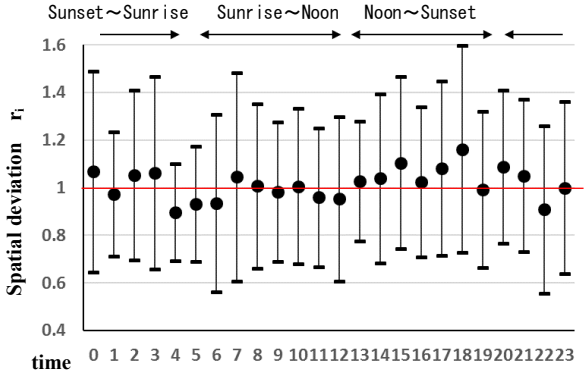

Fig. 3 Diurnal variation of precipitation in the northwest

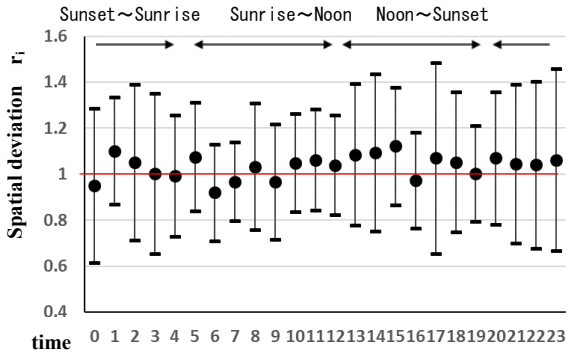

Fig. 4 Diurnal variation of precipitation ≥ 1 mm in northwest

3) In the southwestern part of the urban areas, the tendency

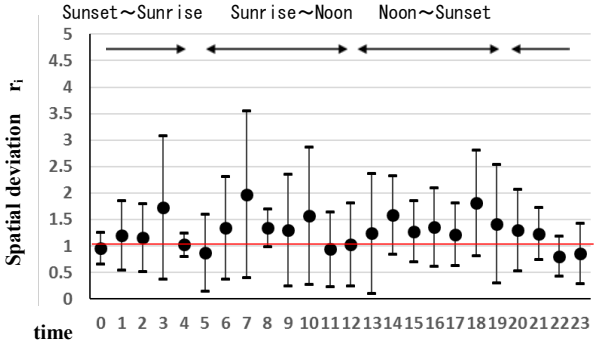

Fig. 5 Diurnal variation of precipitation ≥ 5 mm in northwest

of precipitation and frequency of rain was lower than that of the surrounding areas has been expanded over time.

5. Reference

1) Huff and Vogel: Urban, Topographic and Diurnal Effects on Rainfall in the St. Louis Region J.Appl .Meteor,17,1141 −1152, 1978
2) Wesccot: Summertime cloud–to-ground lightning activity around major Midwestern urban areas J.Appl .Meteor, 34,1633-1642, 1995
3) Balling, R. C. Jr. and S.W. Brazel: Changes in Phoenix, Arizona summertime diurnal precipitation patterns. Theor. Appl .Climato1,38,50-54, 198
4) Jauregui : Urban effects on convective precipitation in Mexico City, Atmos, Environ, 30, 3383-3389, 1996

Performance of sewage treatment and bioenergy production using duckweed

○Hiroshi IWANO[1]*, Takashi OTANI[1], Syo HATOHARA[1] ,Tadashi TAGAWA[2], Hideyuki TAMAKI[3], Yu-you LI[1] & Kengo KUBOTA[1]

[1] Department of Civil and Environmental Engineering, Tohoku University, 6-6-06 Aoba, Aramaki, Aoba-ku, Sendai, Miyagi, 980-8579, Japan.
[2] Department of Civil Engineering, National Institute of Technology, Kagawa College, 355 Chokushicho, Takamatsu, Kagawa, 761-8058, Japan
[3] Bioproduction Research Institute, National Institute of Advanced Industrial Science and Technology (AIST), Central 6, Higashi 1–1–1, Tsukuba, Ibaraki 305–8566, Japan
*E-mail: hiroshi.iwano.q7@dc.tohoku.ac.jp

Abstract

In this study, two species of duckweed (*Lemna* sp. and *Spirodela* sp.) were cultivated using three different treated sewage (i.e., sewage treated by primary sedimentation, conventional activated sludge process, and downflow hanging sponge process (DHS)) to evaluate sewage treatment efficiency, biomass production performance and bioenergy production potential. Sewage treatment and biomass production were stable with DHS- and primary-treated sewage, but not with conventional activated sludge process-treated sewage. *Spirodela* sp. was superior to *Lemna* sp. in terms of nitrogen removal performance. On the other hand, biomass production rate of *Lemna* sp. was greater than *Spirodela* sp.. Methane production potential of *Lemna* sp. and *Spirodela* sp. were 320 and 304 NmL/g-VS, respectively, and eventually approximately 65% of the input COD was converted to methane. These results indicated that duckweed is a suitable substrate for methane fermentation.

Keywords: duckweed, sewage treatment, anaerobic digestion

1. Introduction

In recent years, it has attracted attention to produce bioresources using nutrients such as nitrogen and phosphorus in sewage/wastewater, rather than removing them using expensive treatment systems. One approach is to utilize aquatic plants, especially duckweed. Duckweed can grow with uptaking nutrients from various wastewater such as sewage, swine wastewater and effluent from anaerobic digester treating sewage sludge. A growth rate of duckweed is fast, and duckweed is easy to be harvested because they are floating on water surface. Duckweed contains a large amount of starch and protein and less lignin and cellulose. Due to this characteristic, duckweed is being attractive as a source for biofuel (e.g., bioethanol and biomethane), livestock feed, and even human food.

The potential of bioresource recovery using sewage as a medium is huge due to its great amount. The characteristics of sewage change upon the degree of the treatment, and it has been developed many processes for treating sewage. One of the most applied process is a conventional activated sludge process. In this process, sewage is primary treated in primary sedimentation tank, where large particles of organic matters (i.e., suspended solids) are removed. Sewage after primary sedimentation tank contains a certain degree of organic matters, ammonium-nitrogen, and phosphorus. The primary-treated sewage is subjected to a reaction tank, where microorganisms take a place for nutrient removal, especially for BOD removal. Low BOD concentration and a little bit lower concentrations of ammonium-nitrogen and phosphorus (compared with primary-treated sewage) are a characteristic of conventional activated sludge-treated sewage. Some sewage treatment processes can achieve nitrification, and generate nitrate. One process achieving successful BOD removal and nitrification is down-flow hanging sponge (DHS). DHS is an aerobic biological treatment process that employs polyurethane sponges as the carrier for retaining bacteria. The energy requirement for the operation of DHS is very low due to no need of aeration, and the amount of excess sludge generated from DHS is extremely low. The primary-treated sewage is often subjected to DHS, and the effluent water from DHS contains low BOD (compatible to a conventional activated sludge) and nitrate.

In this study, treated sewage with three different characteristics (i.e., high ammonium-nitrogen and phosphorus concentration with higher BOD [primary-treated sewage], moderate ammonium-nitrogen and low phosphorus concentration with low BOD [activated sludge-treated sewage], and moderate nitrate-nitrogen and phosphorus concentration with low BOD [DHS-treated sewage]) was used to evaluate biomass production from treated sewage using duckweed. In addition, the sewage treatment performance in duckweed cultivation pond was evaluated. Eventually, bioenergy potential of duckweed was evaluated for energy production by methane fermentation.

2. Materials and Methods

2.1 Duckweed pond system

Two species of duckweed, *Lemna* sp. and *Spirodela* sp., were used for experiments. After one week acclimation to each treated sewage, approximately 30 g (wet-weight) of duckweed was subjected to 7.4 L of a duckweed pond with a raceway flow system (DP) and sewage treated by different processes (i.e., a primary sedimentation process (PS), a conventional activated sludge process (AS), and a DHS process) was supplied to DP with HRT of 1 day. The experiment was conducted at 25˚C under about 8,000 lx (16 h/day irradiation). Water quality of influent and effluent water was analyzed to evaluate sewage treatment efficiency by duckweed, and grown duckweed was harvested every week to evaluate biomass production performance.

2.2 Biodegradability test of duckweed

The biodegradability test of *Lemna* sp. and *Spirodela* sp. was carried out for 30 days at 35˚C using a 124 ml vial bottle. The composition of generated biogas was analyzed by gas chromatography and biodegradability of duckweed was calculated as methane gas production potential per VS.

3. Results and Discussion

3.1 Sewage treatment and biomass production

Monitoring results of NH_4^+-N, NO_2^--N, NO_3^--N, and PO_4^{3-}-P concentrations in DP-treated water (with *Lemna* sp.) and wet-weight change of *Lemna* sp. in DP during the treatment are shown in Figure 1.

When AS-treated sewage was supplied, sewage treatment efficiency and biomass production performance were unstable. The total ionic nitrogen (TIN = NH_4^+-N + NO_2^--N + NO_3^--N) removal rate of *Lemna* sp. decreased from 0.54 N-g/m^2/day (1st week) to 0.24 N-g/m^2/day (4th week). As with the biomass production rate, the biomass production rate decreased from 7.3 ton-dry-weight/ha/year (1st week) to 0.2 ton-dry/ha/year (3rd week), and eventually biomass production rate became negative in the 4th week. Since the PO_4^{3-}-P concentration in AS-treated sewage was very low compared with PS- and DHS-treated sewage, it was suggested that phosphorus may be a limiting factor for the growth of duckweed.

On the other hands, sewage treatment efficiency and biomass production performance were stable in the experiments using PS- or DHS-treated sewage. The TIN concentration and the PO_4^{3-}-P concentration decreased from 36.4 mg-N/L to 27.3 mg-N/L in average (0.50 g-N/m^2/day) and from 3.7 mg-P/L to 1.7 mg-P/L in average (0.11 g-P/m^2/day), respectively, with *Lemna* sp.. The concentrations of TIN and PO_4^{3-}-P decreased from 36.4 mg-N/L to 22.2 mg-N/L in average (0.79 g-N/m^2/day) and from 3.7 mg-P/L to 1.6 mg-P/L in average (0.12 g-P/m^2/day), respectively, with *Spirodela* sp.. The average TIN removal rate were 25% for *Lemna* sp. and 39% for *Spirodela* sp.. The PO_4^{3-}-P removal rates were similar for both species. The maximum biomass production rate was 19.7 ton-dry/ha/year (2nd week) for *Lemna* sp., and 14.6 ton-dry/ha/year (1st week) for *Spirodela* sp. when PS-treated sewage was subjected.

In the experiment using DHS-treated sewage, the TIN and PO_4^{3-}-P concentrations decreased from 19.3 mg-N/L to 12.2 mg-N/L in average (0.40 g-N/m^2/day) and from 1.6 mg-P/L to 0.7 mg-P/L in average (0.05 g-P/m^2/day), respectively, with *Spirodela* sp.. The average TIN removal rates were 25% and 37% for *Lemna* sp. and *Spirodela* sp., respectively. The average removal rates of PO_4^{3-}-P were 57% for both species. Likewise, the maximum biomass production rate was 11.7 ton-dry-weight/ha/year for *Lemna* sp. (2nd week), and 10.6 ton-dry-weight/ha/year for *Spirodela* sp. (1st week). Note that remarkable algae growth was observed when the initial supply of duckweed was reduced to 15 g from 30 g, indicating that duckweed should be supplied to cover the surface area in order to carry out stable sewage treatment and biomass production.

3.2 Biodegradability of duckweed

Methane gas production was immediately observed after the start of the experiment. Methane gas production rates of both duckweeds were high and approximately 50% of an input COD was converted to methane in the first 4 days. Then, sudden decrease in gas production rate was observed and eventually about 65% of the input COD was converted to methane. Methane gas production potentials of *Lemna* sp. and *Spirodela* sp. were 320 and 304 NmL/g-VS, respectively. The results demonstrate that both duckweeds are a suitable substrate for methane fermentation.

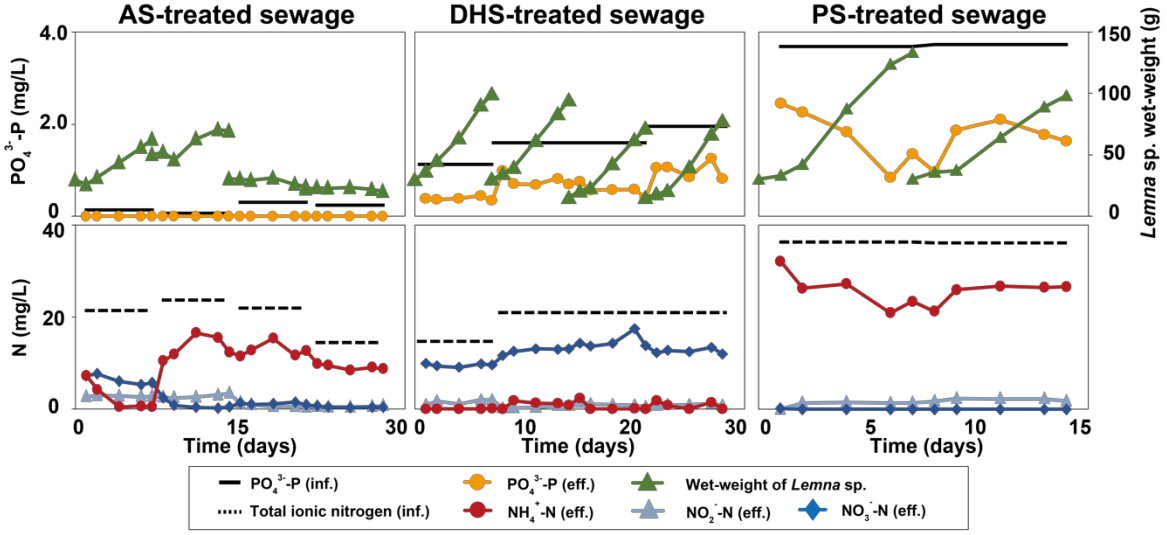

Figure 1. Monitoring of biomass production of *Lemna* sp., NH_4^+-N, NO_2^--N, NO_3^--N, and PO_4^{3-}-P after subjecting AS, DHS, or PS in DP.

Mesophilic and Thermophilic Temperature Phased Anaerobic Digestion of Paper Waste Containing Food waste: the Effects of Hydraulic Retention Time

○Aijun ZHU[1]*, Jing WU[1], Yu Qin[2] & Yu-You Li,[1,2]
[1] Department of Frontier Science for Advanced Environment, Graduate School of Environmental Sciences, Tohoku University, 6-6-20 Aoba, Aramaki-Aza, Aoba-Ku, Sendai, Miyagi 980-8579,
[2] Department of Civil and Environmental Engineering, Graduate School of Engineering, Tohoku University, 6-6-06 Aoba, Aramaki-Aza, Aoba-Ku, Sendai, Miyagi 980-8579, Japan;
*E-mail: zhu.aijun.t4@dc.tohoku.ac.jp

Abstract

The aim of this study was to investigate the effect of hydraulic retention time (HRT) on methane production using a single-stage anaerobic process in different temperature phase . Two continuously stirred tank reactors (CSTRs) were used under thermophilic (55±1°C) and mesophilic(35±1°C) conditions in order to enhance methanogenesis. A mixture of paper waste and food waste (1:1, TS/TS) was utilized. The reactor was operated at different HRTs to optimize the methane production and organic removal efficiency. Comparison of the the mesophilic and thermophilic anaerobic digestion of paper waster containing food waste.

The maximum CH_4 production rate was achieved at HRT of 7.5 d in thermophilic condition. The TS, VS, carbohydrate and COD removal efficiency was almost same at different HRT and protein showed negative removal efficiency.

Keywords: temperature phased; anaerobic digestion; paper waste; food waste; Hydraulic retention time

1. Introduction

Renewable energy sources have received great interest from the international community during the last decades. Organic fraction of municipal solid waste (food waste) is one of the most promising energy sources. However, despite its high carbohydrate content, the anaerobic treatment of food waste is quite problematic due to its low bicarbonate alkalinity high COD concentration and tendency to rapid acidification. Except for the resistant to biodegradation, the low C/N ratio of food wasteis also a serious problem to the anaerobic digestion. Although, an optimum C/N range in feedstock for the anaerobic digestion is still debatable in the literature, 20/1–30/1 is a most acceptable range.

One method to avoid excessive ammonia accumulation is to adjust low feedstock C/N ratios by adding high carbon content materials, thereby improving the digestion performance. Most food waste consists of paper material (including office paper and newspaper), which has a C/N ratio ranging from 173/1 to greater than 1000/1. Both wastes are produced in large quantities and in many places, and much research has focused on this particular issue. Co-digestion using paper waste containing food waste as substrate may enhance the performance of the anaerobic digestion (AD) due to better carbon and nutrients balance. That is, the use of a co-substrate that in most cases improves the biogas yields due to positive synergisms established in the digestion medium and the supply of missing nutrients by the co-digestion.

A series of operational parameters including pH, temperature, reactor configuration, Among them, hydraulic retention time and temperature have been reported as one of the most important parameters significantly affecting microbial ecology in CSTR digesters and must be thus optimized for the particular feedstock fermented in the digester. Organic loading rate and hydraulic retention time have been investigated in the literature due to their effect on biogas production. More specifically, our aim was to study the effect of HRT and different temperature phase, as the critical operating parameters on methane production. The purpose of this work was to assess the possibility of co-digestion of food waste and high carbon content of waste paper at different HRT.

2. Materials and Methods

2.1 Materials

The compositions of food waste used as substrate in the test based on previous study which consisted of 30% fruits, 36% vegetables, animal 14% and staple food 20%.. The collected food waste were ground and homogenized to less than 5 mm with tap water in a blender and were stored at 4°C before feeding. FW was supplemented with the trace elements, Fe, Co and Ni: 100 mg/L of Fe ($FeCl_2 \cdot 4H_2O$), and 10 mg/L of both Co ($CoCl_2 \cdot 6H_2O$) and Ni ($NiCl_2 \cdot 6H_2O$) .

The paper waste was consisted of office paper toilet paper and newspaper which are the most large amount of recycle paper in Japan. The ratio of three paper waste was 1 : 1 : 1, cut by shredder before mixing with food waste for feeding.

Seed sludge was from a mesophilic sewage sludge digester at the Sendai municipal sewage treatment plant located along Sendai, Japan.

Table 1 The operating conditions and removal rate in digester

		mesophilic			thermophilic				
		Run 1	Run 2	Run 3	Run 1	Run 2	Run 3	Run 4	Run 5
temperature		35℃				55℃			
substrate		50%PW	40%PW	40%PW	50%PW	50%PW	50%PW	50%PW	50%PW
HRT(d)		30	20	10	30	20	10	7.5	5
Operation time		1-89	90-142	143-170	1-47	48-119	120-142	143-171	172-192
OLR g COD/L/d		4.3	6.53	13.06	4.3	6.45	12.89	17.1	25.7
removal rate %	TS	65.6±5	71.3±2.1	39.3±4	78.1±1.1	73.6±4.1	69.6±0.2	69.2±0.1	54.77±3.1
	COD_{Cr}	67.22	74.33	30.27	78.94	74.76	72.75	71.17	59.67
	(CH_2O)	78.03	82.53	75.88	91.53	89.06	87.48	86.34	83.99
	protein	16.55	10.97	6.68	29.46	13.05	8.29	9.89	2.12

2.2 Analysis methods

Daily biogas production is measured by wet gas meter, the composition of biogas (CH_4, CO_2 and N_2) were measured by a ShimadzuGC-8A gas chromatograph. and pH, COD, TS, ammonium nitrogen, alkalinity, VS and VSS were measured according to Standard Methods. Sludge samples were sampled twice a week from the digesters and the substrate tank to determine the total and soluble parameters. Samples for the analysis of soluble items, such as soluble COD (SCOD), total ammonia nitrogen (TAN), VFAs and alkalinity, were centrifuged at 8,000 rpm for 15 min and then filtered with 0.45 μm filters before they were analyzed. A GC, equipped with a flame ionization detector ((GC-FID, Shimadzu GC-14B) and a DB-WAXetr column, was utilized to detect VFAs and ethanol. A 0.5 mL filtrate was collected in a 1.5 mL GC vial, and 0.5 mL 0.1 mol/L HCl solution was also added to achieve an acidic pH.

2.3 Reactors start-up and operation

A mixture of paper waste and food waste (in the TS ratio of 1:1) was used, based on our previous experiment. Experiments were carried out in a single-stage continuous anaerobic process. The anaerobic reactors were cylindrical in shape, made with a double wall, having an operating volume of 3 L, and were operated at constant temperature (55±1°C) via a heaters and water jackets. The feedstock was stored in a tank maintained constant temperature at 4 °C.

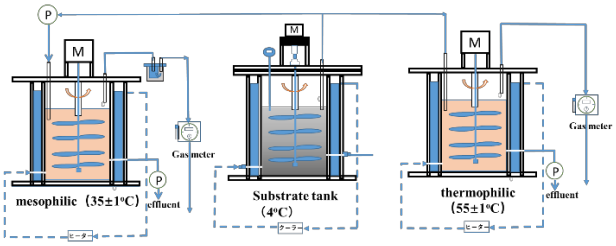

Fig. 1. Schematic diagram of the single-stage system used in this study for methane production

The continuous operation of the reactor started at HRT of 30 d. Sludge samples were sampled twice a week from reactors under continuous stirring conditions and analysed, for monitoring each reactors performance. Experiments were conducted successively to determine the optimum HRT for methane production. Organic loading rate (OLR) was increased by decreasing the operating HRT. The reactor was operated at different HRTs with feeding mixture of paper waste and food waste. The tested operating conditions and removal rate in the system are summarized in Table 1.

3.Results and Discussion

The experimental results about organic removal efficiency obtained at steady-state conditions for the different HRTs. The TS, VS, carbohydrate and COD removal efficiency was almost same at different HRT in thermophilic condition, the all best performance as positive removal was achieved in HRT＝30 d, TS(77.3%), VS(81.6%) , carbohydrate (91.5%) and COD(78.9%).Meanwhile, the protein showed negative removal efficieny.

In the mesophilic fermentation, stable methane fermentation in high organic loading rate utilizing mixture of food waste and paper was possible at HRT 20, 30 days. And the mixing ratio of paper was found to have an important role in the whole process. The processing was operating stably if the paper ratio was less than 40%, otherwise the propionic acid began to accumulate, pH was decreased, methanogenesis was inhibited, tending to acidification When the ratio of paper was 40%, HRT was set to 20 days, the process could be operated steadily, but if HRT was shortened to 10 days, the VFA accumulated rapidly and biogas production ceased.

In the thermophilic phase, stable operation was possible even when the waste mixed with food waste and paper (TS) 1: 1 ratio, the HRT was shortened from 30 days to 7.5 days, but the HRT was more shortening, the VFA accumulated, so the process was failed. Propionic acid tends to accumulate in both the mesophilic and thermophilic condition when the reaction of the process does not progress properly. Then, it made other various Volatile Fatty Acid accumulated and inhibition occurred.

Use of PMA-PCR for revelation of viable microbial members in anaerobic digesters

○Jialing Ni[1], Shingo Hatori[1], Yu-You Li[1], Kengo Kubota[1]
[1]Department of Civil and Environmental Engineering, Graduate School of Engineering, Tohoku University, Sendai, Miyagi 980-8579, Japan.
E-mail: jialing@dc.tohoku.ac.jp

Abstract

Twelve digester sludge samples were treated with PMA to study actually viable microbial community in 5 sludge fed digestion systems. The alpha diversity indicated an obvious decrease in numbers of Operational taxonomic unit (OTU), Chao1 index and Shannon index. The microbial community analysis results showed that the obvious decrease of methane-producing bacteria, and the class *Alphaproteobacteria* and *Betaproteobacteria* remarkably decreased by 40.02% - 96.07% and 13.95% - 98.71%, respectively, after the PMA treatment in relative abundance. Digester sludge samples treated with PMA showed a farther distance than the original ones from primary sedimentation sludge and excess sludge. This study achievably detected the PMA-PCR based 16S rRNA gene sequencing method can reflect the microbial structure of microorganisms with activity in AD samples.

Keywords: Propidium monoazide, 16S rRNA gene sequencing, digester sludge, compromised membrane

1. Introduction

Anaerobic digester wildly used in the world nowadays makes it possible to achieve pollutant removal combined with energy generation and sludge reducing. Next generation sequencing is a very available method that can not only detect the microorganisms connecting anaerobic digestion, but also reveal matter decomposing under anaerobic condition, through microbial community structure analysis. The analysis of 16S rRNA gene extracted from samples without special treatment could not represent the active microbial populations in the certain moment. For instance, in the situation that some microbial populations without activity are remained after aerobic treatment in excess sludge entering into a digester will hardly be proved whether they did make contribution to the digestion process or not.

One method to analyze the DNA from viable cells with intact membrane is a PMA-PCR method. PMA has the characteristic that it cannot get into microbial cells with intact cell membrane (assumed to be live cells). It only penetrates into cells with compromised membrane (assumed to be dead cells) and binds to DNA in the cells. Upon the exposure to bright light, PMA covalently crosslinks DNA, by which dissociation of DNA is prevented even during the thermal treatment during PCR. The cross-linked DNA is not amplified by PCR, so it is not reflected in the community structure analysis result. Our research is to investigate microbial community structure in anaerobic sludge digesters further exploring the actually active microbial community by using PMA-PCR method.

2. Materials and Methods

2.1 Sample collection and PMA treatment

The samples were collected from five different sewage works in Japan (AKT, NGT, NIT, SEN and TNN sewage works). In total, 34 sludge samples were collected for this study (12 DS samples, 11 PS samples, and 11 ES samples).

PMAxx (Biotium) was added to the DS samples. After incubation in dark, light exposure was performed.

2.2 16S rRNA sequencing and analysis

After DNA extraction, the qPCR analysis was performed by using a LightCycler® 2.0. And PCR was conducted with the primer set of 341F-806R-mix targeting the V3 -V4 region of the 16S rRNA gene. Sequencing was performed using an Illumina MiSeq platform. Analysis of sequence data was done using the QIIME software with the Greengenes database. Operational taxonomic unit (OTU) was made with the 97% sequence identity. The Silva database (Silva 132 NR99) and the NCBI blast search tool were also used to confirm the assignment of the taxonomy of several important OTUs.

3. Results and Discussion

Since PMA treatment can eliminate the influence of extracellular and dead cells-derived DNA, quantification of gene copy number allows to estimate the ratio of viable cell in a certain environment. Detail information about qPCR results of all the samples is shown in **Table1**. Ribosomal RNA gene copy numbers of the DS and DS_PMA samples were $4.3\text{-}8.0\times10^5$ and $4.1\text{-}6.0\times10^5$ copies/ngDNA, respectively. Decreasing rate of gene copy number was 19.1% in average. In our study, through comparing the qPCR results with and without PMA treatment, 17.4% to 35.6% of DNA didn't amplify in qPCR process with PMA treatment, which can be considered as dead cells, which don't have intact membrane. Taking into account the accuracy limitation of qPCR, it is reasonable to get the conclusion that qPCR results was very close to the results of Mei and colleagues who pointed out that the involved microbial residue approximately less than 10% in most of the full-scale digesters. Therefore, the PMA-PCR based 16S rRNA gene sequencing method can reflect the microbial structure of microorganisms with activity in AD samples.

The minimum number of sequence reads in all 46 samples was 48,919, and randomly picked 35,000 sequence reads

were used for further analysis in order to keep the same sequencing depth. The number of OTU and two diversity indices, Chao1 and Shannon, of DS and DS_PMA samples as well as PS and ES samples were calculated to estimate and compare the diversity of all samples. A total of 8,756 OTUs was retrieved from the 46 samples. The numbers of OTUs ranged 790-1726 for DS, 534-1267 for DS_PMA, 1045-1767 for ES, and 1264-1727 for PS. The reduced numbers of OTU, Chao1, and Shannon were in the range of 122 to 459, 120 to 594, and 0.27 to 0.89, respectively. The ES and PS samples showed much more diversity than the DS and DS_PMA samples.

Fig1 shows the relative abundance of microorganisms in each sample at the phylum and/or class levels. The phyla with the population less than 1.0% are summarized in "Other". *Proteobacteria*, *Bacteroidetes*, *Firmicutes*, *Chloroflexi* and WWE1 were dominant members.

The changes on the relative abundances of the *Proteobacteria* were remarkable. The relative abundance of the phylum *Proteobacteria* reduced by 49%, 30%, 41%, 44%, and 4% on average in the AKT, NGT, SEN, TNN, and NIT samples, respectively, after the PMA treatment. The class *Alphaproteobacteria* and *Betaproteobacteria* occupied several percent of the total community without PMA treatment, but they remarkably decreased their population by 40% (SEN1) - 96% (TNN1) and 14% (NIT1) - 99% (AKT1), respectively, after the PMA treatment.

Top 25 OTUs whose relative abundance decreased the most in descending order. The OTU 44890 and the OTU 34527 showed 99% and 98% sequence identity, respectively, to Methanosaeta concilii, known as a acetoclastic methanogen. OTU 44890 decreased the most after PMA treatment (6676 sequence reads reduced of all the total sequence reads belonging to DS for about 40.9%). The results also concluded that members of Betaproteobacteria that Rivière and colleagues reported in anaerobic digested sludge as one of the core groups may not be, on the other hand, WWE1 group may be belonged to the core groups.

The similarity and differences of each microbial community structure are analyzed by principal coordinates analysis (PCoA) (**Fig2**). The digested sludge sample treated with PMA shifted the same directions farther away from primary sedimentation sludge and excess sludge than digested sludge sample without PMA treatment. This result shows that some specific microbial microorganisms derived from PS or ES was removed from the structure analysis result of DS by PMA treatment**.**

4. Conclusions

This study revealed that Combining PMA-PCR with 16S rRNA sequencing analysis can exclude microbial community involved from primary sedimentation sludge and excess sludge with compromised membranes, and it is possible that alive microorganisms actively playing a role in the anaerobic digestion could be detected by this study. In addition, the results of qPCR suggested that that near 20-30% of the total prokaryotic microorganisms can be considered as inactive microorganisms in most digesters. And it is also possible to eliminate the toxicity of PMA to microbes in environmental samples and the confusion of biofilm penetration to a degree. OTUs belonging to the *Betaproteobacteria* in anaerobic sludge digesters may not be one of the core groups.

5. Acknowledgments

The authors would like to thank Inter-Graduate School Doctoral Degree Program on Science for Global Safety for the funding support.

Table 1 qPCR results of all the samples.

Sample name	DNA concentration (10^5 gene copies/ng DNA)		
	DS (copies/ng)	DS_PMA (copies/ng)	decreasing rate (100%)*1
AKT1	8.0±0.64	5.2±0.27	36
AKT2	6.7±0.75	5.2±0.52	21
AKT3	4.3±0.51	4.3±0.80	0
NGT1	5.1±0.87	6.0±0.58	-16
NGT2	6.1±0.63	4.6±0.11	25
NIT1	5.7±0.57	4.5±1.07	20
NIT2	5.9±0.57	4.6±0.06	22
SEN1	5.0±0.38	5.0±0.47	1
SEN2	5.8±0.31	4.3±0.15	26
SEN3	5.6±0.64	4.7±0.79	17
SEN4	5.8±0.39	4.2±0.39	27
TNN1	5.9±0.13	4.1±0.67	31

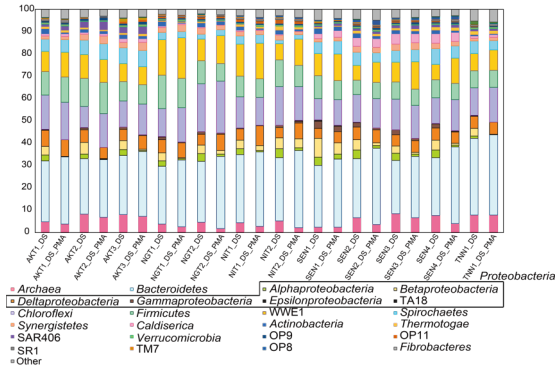

Fig.1 Relative abundance of digested sludge samples

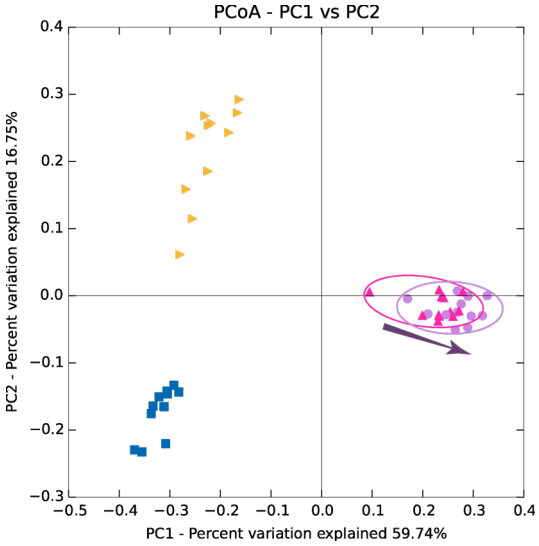

Fig.5 Principal coordinates analysis (PCoA) of prokaryotic community structures

Optimization of cultivation of humic-reducing bacteria based on ORP/pH feedback

○Runda Du[1]*, Jingmei Sun[2], Yu-You Li[1]
[1]Department of Civil and Environmental Engineering, Tohoku University, Sendai, Miyagi 980-8579, Japan
[2]Department of Environmental Engineering, School of Environmental Science and Engineering, Tianjin University, Jinnan District, Tianjin 300350, China
*E-mail: du.runda.t3@dc.tohoku.ac.jp

Abstract

Humic-reducing bacteria can be used as a kind of ecological remediation agent in the process of water restoration. Therefore, the research and development of its high-density culture technology are attached to great importance. In this study, humic-reducing bacteria were cultured with high-cell-density culture using active sludge acclimated by AQDS and its feeding strategy based on ORP/pH feedback was studied. The optimum nutrient conditions for the growth of humic-reducing bacteria were explored by three-factor four-level orthogonal experiment and the metabolic reaction process was further analyzed. The results showed that glucose, as carbon source, could cause acid fermentation and lead to sludge reduction. The reduction process of AQDS significantly improved the observed sludge yield (Y_{obs}=0.622~0.786), thus it promoted the rapid growth of biomass. In the reactor stage, daily parameters such as TOC, pH, ORP were monitored to search for the correlations between microbial growth and metabolism in the system and the changes of ORP or pH, the results showed that the increase of HRT and the addition of agitation could contribute to redox process and the propagation of active sludge. The feeding control strategy was determined: when ORP was close to -150 mv and the pH was higher than 8.0, the reactor should to be enriched.

Keywords: humic-reducing, high-cell-density cultivation, ORP

1. Introduction

Many researches have found that humic-reducing bacteria widely exist in nature, and they can accelerate reduction of toxic substances such as Azo, nitro substituted aromatic compounds and polymerized organic compounds in wastewater. They also have potential applications in remediation situation.

To supply sufficient bioagent (e.g. humic-reducing bacteria) for remediation bio-augmentation, we have to do with propagation or expanding culture situations. However, monoculture of an anaerobic bacterium is so complicated and slow-growing. Furthermore, bioagent with monoculture are susceptible to the aborigines and lost their ecological niche in sediment system. As opposed to monoculture, sludge has a larger microbial community, higher biodiversity and stronger eco-stability. So, we chose to use active sludge acclimated by AQDS, and hence, there was a need for building up a high-density culture strategy. Considering that humic-reducing is closely related to redox, the feeding strategy was designed based on ORP/pH feedback.

According to existing results, the growth and metabolic process of humic-reducing bacteria are accompanied by ORP's sudden jump (this can be explained by Nernst Equation), and the change of pH is also accompanied by the abrupt change of ORP. This coupled with the specific humic-reducing reaction. The microbes thus can be controlled in specific metabolic phase by clarify the relationship between the change of ORP/pH and the growth of microbes. Adequate use of carbon source, nutrients and energy and elimination of side-effects (e.g. acidic fermentation) are expected by using ORP/pH feedback strategy.

2. Materials and Methods

2.1 Source of sludge

The activated sludge used in this experiment is obtained by the research group in the early stage. The sludge is taken from the sludge of the secondary settling tank of a sewage treatment plant and then acclimated by AQDS.

2.2 Methods of pre-experiment

An orthogonal experiment was designed with three factors (types and concentrations of carbon source, C/N ratio) and four levels to find the optimal conditions for biomass production. The substrate is composed of carbon source, 0.5 g/L NH_4Cl, 0.5 g/L $KH_2(PO_4)$, 0.5 g/L $CaCl_2$, 0.6 g/L $Mg(SO_4)_2$, 10 ml/L concentrate of trace element.

According to the formula, the corresponding concentrations of nutrients were added to the 250 ml of serum bottles, and then each bottle was inoculated with 5 g-VSS/L of acclimated sludge.

2.3 Operation of the reactor

The acclimated sludge was inoculated in five reactors, and according to the optimal carbon source and carbon source concentration obtained by the pre-experiment, 25 L of substrate was supplied to all the reactor. The substrate is composed of 15 g/L Sodium acetate, 0.25 g/L $(NH_4)_2SO_4$, 0.05 g/L $KH_2(PO_4)$, 0.5 g/L $CaCl_2$, 0.2 g/L $Mg(SO_4)_2$, 0.00875 g/L Lawsone, 0.1 g/L Na_2SO_3. The specific parameters of the reactor are in the Table 1.

Table 1 Parameters of the reactor

Number	1	2	3	4	5
HRT(h)	24	24	8	4	1
Agitation	Y	N	N	N	N

3. Results and Discussion

3.1 Analysis of ORP in pre-experiment

As shown in Fig. 1(a-d), ORP of sodium acetate and beef extract can reach a lower level (below -400 mv) than that of glucose and yeast extract. In general, ORP of the substrates with different carbon sources shows similar trends. As the feed cycles increase, the initial level of ORP after feeding becomes lower and has smaller range of mutation during feeding, which may be due to the accumulation of reducing metabolites. ORP of the substrates with different carbon sources can decrease and stabilize within a certain range in each cycle, and the effect of different carbon source loading rates on the stability interval is not significant. Therefore, concentration of carbon source is not the key factor to regulate ORP.

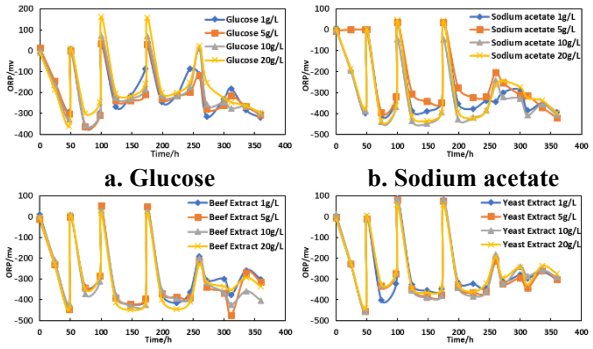

a. Glucose b. Sodium acetate

c. Beef Extract d. Yeast Extract

Fig. 1(a-d) ORP in different substrates of pre-experiment phase

The carbon source in the system is consumed along with the AQDS being reduced and the reduction of ORP. For glucose, according to the Nernst equation:

$$E = E^0 - \frac{RT}{nF}\ln\left[\left(\frac{C_{AH_2QDS}}{C_{AQDS}}\right)^{12}\cdot\left(\frac{C^6_{H_2CO_3}}{C_{C_6H_{12}O_6}}\right)\right]$$

The lower ORP is, the conversion of the carbon source and the reduction of AQDS are more complete. That is to say, the reduction of ORP reflects the degree of carbon source consumption and AQDS reduction, which can be used as a basis for preliminary analysis of the growth state of humic-reducing bacteria. It can be also seen that the effect of C[AH_2QDS]/C[AQDS] on ORP is significantly greater than that of carbon source, which is consistent with the conclusion above: ORP change and stability are less related to carbon source loading rate.

3.2 Proliferation and observed yield of sludge in pre-experiment phase

From Fig. 2, as the glucose loading rate rises, the sludge has a tendency to decrease because of the acidic fermentation of the acclimated sludge when using glucose. The accumulation of organic acids makes damage to DNA and protein, which leads to cell decline. The concentration of MLSS also decreases when the yeast extract reaches 20 g/L because yeast extract is decomposed by microbes into carbohydrate.

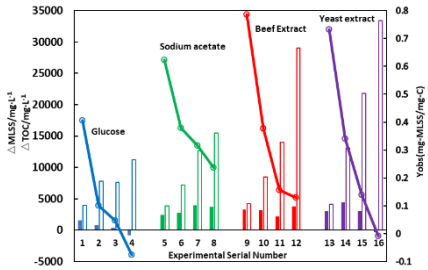

Fig. 2 △MLSS、△TOC and Y_{obs}(observed sludge yield)

3.3 Reactor phase

When acclimated activated sludge containing humic-reducing bacteria uses sodium acetate as carbon source for growth and metabolism, the change of ORP and pH show a kind of correlation that pH increases with the decrease of ORP, and they stabilize around a certain value or in a certain interval before supplementing the carbon source. The lengthening of HRT and the agitation are beneficial to the redox reaction and the proliferation of activated sludge.

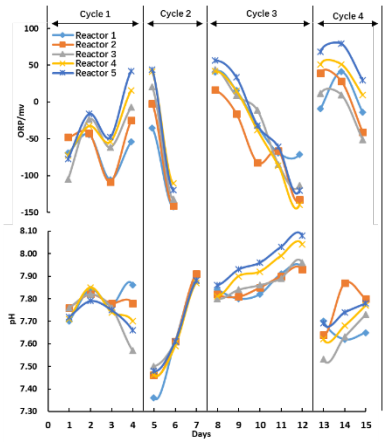

Fig. 3 pH and ORP in system of reactor phase

4. Conclusions

4.1 pre-experiment phase

(1) Glucose as carbon source produces acid fermentation that causes sludge reduction.

(2) The reduction of AQDS is the main factor in the decline of ORP, and the impact of carbon source loading rate on ORP changes is small.

(3) 5 g-COD/L yeast extract and 10 g-COD/L sodium acetate are suitable as carbon source for high-cell-density cultivation. Considering economic factors, sodium acetate is selected as the carbon source, and its concentration is not less than 10 g- COD/L.

4.2 reactor phase

(1) As ORP in the system decreases, pH increases indicating that the metabolism of sodium acetate coupled with AQDS is a reaction process that produces alkalinity.

(2) Determine the threshold of feeding as: ORP=-150 mv or pH=8.0

(3) Lengthening the HRT and increasing the hydraulic disturbance intensity can further promote the proliferation of sludge.

The effects of pre-acidification on the granuler sludge perperties in the anaerobic treatment of starch wastewater

○Bo Feng[1]*, Jing Wu[2], Bo Jiang[2] & Yu-You Li[2]
[1] Graduate School of Environmental Studies, Tohoku University, 6-6-06 Aoba, Sendai 980-8579, Japan
[2] Department of Civil and Environmental Engineering, Graduate School of Engineering, Tohoku University, 6-6-06 Aza-Aoba, Aramaki, Aoba-ku, Sendai, Miyagi 980-8579, Japan.
*E-mail: feng.bo.r3@dc.tohoku.jp

Abstract
In this study, two different anaerobic digestions (AD) processes for the treatment of starch wastewater (SW) were compared to determine the effect of adding a pre-acidification unit to this promising cost-saving process known for its bioenergy advantages. A single-phase UASB reactor (the SP process) and a modified pre-acidification tank/EGSB reactor combined process (the TP process) were continuously fed with SW under organic loading rates (OLR) from 1 to 12g-COD/L/d by shortening the hydraulic retention time (HRT) from 24 to 2h. The SW treatment performances of both processes were compared in terms of their capability to remove organic nutrients, the morphological properties of the granular sludge, and their stability. Results showed that the soluble chemical oxygen demand (SCOD) removal efficiencies were higher than 80% in both processes. However, granule floatation and disintegration were noticed in the SP process when the HRT as shortened to 6h at an OLR of 4g-COD/L/d. These results indicate that the use of a pre-acidification unit (the TP process) is an effective strategy to enhance sludge stability in the AD process in treating SW.
Keywords: Starch wastewater; Anaerobic treatment; Pre-acidification; EPS; Granular physicochemical properties

1. Introduction

With the total starch consumption in 2011 at approximately 70 million tons, world-wide starch production maintains an upward trend. In China, the world's largest producers of sweet potatoes, around 1.5 million ton of sweet potato was used in starch production in 2011. Notably, the starch residue is discarded at many points in the production chain. For example, during the roughing process, in excess of 10 cubic meters of starch wastewater (SW) is typically discharged in the processing of one ton of sweet potato root. The organic content of the raw SW drained from the starch workshop is high and its pH value is low. The large-scale discharge of such waste streams, once large-scale discharged into natural waters without any treatment, can lead to a range of ecological problems.

Awareness of the environmental hazards of waste streams has led to the development of various treatment strategies. Among the alternatives, biological treatment is one of the most recommended technologies. Starch is non-toxic, with a relatively high BOD/COD ratio of 0.4-0.7, and is biodegradable. Anaerobic digestion (AD), is a biological process which converts organic compounds into different products under the oxygen-free condition. The biogas produced by AD process contains 50-75% methane and 5-10% hydrogen, and is a potential biofuel. The Up-flow Anaerobic Sludge Blanket (UASB) technology, one of the AD processes, is employed in 80% of the anaerobic wastewater treatment plants around the world. A modified version of the UASB is the Expanded Granular Sludge Blanket (EGSB) technology: this allows the effluent to be internally circulated to improve contact among the granules with the substrate and provides an alkalinity buffer for the reactor.

Much of the focus of investigations into the performance of the UASB treatment of SW has been on shortening the hydraulic retention time (HRT) to observe the organics removal and biogas production under the elevated organic loading rate (OLR). Lu employed a single-phase (SP) UASB process to treat low-strength SW, and noted that when the OLR reached 6g-COD/L/d with an HRT of 4h, the increase in the extracellular polymeric substance (EPS) content in the granular sludge triggered granules floatation and reactor foaming. This suggests that the treatment of SW in a UASB reactor may involve uncertain sludge physicochemical properties (PCPs).

The organics conversion of carbohydrates in the AD process broadly includes two steps, acidogenensis and methanogenesis. The biokinetic and physiologic characteristics of the related-microorganisms of the two steps are different. The pre-acidification unit, a primary part of the two-phase (TP) AD process, is where acidogenesis is separated from methanogenesis, to ease the rate-limitation of methanogenesis in the bioreactors. In the pre-acidification unit, complex organic compounds are mainly converted to small molecule organics easily biodegradable substances for methanogenesis, such as butyric, propionic and acetic acids, all classified as volatile fatty acids (VFAs). Earlier studies have reported excellent treatment performance of the UASB reactor for short-chain fatty acids, including considerable nutrient removal feasibility, the fully developed granule microstructure and satisfactory granular settling properties. The pre-acidification/UASB process has been reported to successfully improve the AD performance in various waste streams, e.g., coffee-grounds, cheese whey, brewery and chicken manure wastes.

Hence, we considered the possibility that the adverse effects of SW on granular sludge may be overcome by introducing a pre-acidification unit before EGSB treatment.

2. Materials and Methods

2.1 Wastewater and seed sludge inoculation

The SW employed in this study was synthesized according to the diluted real SW from a paper mill industry in Japan, and contained 1000mg/L of COD from modified (soluble) starch (Wako, purity: 99.0%). Supplements of the essential elements and 1000-3500mg/L of NaHCO3 which was used to supplement alkalinity. Mesophilic anaerobic granular sludge was withdrawn from a full-scale UASB reactor in a brewery wastewater treatment plant, Japan. For the pre-acidification unit of TP process, 5.5L of the substrate was mixed with 0.5L of digested sludge from a domestic wastewater treatment plant, in Japan. 1M of hydrochloric acid (HCl) was used to adjust the pH of the mixed sludge to 5.5, an appropriate value for carbohydrate-based acidogenesis.

2.2 Lab-scale reactors and the operational conditions

A schematic diagram of the reactor setup including the accessories is provided in Fig.1. The apparatus used in the long-term experiment comprised a UASB reactor (SP) and a CSTR-EGSB process (TP). the working volume was 6L and the vertical height was 0.8m. Water baths (NTT-20S, EYELA) were equipped to maintain the temperature of both processes at 35±1℃. The recycle ratio of the EGSB in TP process was 1.0 to replenish reactor alkalinity. A plastic tank with an effective volume of 200L was employed to store the substrate. A condenser (Yamato, BE201) was inserted into the plastic tank to refrigerate the substrate at 4°C. Peristaltic pumps (Masterflex, EW-07528-10) were used for substrate delivery and the recirculation of the effluent in the EGSB reactor. Two wet gas flow meters (SHINAGAWA W-NK-0.5) were used to measure the daily production of biogas. The substrate was continuously fed to both processes. The two processes were started up at an HRT of 24h (SU stage), and the stepwise withdrawal shortened the HRT, thereby increasing the OLR.

3. Results and Discussion

3.1 Overall treatment performance of TP and SP processes

In this study, two different anaerobic digestions (AD) processes for the treatment of starch wastewater (SW) were compared to determine the effect of adding a pre-acidification unit to this promising cost-saving process known for its bioenergy advantages. Results showed that the soluble chemical oxygen demand (SCOD) removal efficiencies were higher than 80% in both processes. However, granule floatation and disintegration were noticed in the SP process when the HRT as shortened to 6h at an OLR of 4g-COD/L/d. In-depth analysis of the elemental composition and content of the extracellular polymeric substances (EPS) in the granular sludge indicated an increase in the protein content in the loosely-bound EPS (LB-EPS) due to the paste-like membrane structure attached to the granules. Sludge disintegration in the SP process may have been triggered by the electrostatic repulsion between the negatively charged protein content. In the TP process, the granular sludge shows satisfactory physicochemical properties (PCPs).

3.2 Temporal variation of granular sludge PCPs along the reactor height

Longitudinal diameter distributions along both reactors were generally consistent when the HRT was higher than 12h. During these periods, the granular size distribution fitted well to the Gaussian distribution model (the correlation coefficients (R2) were 0.7351-0.9999). Liu applied an electric field in a UASB reactor to enhance the anaerobic granulation, and reported similar statistical characteristics in the healthy and mature anaerobic granules. When the HRT conditions were higher than 12h, more than 25% of the granules in the upper part of the granular sludge had a diameter range of 1.0-2.0mm, in the middle part, it was around 40%, and around and it was 50% at the bottom part. The longitudinal distributions of the median particle size (extended meaning of mathematical expectation (XC)) stepwise panned right along the X-axis from the "Up" to "Down" part of the two reactors, suggesting that the density of the larger granules made them more buoyant. The granules in both reactors showed a compact structure with a smooth particle surface. According to the granular distribution in the UASB reactor, granules with a diameter size at the range of 2.8-4.0mm were abundant in the "Up" and "Down" part of the reactor when the HRT was shortened to 6h, then the ratios continuously increased up to 34.7% and 40.8% at the HRT of 3h (Fig.4). On the other hand, the granular sludge sampled from each part of the UASB reactor, a sharp increase in granules with a diameter size range of 0.35-0.5mm was found when the HRT was shortened from 12 to 3h. During these HRT conditions, the granule distribution in the UASB reactor (SP) was clearly polarized, statistically disobeying the Gaussian distribution ($R2 < 0.1$). From the perspective of process stability, granule floatation and foaming were observed in the UASB reactor (SP) when the HRT was shortened to 6h and the floatation and foaming became aggravated when the HRT was further shortened. In contrast, no significant changes were noted in the granule distribution and process appearance in the EGSB (TP) when the HRT was shortened from 12 to 3h.

4. Conclusions

(1) The SP process can be successfully used in the treatment of low-strength SW with an OLR far below 4g-COD/L/d.

(2) Granules floatation and disintegration became a serious concern in the SP process when the HRT was 6h with an OLR of 4g-COD/L/d.

(3) The potential for the application of the TP process in the anaerobic treatment of high-strength SW is significant.

Development of urban resource recovery system by methane fermentation and disposal wastewater treatment

○Ming CONG[1*], Yu-You Li[1]
[1] Graduate School of Environmental Studies, Tohoku University, 6-6-06 Aoba, Sendai 980-8579, Japan
*E-mail: soumei0615@gmail.com

Abstract
In this research, we examined the establishment of unit urban resource recovery system integrating highly efficient methane fermentation and disposal wastewater treatment which enables introduction to small-scale business establishments. Methane fermentation process and active sludge process were combined as a unit system. Two unit systems were operated over 420 days in different organic loading rate (OLR) and operating temperature for comparison between mesophilic condition (35±1℃) and thermophilic condition (55±1℃). Siphon-driven self-agitated anaerobic reactors were used for methane fermentation. Scum problem occurred with OLR of 7.3 kg-COD/m^3/d in mesophilic condition. The maximum methane production rate was obtained of 4.2 L/L/d with OLR of 14.7 kg-COD/m^3/d in thermophilic condition. According to the results, combined system had good performance in methane fermentation and wastewater treatment. In addition, it was also revealed that thermophilic condition got better performance than mesophilic condition.

Keywords: Methane fermentation, Food waste, Biogas, Wastewater treatment, Energy recovery

1. Introduction
It is pointed out that management of food waste (FW) is becoming increasingly important due to the rapid progress of urbanization and the rapid population increase. The annual amount of FW generated in the food industry is about 19 million tons, in the food manufacturing industry, the recycling rate in the industry is 95%, the food wholesale industry 58%, the food retailing industry 45% and only 24% in the industry. There are many usual treatment methods such as landfill method, incineration method, compost method, anaerobic digestion method. Although landfilling was well known as a conventional method, problems such as lack of facilities and adverse effects on the environment were pointed out. In the incineration method, expensive costs, humidity control of and exhaust gas regulation were restricted. Therefore, methane fermentation as a solution of bio-gasification method is expected which has two advantages in biomass reducing and biological energy production.

In addition, methane fermentation effluent treatment was also a problem for small methane fermentation plant. Since few cases are set up in rural areas where the fermentation liquor can be reduced as liquid fertilizer. The cost of wastewater treatment and management was come out.

It has been suggested as an effective way of centralized anaerobic FW treatment that FW is crushed first by food waste disposers and sent to a wastewater treatment plant with an anerobic digestion plant though sewerage systems. It could be an efficient way to transportation, order and storage. In this study we found the solution of those problems which was the development of urban resource recovery system by methane fermentation and disposal wastewater treatment.

2. Materials and Methods

2.1 Experimental diagram

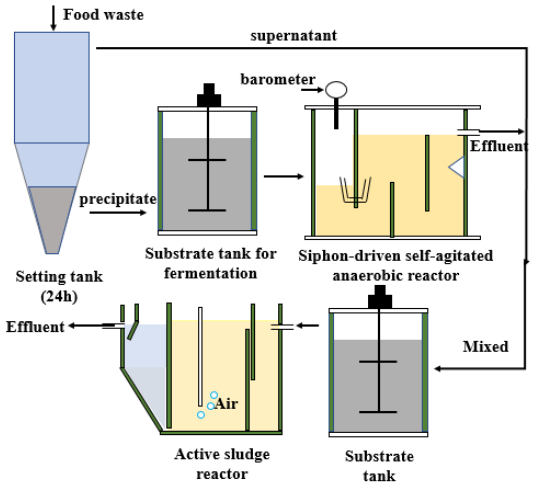

The experiment apparatus was composed of two substrate tank and a Siphon-Driven Self-agitated Anaerobic Reactor (SDSAR) with 10L effective volume and a Active sludge reactor with 5L effective volume. A disposer was used as setting tank to separate precipitate and supernatant.

2.2 Food waste sample collection
The raw and cooked FW was collected from the canteen of the National Institute of Environmental Studies, Japan. A disposal machine (Cuisinart, DLC-NXJ2PS) was used to disintegrate the raw FW. Adds 12 L water to 1 kg FW for the laboratory FW grinding. To maintain a solid content about 5% for direct methane fermentation, this crushed FW was settled in a settlement tank with an effective volume of 15 L for 24 h. Then, the settled FW was transferred and stored in the substrate tank. To prevent the trace elements deficiencies in the reactors, Fe, Co and Ni were added artificially. The trace elements concentration in the substrate was as follows: 100

mg-Fe/L, 10mg-Co/L, and 10 mg-Ni/L, respectively. In this study, no extra buffer was added into the substrate.

3. Results and Discussion

3.1 Results of Biogas production

The treatment performance of methane production in two reactors is shown in Fig.1. At OLR of 3.0 kg-COD/m3/d (HRT 20 d), the methane production rate was under 1 L/L/d for both reactors. The mesophilic reactor performed slightly better than the thermophilic one at methane production under this condition. This could be explained as the thermophilic bacteria need more time (over a month) to develop redox population compared with mesophilic bacteria. Since stable methane production was obtained in the reactors, the HRT was changed from 20 to 10 d from day 106. The methane production in two reactors increased to around 2 L/L/d with HRT decrease. However, after day 160, at OLR of 7.3 kg-COD/m^3/d, scum accumulated in the mesophilic reactor and caused problems with blocking and gas production reduction.

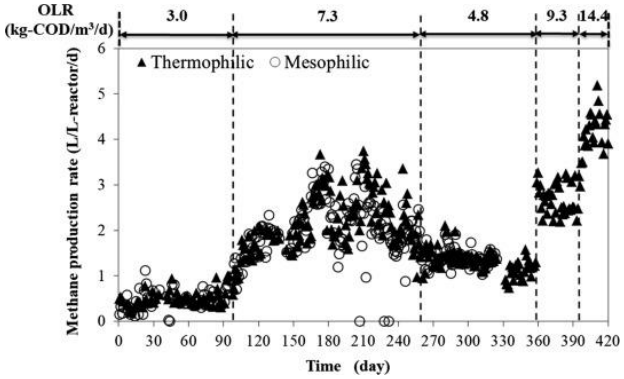

Fig.1 The comparison of biogas production rate and COD removal rate in Thermophilic condition and Mesophilic condition.

3.2 Results of active sludge rector

The treatment performance of active sludge reactors is shown in Fig.2. The effluent performance of both reactors was lower than drainage standard until day 146. According to the HRT shortening in both two reactors. The concentration of DO and MLSS became lower. BOD concentration of effluent was over 1200mg/L. Because of the instability of the properties of the fermented liquid of the previous term, the dilution method was changed from 170 days to stabilize the BOD volume load (fermentation solution: supernatant water: water = 1: 3: 1). From Phase 4, the fermentation solution dilution method returned to 1: 4, and from 330 days to 400 days, the AOD BOD concentration fell below the standard value. From the results of BOD, the temperature was better than the medium temperature. The average values of high temperature and medium temperature were 243 ± 301 and 276 ± 338 mg/L, respectively.

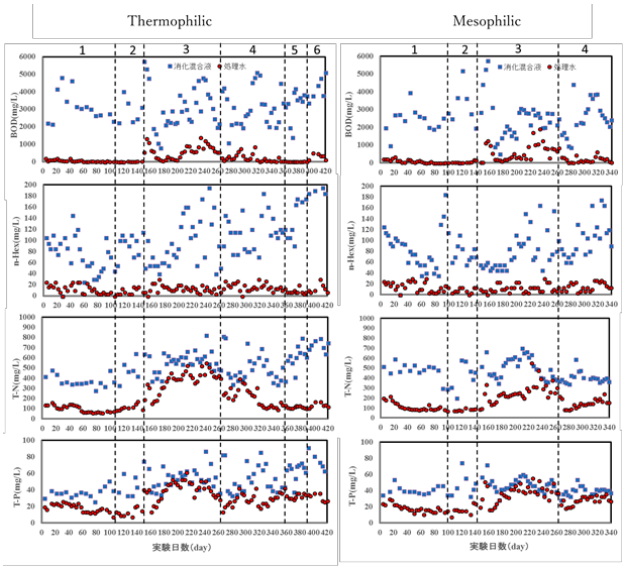

Fig.2 The performance of effluent from active sludge reactors with BOD removal rate and nitrogen removal rate.

4. Conclusions

1. The effects of OLR and operating temperature on the performance of SDSAR for the food waste treatment were investigated. It is observed that with HRT above 15 d and OLR below 4.8 kg-COD/m^3/d, relatively high COD removal in the range of 84.5–92.3% was obtained in both reactors. It is suggested that the SDSAR could successfully avoid VFA accumulation compared with other anaerobic digesters. However, the limits of the loading capacity of the mesophilic SDSAR were observed when OLR was further increased to 7.3 kg-COD/m^3/d by shortening HRT. In contrast, the thermophilic reactor can be operated at OLR as high as 14.4 kg-COD/m^3/d with satisfactory COD removal and biogas production. Based on the results, it is suggested that thermophilic SDSAR is a promising technology for the on-site FW treatment.
2. Methane fermentation by Siphon-driven self-agitated anaerobic reactor achieves that COD removal rate over 80% and methane conversion rate over 70%. It showed the same performance as the same anaerobic treatment tank of the same type that processed garbage as reported.
3. As a result of continuous experiments of treatment, it was possible to sustainably attain good quality of treated water sufficiently lower than sewage exclusion criteria.
4. According to the results of aerobic treatment removal of phosphorus was different from nitrogen, and efficient removal was not possible. Removal of phosphorus is considered to be difficult only with an aerobic tank.

Co-digestion of Food Waste and Sewage Sludge in Anaerobic Membrane Bioreactor

○Yemei Li[1]*, Hui Cheng[1] & Yu-You Li[1,2]
[1]Department of Civil and Environmental Engineering, Graduate School of Engineering, Tohoku University,6-6-06 Aoba, Aramaki-Aza, Sendai, Miyagi 980-8579, Japan.
[2]Department of Frontier Science for Advanced Environment, Graduate School of Environmental Sciences, Tohoku University, 6-6-20 Aoba, Aramaki-Aza, Sendai, Miyagi 980-8579, Japan.
*E-mail: li.yemei.s5@dc.tohoku.ac.jp

Abstract
The increase of food waste which generates during the food transfer chain catchs more and more attention because of the shortage of food and the improvement of living conditions. Sewage sludge, the major by-product from the conventional activated sludge process which is widely used for the removal of organics and nutrients in municipal and industrial wastewater plants. The huge volume and complex composition of sewage sludge makes it the main drawback of the process. Anaerobic digestion is thought to be the most suitable method to treat these two kinds of waste. To improve the digestion efficiency, co-digestion was proposed. In this study, the co-digestion of food waste and sewage sludge in AnMBR system at different temperatures was studied. The results showed an excellent performance gained in AnMBR system at both mesophilic and thermophilic conditions. The mesophilic reactor had a better and more stable performance in the removal of organic matters than the thermophilic one.

Keywords: Food waste, sewage sludge, co-digestion, AnMBR

1. Introduction
With the development of population and living conditions, food wastage, which include food loss and food waste, increases rapidly. It is estimated by the Food and Agriculture Organization of the United Nations (FAO) that over one third of food produced was lost or wasted along the food value chain in 2009. According to FAO's report, cost of societal impacts of food wastage, including the financial value of lost food and indirect consequences of degraded environmental resources and loss of social wellbeing, is 1224.2 billion USD per year globally. Reduce, reuse, recycle or recovery and disposal are mitigation measures that being used to face the situation. The recycle and disposal measures are thought to be the least environmentally friendly. However, for food waste, which means any food being produced for human consumption, but which leaves the food supply chain, landfilling, incineration, composting and anaerobic digestion are the most common treatments. Among all these options, anaerobic digestion (AD) is regarded as the most promising pathway for this kind of waste which containing high moisture and biodegradable organics.

Sewage sludge is made up by biosolids which convert from chemical oxygen demand initially presented in the influent. The sludge is the major by-product of the conventional activated sludge process which is widely used for the removal of organics and nutrients in municipal and industrial wastewater plants. Sewage sludge usually represents 1-2% of the treated wastewater volume. Though the process is high efficiency, cost effectiveness, flexibility and ease of operation, a big generation of sludge is one of its major drawbacks. Furthermore, sewage sludge contains a myriad of toxic substance which creates odors and hygiene concerns. Improper use and disposal of it will cause severe environmental impacts and health hazard to the public. Because of the disposal limitation by the reason of strict environmental regulations, together with the increase of the amount of sewage sludge resulting from the development of modern wastewater treatment, more and more attention has been focused on the full use and treatment of sludge. Normally, sewage sludge is treated biologically to stabilize and improve final dewatering. AD is the most commonly used and well-studied method to do this.

Although, AD is regarded as the most suitable way to treat food waste and sewage sludge, there still some disadvantages exist in the process, such as the high suspended solids and sodium concentration contained in food waste and low organic content in sewage sludge. These negative factors result in an improvable digestion process who need longer retention time, be sensitive to feed and operation conditions, and has reactor limitation. One option to enhance the performance of anaerobic digestion is to improve biogas production via co-digestion of multiple substrates. Co-digestion can enhance digestion performance and enrich key active microbial populations via increase the organic loading rate, dilute concentrations of potentially toxic compounds, improve microbial activity and enhance the nutrient balance. Previous researches found that co-digestion can overall increase biogas production.

In this study, the effective of temperature and food waste to sewage sludge ratio on the performance including biogas production and organic removal rate of co-digestion of food waste and sewage sludge were studied.

2. Materials and Methods

2.1 Substrate Preparation
The substrate used in this study was prepared according to an earlier research which was about the composition of food waste generated in Japan. The food waste was first ground by

a cutting pump. Then it was diluted with tap water and maintained in the substrate tank at the temperature of 4°C. The sewage sludge, including primary sludge and excess sludge, used in this study was generated from a wastewater treatment plant located in Tagajo city area. The sludge was also kept in tank at 4°C until be used. The mixture of food waste and sewage sludge was based on the total solid of these three feedstocks. The researched replace ratios of sewage sludge to food waste were 0%, 25%, and 75%. For the solo food waste as digestion substrate, considering its shortage of trace elements, supplements of the cardinal elements were added. The seed sludge was also taken from the same wastewater treatment plant mentioned previously.

2.2 Reactor System and Operation

The reactor used in this study is called anaerobic membrane bioreactor or AnMBR for short. The AnMBR system was made up by a continuous stirred-tank reactor (CSTR) and a hollow fiber membrane unit. The effective volume of the system was 15 L. The membrane was made by polytetrafluoroethylene, with a mean pore size of 0.2 μm and an effective filtration area of 0.1 m^2. The procedure of digestion was described as follow. The substrate was pumped into CSTR from the substrate tank which was maintained at 4°C by a peristaltic pump. The HRT of the system was hold at 15 d. Then the sludge in CSTR was pumped in to membrane unit also by a peristaltic pump and the sludge in membrane unit flow back to the CSTR on account of gravity. This process made the CSTR and membrane unit a cycle system. The biogas generated in the CSTR was used as aeration source in membrane unit. To research the effect of temperature, there was two AnMBR systems were used. The temperature of these two systems were maintained at 35°C and 55°C.

2.3 Analysis Methods

The volume of biogas generated was recorded by a wet gas meter, and environment temperature and pressure were also taken into consider. The composition of biogas was measured by gas chromatograph (Shimadzu GC-8A, Japan). TS, VS, COD, protein and polysaccharide were measured according to a modified Japan Standard Testing Method for wastewater. The suspended samples were the suspended liquid gained from the centrifugation of 15 mL samples at 8,000 rpm for 15 min. The results of these samples were marked as S while the results of original samples were called T. The removal rate (RR) of organic matters were calculated as Eq. (1).

$$\mathrm{RR} = \frac{(C_{inf} - C_{eff})}{C_{inf}} \times 100\% \quad (1)$$

where C_{inf} and C_{eff} were the concentrations of organic matters in the influent and effluent, respectively.

3. Results and Discussion

Fig. 1 showed the concentrations of TS, VS, COD, protein and polysaccharide in substrate and effluent, and the organic matters removal rate in mesophilic and thermophilic reactor. Fig. 1(a) - 1(d) showed the concentrations of TS, VS, COD, protein and polysaccharide in substrate. Except protein, the concentrations of organic matters decreased with the replacement of sewage sludge. Both total and suspended concentrations expressed the same tendency. From 1(e)-1(l), which showed the effluent concentration and removal rate of organic matters in mesophilic and thermophilic reactor, nearly 100% of total removal efficiency showed an excellent performance of AnMBR system in both mesophilic and thermophilic conditions.

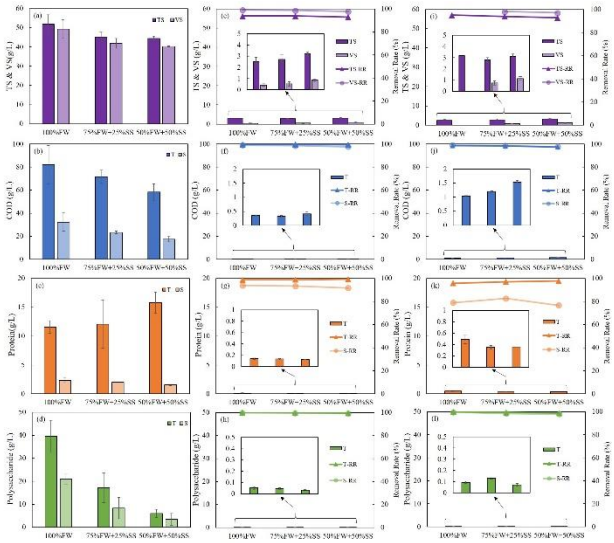

Fig. 1. The concentrations of TS, VS, COD, protein and polysaccharide in substrate and effluent, and the organic matters removal rate in mesophilic and thermophilic reactor. (The concentrations of (a) TS and VS, (b) COD, (c) protein, (d) polysaccharide in substrate; the effluent concentrations and removal rate of (e) TS and VS, (f) COD, (g) protein, (h) polysaccharide in mesophilic reactor; the effluent concentrations and removal rate of (i) TS and VS, (j) COD, (k) protein, (l) polysaccharide in thermophilic reactor.)

A comparison between the digestion performance of mesophilic and thermophilic systems also can be observed from Fig. 1(e) – 1(h) and Fig. 1(i) – 1(l). For all measured indexes, the mesophilic reactor had a better performance than the thermophilic one, especially for COD, protein and polysaccharide. Furthermore, there was no obvious tendency of system performance with the change of the food waste to sewage sludge ratio which showed a stable performance of AnMBR system at mesophilic condition. However, in the thermophilic system, the tendency of removal efficiency decreased with the decrease of the occupancy volume of food waste. Particularly, for protein, the total removal rate was much higher than the suspended one means that there would be some insoluble protein be used by microorganism at thermophilic condition.

4. Conclusions

(1) Both mesophilic and thermophilic system had an excellent co-digestion performance of food waste and sewage sludge.

(2) The mesophilic system had a stable performance with the change of co-digestion substrate while the thermophilic system changed.

The potential appearance of free-chlorine resistant norovirus after disinfection process in wastewater

○Andri Taruna Rachmadi[1], Masaaki Kitajima[2], Kozo Watanabe[3], Sakiko Yaegashi[3,4], Joeselle Serrana[3], Arata Nakamura[1], Toyoko Nakagomi[5], Osamu Nakagomi[5], Kazuhiko Katayama[6], Satoshi Okabe[2], Daisuke Sano[2]
[1] Department of Civil and Environmental Engineering, Tohoku University, Miyagi, Japan
[2] Division of Environmental Engineering, Faculty of Engineering, Hokkaido University, Japan
[3]Department of Civil and Environmental Engineering, Ehime University, Ehime, Japan
[4]Department of Civil and Environmental Engineering, University of Yamanashi, Yamanashi, Japan
[5]Department of Hygiene and Molecular Epidemiology, Nagasaki University, Japan
[6]Laboratory of Viral Infection I, Department of Infection Control and Immunology, Kitasato Institute for Life Sciences, Kitasato University, Tokyo, Japan

*E-mail: rachmadi.andri.taruna.a7@tohoku.ac.jp

Abstract

Human norovirus is present in a high number at wastewater treatment plant (WWTP) influent and become a health hazard, hence its inactivation mainly in the disinfection step is needed before release to aquatic environment. However, the high genomic diversity of norovirus owing to the high mutation rate raises a concern of the emergence of higher resistance population to water disinfection. This study aims to observe if free chlorine, one of the common water disinfectants, will act as selective pressure on norovirus evolution and give them higher resistance. Murine norovirus S7-PP3 was used as human norovirus surrogate. Two independent cycle experiments were performed with ten-time repetition of free chlorine exposure and propagation in host cells (RAW 264.7), followed by a capsid gene analysis using next generation sequencing. As a control, a cycle experiment with 10,000-fold dilution instead of free chlorine exposure was conducted. The chlorine-treated populations showed higher resistant to free chlorine and included higher number of synonymous and nonsynonymous mutations compared to the control population. A nonsynonymous mutation at nucleotide (nt) position of 7280 was observed only in the chlorine-treated populations from both trials. The result of principal coordinate analysis indicated that the chlorine-treated populations at the 5th and 10th cycles were clustered separately from the control populations at the identical cycle numbers, although the original population and all the populations at the 1st cycle were clustered together. In addition, all clones isolated from the chlorine-treated population with a mutation at nt T7280C[VP2:F200S] had higher resistant to free chlorine than clones from the control population. These results suggest that the free chlorine treatment has the effect of selection pressure on murine norovirus evolution, and the mutation at nt T7280C[VP2:F200S] determines the resistant of murine norovirus as human norovirus surrogate to free chlorine.

Keywords: Human norovirus, wastewater, disinfection, free chlorine, selective pressure